NASA Contractor Report 4099

Computational Procedures for Evaluating the Sensitivity Derivatives of Vibration Frequencies and Eigenmodes of Framed Structures

Timothy L. Fetterman and Ahmed K. Noor

GRANT NAG1-728
OCTOBER 1987

NASA

NASA Contractor Report 4099

Computational Procedures for Evaluating the Sensitivity Derivatives of Vibration Frequencies and Eigenmodes of Framed Structures

Timothy L. Fetterman and Ahmed K. Noor
The George Washington University
Joint Institute for Advancement of Flight Sciences
Langley Research Center
Hampton, Virginia

Prepared for
Langley Research Center
under Grant NAG1-728

National Aeronautics
and Space Administration

**Scientific and Technical
Information Division**

1987

CONTENTS

LIST OF FIGURES

LIST OF TABLES

NOMENCLATURE

$[a]$	material compliance coefficients
$[A]$, $[A]_o$, $[\bar{A}]$	matrices used in description of preconditioned conjugate gradient method
a_j	step size in preconditioned conjugate gradient
$[B]$	discrete strain-displacement matrix
$\{B\}$	right-hand side vector used in description of preconditioned conjugate gradient method
b_j	search direction modification factor in preconditioned conjugate gradient
c	constant multiplier of complementary solution for eigenvector derivative from the reduced equations
c_{jk}	linear design variable linking coefficients
C	constant multiplier of complementary solution for eigenvector derivative form the full equations
$[F]$	global flexibility matrix
$\{H\}$	nodal stress parameters
$\{\bar{H}\}$	approximate nodal stress parameters
$[I]$	identity matrix
$[K]$	global stiffness matrix
$[\bar{K}]$	reduced stiffness matrix
$[\tilde{K}]$	global stiffness matrix (mixed formulation)
L	number of finite elements
m	number of dependent design variables
$[M]$	global mass matrix
$[\bar{M}]$	reduced mass matrix
$[\tilde{M}]$	global consistent mass matrix (mixed formulation)
$[N]$, $[\hat{N}]$	Lagrangian interpolation functions
n	number of independent design variables
$\{Q_i\}$	particular solution for eigenvector derivative from the full equations
$\{R\}$	residual vector used in preconditioned conjugate gradient iteration
$[S]$	global generalized stiffness matrix
t	time
$\{u\}$	displacements
$\{\dot{u}\}$	velocities
$\{U\}$	nodal displacements
$\{\bar{U}\}$	approximate nodal displacements
$\{\dot{U}\}$	nodal velocities
$\{\ddot{U}\}$	nodal accelerations
U_c	component of the functional Π, complementary strain energy
$\bar{U}_c$	component of discretized functional $\bar{\Pi}$

v_j	dependent design variable
V	component of the functional Π
$\bar{V}$	component of discretized functional $\bar{\Pi}$
V_k	independent design variable
W	component of the functional Π, kinetic energy
$\bar{W}$	component of discretized functional $\bar{\Pi}$
$\{X_i\}$	eigenvector, displacement components
$\{\bar{X}_i\}$	approximate full eigenvector from reduction method
$[Y]^{(i)}$	matrix containing normalized iteration vectors for generalized dynamic reduction
$[\bar{Y}]^{(i)}$	matrix containing unnormalized iteration vectors for generalized dynamic reduction
$\{Y\}$	steepest descent direction in preconditioned conjugate gradient method
$[Z]^{(i)}$	matrix containing normalized iteration vectors for generalized dynamic reduction in mixed formulation
$[\bar{Z}]^{(i)}$	matrix containing unnormalized iteration vectors for generalized dynamic reduction in mixed formulation
$\{Z\}$	conjugate gradient search direction
α_i	normalization constant for iteration vectors in generalized dynamic reduction
β_i	normalization constant for iteration vectors in mixed formulation generalized dynamic reduction
$[\Gamma]$	reduction matrix with basis vectors as columns
$[\Gamma_H]$	stress basis vectors
$[\Gamma_X]$	displacement basis vectors
$\{\varepsilon\}$	infinitesimal strains
ε	exact error norm for approximate vectors
ε_1	residual error norm for approximate eigenvectors
ε_2	residual error norm for approximate eigenvector derivatives
$\{\theta_i\}$	particular solution for derivative of reduced eigenvector
λ_i	eigenvalue
$\bar{\lambda}_i$	approximate eigenvalue
ν	eigenvalue shift parameter
Π	functional used in the development of the mixed model
$\bar{\Pi}$	discretized functional
ρ	density
$\{\tau\}$	stresses
$\{\phi\}$	reduced unknowns
$\{\psi_i\}$	reduced eigenvector
Ω	volume

Superscript T denotes transposition

SUMMARY

Computational procedures are presented for evaluating the sensitivity derivatives of the vibration frequencies and eigenmodes of framed structures. Both a displacement and a mixed formulation are used. The two key elements of the computational procedure are: a) Use of dynamic reduction techniques to substantially reduce the number of degrees of freedom; and b) Application of iterative techniques to improve the accuracy of the derivatives of the eigenmodes. The two reduction techniques considered in the study are the static condensation (Guyan's reduction) and a generalized dynamic reduction technique.

Error norms are introduced to assess the accuracy of the eigenvalue and eigenvector derivatives obtained by the reduction techniques. The two iterative procedures used in improving the accuracy of the resulting eigenvector derivatives are based on the inverse power method and the preconditioned conjugate gradient technique.

The effectiveness of the methods presented is demonstrated by three numerical examples. The structures considered are composed of beam elements and derivatives are taken with respect to cross-sectional areas and moments of inertia. An elastic line representation of a helicopter structure is also investigated and some of the concentrated masses are used as design variables.

I. INTRODUCTION

1.1 Structural Sensitivity Analysis and Dynamic Reduction Methods

There are an ever increasing number of fields where the ability to calculate the change in the response of a system due to a small change in a particular system parameter is making important contributions. A recent survey [1] reviews applications in such diverse disciplines as physiology, thermodynamics, physical chemistry and aerodynamics. Consequently the branch of science, known as sensitivity analysis, is the object of a great deal of research looking for better and more efficient ways to calculate sensitivity derivatives.

The application of sensitivity analysis to structural response quantities, which has its roots in the development of gradient based automated structural optimization in the 1960's [2], is finding many new applications and gaining recognition as a powerful design tool [3]. Derivatives of static response, eigenvalues and eigenvectors, and transient response are being used in approximate analysis, for guidance in design modification and for improving analytical models. For extremely large and complex structures the calculation of the response and its derivatives can become prohibitively expensive unless some type of approximations are introduced.

Today almost all dynamic response calculations of large structures are carried out using finite element methods. Due to the complex topology it is generally convenient to include much more detail in the model than is required to accurately predict the dynamic response [4]. This has resulted in the development of dynamic reduction methods that allow the number of degrees of freedom to be reduced without sacrificing accuracy. While quite a few methods have been developed for calculating eigenvalues and eigenvectors, no general and efficient method exists for calculating the derivatives from a reduced set of equations. The need to reduce the cost of calculating free vibration sensitivity derivatives is a strong motivation for applying dynamic reduction methods to this problem.

1.2 Derivatives of Vibration Eigenvalues and Eigenvectors

Free vibration eigenvalues and eigenvectors of large dynamic structures are frequently used in evaluating the response. Accordingly, their derivatives with respect to design variables provide useful information to the designer and analyst. For example, the approximate dynamic response of a structure that has been changed only slightly can be calculated quickly and easily. Also, derivatives of eigenvectors can be used as a guide to alter the response of a structure to minimize displacements at certain locations. Another application occurs in the development of analytical models where the derivatives of eigenvalues and eigenvectors can be invaluable for improving the model characterization to agree better with experimental results.

The most straightforward method of calculating eigenvalue and eigenvector derivatives is by finite difference approximations. While this method is easy to implement, sensitivity to perturbation step sizes and the expense of analyzing the structure for at least one perturbation of each design variable are major drawbacks. Although recent progress has been made in the selection of step sizes [5], in many cases the method is computationally more expensive than other direct analytical methods.

The derivatives of eigenvalues can be calculated using a very simple analytical expression [6] that involves the eigenvalue being differentiated and its corresponding eigenvector. This is generally accepted as the preferred method. In contradistinction, the derivatives of eigenvectors can be calculated by several methods with the best choice being somewhat problem dependent. The modal method [6] calculates the derivatives as a linear superposition of the eigenvectors. While it is frequently possible to obtain accurate results using a truncated subset of eigenvectors, it is still computationally expensive and requires convergence checks. Other methods attempt to solve for the derivatives directly but must deal with the singularity of the governing differential equations. One procedure [6] performs algebraic manipulations that unfortunately destroy the banded form of the coefficient matrix; a major drawback when large matrices are involved. Another method [7] maintains the banded form of the coefficient matrix by calculating the derivative as the sum of a complementary and particular solution. In a majority of cases this method provides the best results; however, it does require the decomposition of a coefficient matrix for each distinct eigenvalue. A comparison of a number of methods for calculating vibration eigenvector derivatives is given in reference [8].

All the aforementioned methods for determining eigenvector derivatives provide direct finite-number-of-step formulae. Reference [9] presents an iterative scheme that converges to the derivative of the eigenvector associated with the largest eigenvalue and suggests modifications that allow derivatives of additional eigenvectors to be calculated. The present study focuses on the efficient calculation of the derivatives of the eigenvectors associated with the smallest eigenvalues. However, the procedure is easily modified to converge to these vectors.

1.3 Dynamic Reduction Methods

There are practical engineering problems for which it is necessary to perform a dynamic analysis of very large structures by developing analytical models in terms of motions or forces at discrete points. A few examples include aircraft, rotorcraft, skyscrapers and nuclear power plants [4]. Before developing the model a decision must be made about the level of discretization desired. Models can be very coarse and lump many structural components together or extremely fine and include each structural component separately. The former case has the advantage of resulting in a much smaller number of degrees of freedom (hundreds as compared to thousands for the latter) and usually provides acceptable accuracy but masks much of the detailed information required about the behavior of the actual structural components. To get complete information on the dynamic stresses and displacements occurring in the structural components a very fine model is needed but this results in an extremely large number of degrees of freedom and high computational costs. This dilemma has resulted in the development of dynamic reduction methods which allow the size of the equations to be decreased without losing the fine detail of the model.

The crux of dynamic reduction methods is the relationship between the small number of degrees of freedom defining the reduced model and the vector of unknowns of the original (full) model. This is accomplished by approximating the full vector of unknowns as a linear combination of a small number of global approximation (or basis) vectors, the amplitudes of which constitute the unknowns of the reduced equations. There have been a number of methods proposed for determining the basis vectors and a few of those will be described subsequently.

One of the first and most popular methods of dynamic reduction is known as static condensation or Guyan's reduction [10]. The procedure is to subdivide the vector of unknowns into two sets. One set contains the degrees of freedom considered most important that will be retained while the other contains those of lesser importance that will be eliminated. The two sets of degrees of freedom are usually referred to as free and constrained. The basis vectors are determined from the static relationship between the two sets and neglect the effects of the dynamic terms. This method is very easy to implement, however it requires some experience in choosing the free degrees of freedom, and in most cases only a moderate reduction is possible without sacrificing accuracy [4].

Dynamic condensation [11] is similar to static condensation but includes the dynamic terms in the relation between the free and constrained unknowns by using an iterative procedure. The method offers substantial improvements in accuracy, however because the equations must be reduced for each eigenvalue a great reduction in efficiency results (compared with static condensation).

In both static and dynamic condensation the reduced unknowns are physical degrees of freedom. Another group of reduction methods uses a reduced set of unknowns which have no direct physical significance, thereby relieving the analyst of the task of choosing the free degrees of freedom. The first method of this type [12] proposed the use of Lanczos vectors, which are rich in the desired eigenvectors, for basis vectors. This has the advantage of automatic selection of basis vectors and can allow very substantial reductions in problem size. Subsequently, several variations on this original algorithm have been proposed such as subspace iteration [13] and generalized dynamic reduction [4]. These methods have become very popular in recent years due to their simplicity, accuracy and efficiency.

1.4 Mixed Formulation Finite Elements

In recent years there have been a number of applications in which the use of a mixed formulation in which the fundamental unknowns are both stresses and displacements has shown advantages over the more common displacement-based formulation. Studies in approximate structural reanalysis [14,15] have shown that the use of a mixed method provided higher accuracy for the predicted response, especially for stress quantities. Also, work in nonlinear structural analysis [16] has indicated that the use of reduction methods in conjunction with mixed finite element models can considerably improve the accuracy.

When reduction methods are used in conjunction with the mixed formulation, explicit approximations are made for both the stresses and displacements. The stresses are allowed to be discontinuous across element boundaries and eliminated on the element level. It has been shown [16] that this improves the performance of the method and also avoids the computational expense that would be associated with generating the basis from the complete set of equations directly.

1.5 Review of Previous Pertinent Work

While several examples of the current work being performed in the fields of free vibration structural sensitivity analysis and dynamic reduction methods have been discussed previously, there are surprisingly few cases in which the two are considered jointly. A recent paper on the calculation of eigenvalue sensitivity derivatives [17] proposes two new

solution techniques, one direct and the other iterative, and also addresses the case of repeated eigenvalues. However, no reduction in problem size or significant improvements in efficiency are suggested. Another study [18] suggests improvements to increase the rate of convergence of the modal method; however, it was found in [8] that even with these improvements the method is computationally expensive.

A paper by Robinson [19] describes the implementation of a systematic finite element modification technique in the program EAL for the purpose of improving dynamic models to agree better with experimental results. In this implementation the eigenvector derivatives are calculated by the modal method and he suggests the use of a Rayleigh-Ritz type reduction method to reduce the computational expense. In the described implementation, the modification of the structure is performed in a reduced space defined by the eigenvectors of the original structure. Large reductions in computer execution times are reported.

Another important application of free vibration sensitivity derivatives is in automated structural optimization. Kim and Anderson [20] apply generalized dynamic reduction to automated redesign for frequency changes. The optimization is performed in the reduced subspace and good results are reported; however, changes in eigenvectors are not considered. Also, the optimization equations are formulated in terms of perturbation equations that do not require the calculation of gradients, but this study does give an indication of the ability of the subspaces to accurately represent the full dynamic space.

The calculation of approximate eigenvalue and eigenvector derivatives for a modified system is addressed in a recent paper by Wang [21]. For the special case in which the stiffness and mass terms are homogeneous functions of the design variable he develops expressions using cross mode energies to calculate the approximate derivatives. The results that are reported show a mixed degree of success.

1.6 Objective and Scope of the Present Study

The objective of the present study is to develop an efficient computational strategy for calculating the sensitivity derivatives of vibration frequencies and eigenmodes of framed structures. The key elements of the strategy are:

1. Use of dynamic reduction methods to substantially reduce the number of degrees of freedom.

2. The application of a mixed method in conjunction with reduction methods to the free vibration derivative calculations.

3. Use of iterative techniques for improving the accuracy of the derivatives obtained by using the reduction technique.

The scope of this study includes:

1. Large frame-type structures modelled by finite elements.

2. Sensitivity derivatives of vibration eigenvalues and eigenvectors with respect to cross-sectional design variables and concentrated masses.

II. SENSITIVITY CALCULATIONS VIA REDUCTION METHODS

2.1 Introduction

Reduction methods is the name usually given to a class of hybrid two-step computational procedures that attempt to reduce the dimension of a given problem and permit the solution to be calculated more economically. The first step is the spatial discretization of the system into a number of finite domains within which interpolation functions are used to approximate the unknown fields in terms of unknown nodal parameters. These nodal parameters span what will henceforth be referred to as the full space of the system. The second step is to impose relationships between the degrees of freedom of the full space to define a new coordinate system, usually of much smaller dimension, called the reduced subspace. The transformation of the governing equations from the full space to the reduced subspace is accomplished by using a Rayleigh-Ritz (or Bubnov-Galerkin) procedure. Throughout this report the words full and reduced are used as a prefix to indicate the space in which the response quantities are defined. For example, reduced equations refer to equations defined in the reduced subspace.

In this section the derivation and solution of the reduced equations for the derivatives of vibration eigenvalues and eigenvectors is discussed. Since this is accomplished by a transformation of coordinates the full equations are developed first and are then transformed into the reduced subspace.

2.2 Governing Equations

The free vibrations of structures modelled by displacement-based finite elements are governed by the following system of equations:

$$([K] - \lambda_i [M]) \{X_i\} = 0 \qquad (1a)$$

where

$[K]$ = global stiffness matrix
$[M]$ = global mass matrix (consistent or lumped)
λ_i = ith eigenvalue (square of the frequency of vibration)
$\{X_i\}$ = ith eigenmode (vibration mode shape)

The eigenvectors satisfy the orthonormality relation

$$\{X_i\}^T [M] \{X_j\} = \delta_{ij} \qquad (1b)$$

where

δ_{ij} = Kronecker delta = 1 if $i=j$
= 0 if $i \neq j$

Before assembling the stiffness and mass matrices the specific properties of each element must be known. Changing any one of these properties would change the resulting stiffness and mass matrices and thus the eigenvalues and eigenvectors. To quantify the effect of this change the equations (1) are differentiated with respect to the property, called a

design variable [6]. It is often more convenient to determine the effect of the simultaneous change in the properties of several elements and this is accomplished using design variable linking. The properties of each individual element (dependent design variables v_j) are related to a much smaller number of parameters (independent design variables V_k) by a linking relationship. For example, linear design variable linking is expressed by the relation

$$v_j = \sum_{k=1}^{n} c_{jk} V_k \tag{2}$$

where

n = the number of independent design variables
c_{jk} = the linking coefficients

Differentiating equations (1) with respect to an independent design variable V_k results in

$$([K] - \lambda_i [M]) \frac{\partial \{X_i\}}{\partial V_k} = \left(\frac{\partial \lambda_i}{\partial V_k}[M] + \lambda_i \frac{\partial [M]}{\partial V_k} - \frac{\partial [K]}{\partial V_k} \right) \{X_i\} \tag{3a}$$

and

$$2 \{X_i\}^T [M] \frac{\partial \{X_i\}}{\partial V_k} + \{X_i\}^T \frac{\partial [M]}{\partial V_k} \{X_i\} = 0 \tag{3b}$$

The unknowns in equations (3) are the derivatives of the eigenvalue and eigenvector, $\frac{\partial \lambda_i}{\partial V_k}$ and $\frac{\partial \{X_i\}}{\partial V_k}$. It is noted that when using design variable linking the derivatives of the stiffness and mass matrices must be evaluated using the chain rule of partial differentiation. For the linear design variable linking in equations (2), this results in

$$\frac{\partial [K]}{\partial V_k} = \sum_{j=1}^{m} \frac{\partial [K]}{\partial v_j} \frac{\partial v_j}{\partial V_k} = \sum_{j=1}^{m} \frac{\partial [K]}{\partial v_j} c_{jk} \tag{4a}$$

$$\frac{\partial [M]}{\partial V_k} = \sum_{j=1}^{m} \frac{\partial [M]}{\partial v_j} \frac{\partial v_j}{\partial V_k} = \sum_{j=1}^{m} \frac{\partial [M]}{\partial v_j} c_{jk} \tag{4b}$$

where m is the number of dependent design variables.

An examination of equations (3a) indicates that a direct solution is not possible for two reasons:

1. The right hand side vector contains the derivative of the eigenvalue which is, as yet, unknown.
2. The matrix on the left-hand side is singular.

Before solving equations (3) it is important to determine the multiplicity of the eigenvalue λ_i. Since the solution for nonrepeated eigenvalues is simpler it is presented first and then generalized to the repeated case.

2.2.1 Nonrepeated Eigenvalues

The derivative of the eigenvalue is calculated through premultiplication of equation (3a) by the transpose of the eigenvector and noting equations (1), resulting in the following expression:

$$\frac{\partial \lambda_i}{\partial V_k} = \{X_i\}^T \left(\frac{\partial [K]}{\partial V_k} - \lambda_i \frac{\partial [M]}{\partial V_k} \right) \{X_i\} \tag{5}$$

Nelson [7] solved the problem of a singular coefficient matrix by expressing the derivative of the eigenvector as the sum of a particular and complementary solution.

$$\frac{\partial \{X_i\}}{\partial V_k} = \{Q_i\} + C \{X_i\} \tag{6}$$

The complementary solution $\{X_i\}$ is the eigenvector and the particular solution $\{Q_i\}$ is obtained by constraining one degree of freedom of the solution vector in equation (3a) to zero (e.g. the one corresponding to the largest component of the eigenvector) to eliminate the singularity in the coefficient matrix. The unknown constant C is then determined by substituting the assumed form of the solution (6) into equation (3b). This leads to

$$C = - \{X_i\}^T [M] \{Q_i\} - \frac{1}{2} \{X_i\}^T \frac{\partial [M]}{\partial V_k} \{X_i\} \tag{7}$$

2.2.2 Repeated Eigenvalues

When eigenvalues of multiplicity greater than one are present the solution of equations (3) becomes much more complex due to the nonuniqueness of the associated eigenvectors and the decreased rank of the coefficient matrix. For simplicity an eigenvalue of multiplicity two is assumed in the subsequent discussion however, the method is easily generalized to cases of higher multiplicity (see for example Reference [17]). The free vibration equations for the repeated eigenvalue can be written

$$([K] - \lambda_i [M]) \{X_i\} = 0 \tag{8a}$$

$$([K] - \lambda_{i+1} [M]) \{X_{i+1}\} = 0 \tag{8b}$$

where

$$\lambda_i = \lambda_{i+1}$$

The eigenvectors satisfy the orthonormality relation (1b). Since any linear combination of eigenvectors is also an eigenvector the free vibration equation can also be expressed as

$$([K] - \lambda_i[M])\ \{X'_i\} = 0 \tag{9}$$

where

$$\{X'_i\} = [X_i\ X_{i+1}]\ \{a_i\} \tag{10}$$

The matrix $[X_i\ X_{i+1}]$ stores the eigenvectors columnwise and $\{X'_i\}$ also satisfies the orthonormality relation (1b). Differentiating (9) with respect to an independent design variable V_k results in

$$([K] - \lambda_i[M])\ \frac{\partial\{X'_i\}}{\partial V_k} = \left(\frac{\partial\lambda_i}{\partial V_k}[M] + \lambda_i\frac{\partial[M]}{\partial V_k} - \frac{\partial[K]}{\partial V_k}\right)\ \{X'_i\} \tag{11}$$

Premultiplication of (11) by $[X_i\ X_{i+1}]^T$ and noting equations (8) and (10) leads to the following:

$$[X_i\ X_{i+1}]^T\left(\frac{\partial[K]}{\partial V_k} - \lambda_i\frac{\partial[M]}{\partial V_k}\right)\ [X_i\ X_{i+1}]\ \{a_i\} = \frac{\partial\lambda_i}{\partial V_k}\ \{a_i\} \tag{12}$$

Equation (12) is an eigenvalue problem of dimension two and has the two solutions $\frac{\partial\lambda_i}{\partial V_k}$, $\{a_i\}$ and $\frac{\partial\lambda_{i+1}}{\partial V_k}$, $\{a_{i+1}\}$ which indicates that the repeated eigenvalue may follow two separate paths with the continuous variation of V_k and also leads to two separate right hand side vectors for equation (11) (and thus two eigenvector derivatives). Differentiation of the orthonormality relations for the vectors $\{X'_i\}$ and $\{X'_{i+1}\}$ (obtained from $\{a_i\}$ and $\{a_{i+1}\}$ respectively) results in the following equations:

$$\{X'_i\}^T\ [M]\ \frac{\partial\{X'_i\}}{\partial V_k} = -\frac{1}{2}\ \{X'_i\}^T\ \frac{\partial[M]}{\partial V_k}\ \{X'_i\} \tag{13a}$$

$$\{X'_{i+1}\}^T\ [M]\ \frac{\partial\{X'_{i+1}\}}{\partial V_k} = -\frac{1}{2}\ \{X'_{i+1}\}^T\ \frac{\partial[M]}{\partial V_k}\ \{X'_{i+1}\} \tag{13b}$$

$$\frac{\partial\{X'_i\}^T}{\partial V_k}\ [M]\{X'_{i+1}\} + \{X'_i\}^T\frac{\partial[M]}{\partial V_k}\{X'_{i+1}\} + \{X'_i\}^T[M]\frac{\partial\{X'_{i+1}\}}{\partial V_k} = 0 \tag{13c}$$

As in the previous subsection, solutions to equation (11) are assumed of the form

$$\frac{\partial\{X'_i\}}{\partial V_k} = \{Q_i\} + [X'_i\ X'_{i+1}]\ \{c\} \tag{14a}$$

$$\frac{\partial\{X'_{i+1}\}}{\partial V_k} = \{Q_{i+1}\} + [X'_i \; X'_{i+1}] \; \{d\} \tag{14b}$$

In equations (14), $\{Q_i\}$ and $\{Q_{i+1}\}$ are particular solutions to (11) obtained by constraining two degrees of freedom (those associated with the largest degree of freedom of each eigenvector) in the solution vector and the eigenvectors are complementary solutions. Substitution of the solutions (14) into equations (13) leads to the following expressions for the unknown constants:

$$c_1 = -\frac{1}{2}\{X'_i\}^T \frac{\partial[M]}{\partial V_k}\{X'_i\} - \{X'_i\}^T[M]\{Q_i\} \tag{15a}$$

$$d_2 = -\frac{1}{2}\{X'_{i+1}\}^T \frac{\partial[M]}{\partial V_k}\{X'_{i+1}\} - \{X'_{i+1}\}^T[M]\{Q_{i+1}\} \tag{15b}$$

$$c_2+d_1 = -\{Q_i\}^T[M]\{X'_{i+1}\} - \{X'_i\}^T[M]\{Q_{i+1}\} - \{X'_i\}^T \frac{\partial[M]}{\partial V_k}\{X'_{i+1}\} \tag{15c}$$

It is noted from equation (15c) that the nonuniqueness of the eigenvectors extends to their derivatives.

Equations (3) or (11) can be solved by several alternate methods (see subsection 1.2) but the solution presented herein has the advantage of providing essentially exact results without the need for convergence checks. Its major disadvantage is that the coefficient matrix must be decomposed for each distinct eigenvalue. However, it is shown subsequently that reduction methods can substantially reduce the size of this matrix and the cost of decomposition.

2.3 Dynamic Reduction Methods

Dynamic reduction methods approximate a vector in the full space by a linear combination of a small number of linearly independent basis vectors that define a reduced subspace. The accuracy of the method depends on the degree to which the full vector lies within the reduced subspace and, as such, the determination of the basis vectors is a crucial step that depends strongly on the nature of the full vectors. Since the current work focuses on the derivatives of the eigenvectors, a logical starting point is methods developed for approximating the eigenvectors. The approximation is expressed by the following equation:

$$\{X_i\} \simeq \{\bar{X}_i\} = [\Gamma] \; \{\psi_i\} \tag{16}$$

where

$\{X_i\}$ = the full eigenvector

$\{\bar{X}_i\}$ = the approximate full eigenvector

$[\Gamma]$ = matrix with basis vectors as columns

$\{\psi_i\}$ = reduced eigenvector

The reduced eigenvector $\{\psi_i\}$ consists of generalized coordinates that are amplitudes of the basis vectors.

Using equation (16) the free vibration equations (1) are transformed into the reduced subspace resulting in the following reduced equations:

$$([\bar{K}] - \bar{\lambda}_i [\bar{M}]) \{\psi_i\} = 0 \tag{17a}$$

and

$$\{\psi_i\}^T [\bar{M}] \{\psi_j\} = \delta_{ij} \tag{17b}$$

where

$[\bar{K}] = [\Gamma]^T [K] [\Gamma]$ = reduced stiffness matrix

$[\bar{M}] = [\Gamma]^T [M] [\Gamma]$ = reduced mass matrix

$\bar{\lambda}_i$ = approximate eigenvalue

$\{\psi_i\}$ = reduced eigenvector

Since equations (17) represent a much smaller system of equations than (1), their solution requires substantially less effort and provides approximations to the lower eigenvalues and, through the use of equation (16), the eigenvectors. Several methods have been developed for performing reduced eigenvalue analysis (see for example [4] and [11]) and two of these are discussed in the following subsections.

2.3.1 Static Condensation

One of the first and most popular methods of determining the basis vectors used in equations (16) and (17) is known as static condensation or Guyan's reductions [10]. The procedure begins with the choice of constrained degrees of freedom (a subset of the degrees of freedom of the full space that are assumed massless). Then the equations (1) are partitioned in the form

$$\left(\begin{bmatrix} K^{ff} & K^{fc} \\ K^{cf} & K^{cc} \end{bmatrix} - \lambda_i \begin{bmatrix} M^{ff} & M^{fc} \\ M^{cf} & M^{cc} \end{bmatrix} \right) \begin{Bmatrix} X_i^f \\ X_i^c \end{Bmatrix} = 0 \tag{18}$$

where the superscript f denotes the free (retained) degrees of freedom and the superscript c denotes the constrained degrees of freedom. Expanding the equation in the lower partition of (18) and solving for $\{X_i^c\}$ results in

$$\{X_i^c\} = - ([K^{cc}] - \lambda_i [M^{cc}])^{-1} ([K^{cf}] - \lambda_i [M^{cf}]) \{X_i^f\} \tag{19}$$

If the mass matrices $[M^{cc}]$ and $[M^{cf}]$ are neglected, equation (19) reduces to the following static relation:

$$\{X_i^c\} = - [K^{cc}]^{-1} [K^{cf}] \{X_i^f\} \tag{20}$$

Equations (20) are used to eliminate the constrained degrees of freedom. The matrix of basis vectors of the static condensation procedure can then be expressed by the equation

$$[\Gamma] = \begin{bmatrix} [I] \\ -[\bar{K}^{cc}]^{-1}[\bar{K}^{cf}] \end{bmatrix} \tag{21}$$

The approximation results from neglecting the mass matrices $[M^{cc}]$ and $[M^{cf}]$. The accuracy of the approximation depends on the selection of free and constrained degrees of freedom. There is obviously a certain amount of talent or experience required for the proper selection of the free and constrained degrees of freedom. Also, looking at equation (19) it is apparent that the effect of the neglected masses increases with increasing eigenvalue and therefore, the accuracy of the method decreases with increasing eigenvalue.

With static condensation it is generally possible to perform a moderate amount of reduction and still obtain good results for the lowest few eigenvalues and eigenvectors. However, the desire to obtain an even higher degree of reduction and also to eliminate the need for choosing massless degrees of freedom has led to the development of another group of methods that generate the basis vectors automatically. These are discussed in the succeeding subsection.

2.3.2 Generalized Dynamic Reduction

Since the main purpose of the dynamic reduction methods is the accurate calculation of eigenvectors, procedures have been developed that start with arbitrarily chosen vectors and then attempt to enrich the content therein of a selected group of eigenvectors (see for example [12] and [13]). The enriched vectors, called Lanczos vectors, are then used as basis vectors. In generalized dynamic reduction [4], the Lanczos vectors are generated by performing a required number of iterations through the recursion relation

$$([K] - \nu[M]) [\bar{Y}]^{(r+1)} = [M] [Y]^{(r)} \tag{22a}$$

where

$$[Y]^{(r)} = [\{Y_1\} \{Y_2\} \dots \{Y_n\}] \tag{22b}$$

and

$$\{Y_i\}^{(r+1)} = \alpha_i^{(r+1)} \{\bar{Y}_i\}^{(r+1)} \tag{22c}$$

In equations (22), the constant $\alpha_i^{(r+1)}$ is used to normalize $\{\bar{Y}_i\}^{(r+1)}$. As mentioned previously, the initial iteration vectors $[Y]^{(0)}$ are chosen arbitrarily. Experience has shown that the use of a pseudorandom number generator (e.g. generated by the multiplicative congruential method, see Reference [22]) in initializing $[Y]^{(0)}$ helps insure that all eigenvectors are represented and increases the chances that a mode will not be missed. In addition, if a structure contains large concentrated masses it has been found advantageous to include unit vectors to excite these masses. Since eigenvectors other than the ones associated with the smallest eigenvalues

are sometimes of interest, a nonzero value for the shift parameter ν allows equation (22) to converge to the eigenvectors desired.

In addition to being rich in the eigenvectors of interest the basis vectors must also be linearly independent. The final iteration vectors from equation (22) are orthonormalized by performing the Gram-Schmidt orthogonalization procedure. Often this must be performed several times to achieve the high degree of linear independence required to insure the solvability of equation (17). The orthogonalization also helps to amplify the content of eigenvectors slightly further away form the shift value ν, in the basis vectors.

Generalized dynamic reduction usually allows a greater reduction in the number of degrees of freedom than static condensation and at the same time provides greater accuracy. The number of modes that can be obtained accurately from the reduced equations is usually less than one-half the number of basis vectors. With static condensation this limits the number of modes that can be calculated, but generalized dynamic reduction used with multiple shift values ν and multiple reductions can be used in calculating many more eigenvectors than the number of basis vectors used.

2.4 Reduction of the Governing Finite Element Equations

The preceding section has dealt with dynamic reduction methods for calculating eigenvalues and eigenvectors. The next step is to apply these to the calculation of the required derivatives. Differentiating equations (16) and (17) with respect to an independent design variable results in

$$\frac{\partial\{X_i\}}{\partial V_k} \approx \frac{\partial\{\bar{X}_i\}}{\partial V_k} = [\Gamma] \frac{\partial\{\psi_i\}}{\partial V_k} + \frac{\partial[\Gamma]}{\partial V_k} \{\psi_i\} \tag{23}$$

and

$$\left([\bar{K}] - \lambda_i [\bar{M}] \right) \frac{\partial\{\psi_i\}}{\partial V_k} = \left(\frac{\partial\bar{\lambda}_i}{\partial V_k} [M] + \lambda_i \frac{\partial[\bar{M}]}{\partial V_k} - \frac{\partial[\bar{K}]}{\partial V_k} \right) \{\psi_i\} \tag{24}$$

where

$$\frac{\partial[\bar{K}]}{\partial V_k} = [\Gamma]^T \frac{\partial[K]}{\partial V_k} [\Gamma] + [\Gamma]^T [K] \frac{\partial[\Gamma]}{\partial V_k} + \frac{\partial[\Gamma]^T}{\partial V_k} [K] [\Gamma]$$

and

$$\frac{\partial[\bar{M}]}{\partial V_k} = [\Gamma]^T \frac{\partial[M]}{\partial V_k} [\Gamma] + [\Gamma]^T [M] \frac{\partial[\Gamma]}{\partial V_k} + \frac{\partial[\Gamma]^T}{\partial V_k} [M] [\Gamma]$$

The matrix $\partial[\Gamma]/\partial V_k$ in equations (23) and (24) represents the changes in the basis vectors due to changes in the design variables. It is not desirable to calculate this matrix since it would be at least as computationally expensive as calculating the derivatives of the eigenvectors from the full equations. The purpose of this procedure is to reduce the expense and the contribution of the derivatives of the basis vectors must be neglected to retain the desired efficiency. With this assumption the reduced derivative of the mass and stiffness matrices from equation (24) become

$$\frac{\partial[\bar{K}]}{\partial V_k} = [\Gamma]^T \frac{\partial[K]}{\partial V_k} [\Gamma] \tag{25a}$$

and

$$\frac{\partial[\bar{M}]}{\partial V_k} = [\Gamma]^T \frac{\partial[M]}{\partial V_k} [\Gamma] \tag{25b}$$

and the derivative of the eigenvector is approximated as

$$\frac{\partial\{X_i\}}{\partial V_k} \simeq \frac{\partial\{\bar{X}_i\}}{\partial V_k} = [\Gamma] \frac{\partial\{\psi_i\}}{\partial V_k} \tag{26}$$

It is noted that neglecting the derivative of the basis vectors is equivalent to assuming the derivative of the eigenvector lies in the subspace defined by the basis vectors.

Since the form of equation (24) is identical to that of equation (3) only of much smaller order, it can be solved by the same method. For eigenvalues of multiplicity one the approximate derivative of the eigenvalue is calculated from

$$\frac{\partial\bar{\lambda}_i}{\partial V_k} = \{\psi_i\}^T \left(\frac{\partial[\bar{K}]}{\partial V_k} - \bar{\lambda}_i \frac{\partial[\bar{M}]}{\partial V_k} \right) \{\psi_i\} \tag{27}$$

The reduced derivative of the eigenvector is assumed to be of the form

$$\frac{\partial\{\psi_i\}}{\partial V_k} = \{\theta_i\} + c\,\{\psi_i\} \tag{28}$$

where the reduced eigenvector $\{\psi_i\}$ is a complementary solution and $\{\theta_i\}$ is a particular solution to equation (24) obtained by constraining one component of the solution vector. In the reduced equations the degree of freedom associated with the smallest term on the diagonal of the coefficient matrix is constrained to zero. The constant c is then calculated from

$$c = -\{\psi_i\}^T [\bar{M}] \{\theta_i\} - \frac{1}{2} \{\psi_i\}^T \frac{\partial[\bar{M}]}{\partial V_k} \{\psi_i\} \tag{29}$$

For repeated eigenvalues a procedure analogous to that used above, but using the method described in subsection 2.2.2 can be used.

The foregoing procedure for calculating approximate derivatives of eigenvalues and eigenvectors with respect to design variables greatly reduces the computational effort compared to the solution of the full equations. The performance of these methods on several finite element models is discussed in section five in conjunction with the numerical studies.

III. APPLICATION OF A MIXED FINITE ELEMENT MODEL TO SENSITIVITY CALCULATIONS

3.1 Introduction

In the preceeding section reduced equations are developed for calculating the derivatives of free vibration eigenvalues and eigenvectors based on a displacement formulation. The displacement formulation is the most commonly used; however, in some applications a mixed formulation, which takes both stresses and displacements as unknowns, has several advantages (see subsection 1.4 for references). Studies in nonlinear analysis have shown that the use of a mixed model in conjunction with reduction methods can provide improved accuracy over reduction methods used with a displacement formulation [23]. Also, in several types of structures (e.g. trusses, plates, membranes) approximate reanalysis is improved by taking the inverse of the sizing quantities as design variables [24]. In the mixed formulation this is a natural choice.

3.2 Element Formulation

The mixed finite element formulation is based on the Hellinger-Reissner variational principle [25]. The following functional, which represents a modified version of Hamilton's principle, is used in the development of the governing equations:

$$\Pi = \int_{t_1}^{t_2} \left(W - (V - U_c) \right) dt \tag{30}$$

where

$$V = \int_{\Omega} \{\varepsilon\}^T \{\tau\} \, d\Omega$$

$$U_c = \frac{1}{2} \int_{\Omega} \{\tau\}^T [a] \{\tau\} \, d\Omega$$

and

$$W = \frac{1}{2} \int_{\Omega} \rho \, \dot{\{u\}}^T \dot{\{u\}} \, d\Omega$$

The integrations are performed over the volume of the structure Ω. The infinitesimal strains $\{\varepsilon\}$ correspond to the displacements $\{u\}$ of the structure from its undeformed state and the stresses $\{\tau\}$ result from these strains. The matrix $[a]$ contains the material compliance coefficients. It is noted that no external forces are included in the functional since the present study is considering only free vibrations. If considered, body forces, surface tractions and point loads would be added to the term W.

The functional in equation (30) is discretized by subdividing the structure into finite elements and approximating the fundamental unknowns within each element using Lagrangian interpolation functions. The displacements and stresses of the j^{th} element are given by the relations

$$\{u^j\} \simeq [N^j]\ \{U^j\} \tag{31}$$

$$\{\tau^j\} \simeq [\hat{N}^j]\ \{H^j\} \tag{32}$$

where $\{U\}$ are the nodal displacements and $\{H\}$ are stress parameters. It was shown in [23] that better accuracy is obtained from mixed elements when the interpolation functions for the stresses are one degree lower than those used for approximating the displacements. Accordingly, $[\hat{N}]$ represents a matrix of lower degree shape functions than $[N]$. Also, the stress field is allowed to be discontinuous across element boundaries so that the stress parameters can be eliminated on the elemental level.

Applying the aforementioned finite element approximation results in the following discretized functional:

$$\bar{\Pi} = \int_{t_1}^{t_2} \left(\bar{W} - (\bar{V} - \bar{U}_c) \right) dt \tag{33}$$

where

$$\bar{V} = \sum_{j=1}^{L} \int_{\Omega^j} \{U\}^T [B]^T [\hat{N}]\ \{H\}\ d\Omega$$

$$\bar{U}_c = \sum_{j=1}^{L} \frac{1}{2} \int_{\Omega^j} \{H\}^T [\hat{N}]^T [a]\ [\hat{N}]\ \{H\}\ d\Omega$$

and

$$\bar{W} = \sum_{j=1}^{L} \frac{1}{2} \int_{\Omega^j} \rho\ \{\dot{U}\}^T [N]^T [N]\ \{\dot{U}\}\ d\Omega$$

The summations are over the number of elements L, and $[B]$ is the discrete strain-displacement matrix.

Varying the displacement and stress parameters independently and simultaneously results in discrete governing equations which consist of both constitutive relations and equilibrium equations. For the jth element these equations are cast in the following form:

$$\begin{bmatrix} -F & S \\ S^T & 0 \end{bmatrix}^j \begin{Bmatrix} H \\ U \end{Bmatrix}^j + \begin{bmatrix} 0 & 0 \\ 0 & \tilde{M} \end{bmatrix}^j \begin{Bmatrix} H \\ \ddot{U} \end{Bmatrix}^j = 0 \tag{34}$$

The submatrices in these equations are:

$$[F]^j = \int_{\Omega^j} [\hat{N}]^T [a]\ [\hat{N}]\ d\Omega = \text{elemental flexibility matrix}$$

$$[S]^j = \int_{\Omega^j} [\hat{N}]^T [B]\ d\Omega = \text{elemental generalized stiffness matrix}$$

$$[\tilde{M}]^j = \int_{\Omega^j} \rho\ [N]^T [N]\ d\Omega = \text{elemental consistent mass matrix}$$

For free vibrations the nodal displacements $\{U\}$ are of the form

$$\{U(\Omega,t)\} = e^{i\sqrt{\lambda}t} \{X(\Omega,\lambda)\} \tag{35}$$

and equations (34) become

$$\begin{bmatrix} -F & S \\ S^T & 0 \end{bmatrix}^j \begin{Bmatrix} H_i \\ X_i \end{Bmatrix}^j - \lambda_i \begin{bmatrix} 0 & 0 \\ 0 & \tilde{M} \end{bmatrix}^j \begin{Bmatrix} H_i \\ X_i \end{Bmatrix}^j = 0 \tag{36}$$

Since the stress field is allowed to be discontinuous across interelement boundaries, the upper partition of (36) can be solved for $\{H^j\}$ at the element level. This allows the elimination of the stress parameters from the lower partition. The resulting elemental equations can then be assembled in the form

$$([\tilde{K}] - \lambda_i [\tilde{M}]) \{X_i\} = 0 \tag{37}$$

where

$$[\tilde{K}] = \sum_{j=1}^{L} [S^j]^T [F^j]^{-1} [S^j] = \text{global stiffness matrix}$$

and

$$[\tilde{M}] = \sum_{j=1}^{L} [\tilde{M}^j] = \text{global consistent mass matrix}$$

The above system of equations is of the same order as a corresponding displacement model.

3.3 Derivatives of Eigenvalues and Eigenvectors

Equation (37) is similar in form to the governing equations of the displacement formulation (equation(1)) and the sensitivity derivatives of the eigenvalues and eigenvectors can be calculated as outlined in equations (3)-(7). The only difference is the derivative of stiffness matrix which in this case is

$$\frac{\partial[\tilde{K}]}{\partial V_k} = \sum_{j=1}^{L} [S^j]^T \frac{\partial([F^j]^{-1})}{\partial V_k} [S^j] \tag{38}$$

This approach will work, but has no advantage over the displacement formulation since it requires the differentiation of the inverse of the flexibility matrix (essentially a stiffness matrix). In cases where it is advantageous to choose the inverse of the sizing variables as design variables (discussed at the beginning of this section) it would be more efficient to differentiate the flexibility matrix and thus an alternate formulation of the derivative equation is required. Differentiation of equation (36) with respect to an independent design variable V_k results in the following:

$$\left(\begin{bmatrix} -F & S \\ S^T & 0 \end{bmatrix}^j - \lambda_i \begin{bmatrix} 0 & 0 \\ 0 & \tilde{M} \end{bmatrix}^j \right) \begin{Bmatrix} \frac{\partial H_i}{\partial V_k} \\ \frac{\partial X_i}{\partial V_k} \end{Bmatrix}^j$$

$$= \left(\frac{\partial \lambda_i}{\partial V_k} \begin{bmatrix} 0 & 0 \\ 0 & \tilde{M} \end{bmatrix}^j + \lambda_i \begin{bmatrix} 0 & 0 \\ 0 & \frac{\partial \tilde{M}}{\partial V_k} \end{bmatrix}^j - \begin{bmatrix} -\frac{\partial F}{\partial V_k} & 0 \\ 0 & 0 \end{bmatrix}^j \right) \begin{Bmatrix} H_i \\ X_i \end{Bmatrix}^j \qquad (39)$$

The solution of the upper partition of (39) for the derivative of the stress parameters, again on the element level, and the solution of the upper partition of (36) for the stress parameters can be used to eliminate all stress quantities from the lower partition of (39). The assembled global equations then take the form

$$([\tilde{K}] - \lambda_i [\tilde{M}]) \frac{\partial \{X_i\}}{\partial V_k}$$

$$= \left(\frac{\partial \lambda_i}{\partial V_k} [\tilde{M}] + \lambda_i \frac{\partial [\tilde{M}]}{\partial V_k} + \frac{\partial [\tilde{K}]}{\partial V_k} \right) \{X_i\} \qquad (40)$$

where

$$\frac{\partial [\tilde{K}]}{\partial V_k} = \sum_{j=1}^{L} [S^j]^T [F^j]^{-1} \frac{\partial [F^j]}{\partial V_k} [F^j]^{-1} [S^j]$$

The right hand side vector contains the derivative of the flexibility matrix as desired. Equation (40) is in the general form of equation (3) and can be solved by any of the several methods developed for calculating eigenvalue and eigenvector derivatives.

3.4 Reduction Methods

The basic idea behind the use of reduction methods in conjunction with mixed models is to define a small number of parameters related to both the displacement and stress degrees of freedom of the full model and reduce the equations to these coordinates. This is accomplished by defining a basis vector representing each reduced coordinate. The stresses and displacements are then approximated as a linear combination of the linearly independent basis vectors. In partitioned matrix format this approximation is

$$\begin{Bmatrix} H \\ U \end{Bmatrix} \simeq \begin{Bmatrix} \bar{H} \\ \bar{U} \end{Bmatrix} = \begin{bmatrix} \Gamma_H \\ \Gamma_X \end{bmatrix} \{\phi\} \qquad (41)$$

where $[\Gamma_H]$ and $[\Gamma_X]$ are matrices with the stress and displacement basis vectors as columns, respectively, and $\{\phi\}$ are the reduced unknowns. A major advantage of the mixed model is the direct approximation of the stresses.

The basis vectors are determined in a two-step procedure. The displacement basis vectors $[\Gamma_X]$ are determined first by one of the methods used in section two. In static condensation, some of the displacement degrees of freedom are assumed massless and eliminated (see section 2.3.1). For the mixed model this leads to the following basis vectors:

$$[\Gamma_X] = \begin{bmatrix} [I] \\ -[\tilde{K}^{cc}]^{-1}[\tilde{K}^{cf}] \end{bmatrix} \tag{42}$$

where

$$[\tilde{K}] = \begin{bmatrix} \tilde{K}^{ff} & \tilde{K}^{fc} \\ \tilde{K}^{cf} & \tilde{K}^{cc} \end{bmatrix}$$

is a partitioned form of the stiffness matrix defined in equation (37). The superscript f denotes degrees of freedom with mass and the superscript c those without.

Generalized dynamic reduction can also be used to determine the displacement basis vectors (see section 2.3.2). Initial iteration vectors are chosen arbitrarily and placed as columns in the matrix $[Z]^{(0)}$. A required number of iterations is performed through the recursion relations

$$([\tilde{K}] - \nu [\tilde{M}]) [\bar{Z}]^{(r+1)} = [\tilde{M}] [Z]^{(r)} \tag{43a}$$

where

$$[Z]^{(r)} = [\{Z_1\} \{Z_2\} \dots \{Z_n\}]^{(r)} \tag{43b}$$

and

$$\{Z_i\}^{(r+1)} = \beta_i^{(r+1)} \{\bar{Z}_i\}^{(r+1)} \tag{43c}$$

where the matrices $[\tilde{K}]$ and $[\tilde{M}]$ are defined in equations (34) and (37) and $\beta_i^{(r+1)}$ is used to normalize $\{\bar{Z}_i\}^{(r+1)}$. The final iterates are orthonormalized to form a linearly independent set.

The second step is the determination of the stress basis vectors. As mentioned previously, for efficiency the matrices [F] and [S] in equation (34) are only calculated at the element level and never assembled globally except for an element by element contribution to the stiffness matrix as defined in equation (37). For this reason the stress basis vectors are also calculated only at the element level. The stress and displacement degrees of freedom in the jth element are related by the equation

$$[F^j] \{H^j\} = [S^j] \{U^j\} \tag{44}$$

Using the approximation given in equation (41) the above relation can be solved for the stress basis vectors to yield

$$[\Gamma_H^j] = [F^j]^{-1}[S^j][\Gamma_X^j] \tag{45}$$

where $[\Gamma_X^j]$ is a matrix containing the rows of $[\Gamma_X]$ corresponding to the displacement degrees of freedom of the jth element.

Equation (41) is substituted into the discretized functional (equation(33)) and the resulting Rayleigh-Ritz analysis leads to the reduced equations

$$([\bar{K}] - \bar{\lambda}_i [\bar{M}])\{\psi_i\} = 0 \tag{46}$$

The reduced matrices are given by

$$[\bar{K}] = \sum_{j=1}^{L} [\Gamma_H^j]^T[F^j][\Gamma_H^j] + [\Gamma_H^j]^T[S^j][\Gamma_X^j] + [\Gamma_X^j]^T[S^j]^T[\Gamma_H^j]$$
$$= \text{reduced stiffness matrix} \tag{47}$$

$$[\bar{M}] = [\Gamma_X]^T[\tilde{M}][\Gamma_X] = \text{reduced mass matrix} \tag{48}$$

where $[F^j]$, $[S^j]$ and $[\tilde{M}]$ are defined in equations (34) and (37) and it is noted that $[\bar{K}]$ is formed from element contributions. Also, for free vibration, the reduced unknowns $\{\phi\}$ are assumed to be of the form

$$\{\phi(\Gamma,t)\} = e^{i\sqrt{\bar{\lambda}}t}\{\psi(\Gamma,\lambda)\} \tag{49}$$

The reduced equation for the eigenvalues and eigenvectors (46) looks very similar to the reduced equation (17) from the displacement formulation with the exception of the reduced stiffness matrix which has a very different form.

A reduced equation for the derivative of the eigenvalues and eigenvectors can be developed by differentiating the reduced equation (46) with respect to an independent design variable V_k, resulting in the following:

$$([\bar{K}] - \lambda_i[\bar{M}])\left\{\frac{\partial\psi_i}{\partial V_k}\right\}$$
$$= \left(\frac{\partial\lambda_i}{\partial V_k}[\bar{M}] + \lambda_i[\Gamma_X]^T\frac{\partial[\tilde{M}]}{\partial V_k}[\Gamma_X] + \frac{\partial[\bar{K}]}{\partial V_k}\right)\{\psi_i\} \tag{50}$$

where

$$\frac{\partial[\bar{K}]}{\partial V_k} = \sum_{j=1}^{L} [\Gamma_H^j]^T\frac{\partial[F]}{\partial V_k}[\Gamma_H^j]$$

The basis vectors in equation (42) are assumed to be invariant with respect to the design variable which, as discussed previously, is necessary to

obtain the desired efficiency. The advantage of this formulation over the displacement formulation results from the use of the derivatives of the flexibility coefficients on the right hand side (as opposed to the derivatives of the stiffness coefficients in (24)). Equations (46) and (50) can be solved by any of the methods described previously, and the eigenvector derivatives recovered from the relation

$$\begin{Bmatrix} \frac{\partial H_i}{\partial V_k} \\ \frac{\partial X_i}{\partial V_k} \end{Bmatrix} \simeq \begin{Bmatrix} \frac{\partial \bar{H}_i}{\partial V_k} \\ \frac{\partial \bar{X}_i}{\partial V_k} \end{Bmatrix} = \begin{bmatrix} \Gamma_H \\ \Gamma_X \end{bmatrix} \begin{Bmatrix} \frac{\partial \psi_i}{\partial V_k} \end{Bmatrix} \tag{51}$$

Numerical results obtained by using the mixed formulation are discussed in section five and compared with those from the displacement formulation.

IV. ACCURACY AND ITERATIVE REFINEMENT

4.1 Introduction

Methods for calculating the derivatives of eigenvalues and eigenvectors from reduced equations are developed in the preceding two sections. The usefulness of the proposed procedure requires the ability to assess the accuracy of the eigenvector derivatives and a method for improving the accuracy of the derivatives that do not meet the required tolerance. In order to accomplish these two objectives it is necessary to return to the full equations. Two methods are presented that use iterative techniques involving a shifted stiffness matrix to improve the eigenvector derivatives. As a by-product of the performance of generalized dynamic reduction this shifted stiffness matrix is decomposed and as such, the implementation of these methods adds minimal computational expense.

4.2 Solution Errors

A key element of approximate solution methods is the ability to evaluate the accuracy of the approximate solution without knowing the exact solution. In the present study this is accomplished by calculating a normalized residual error from the full equations. For example, the accuracy of the approximate eigenvalues and eigenvectors is evaluated using the following error norm [13]:

$$\varepsilon_1 = \frac{\| ([K] - \bar{\lambda}[M])\{\bar{X}\} \|_2}{\| [K]\{\bar{X}\} \|_2} \tag{52}$$

The numerator is the Euclidean norm of the residual vector from equation (1a) and the denominator is a normalization factor (the norm of the internal force vector). Although this does not provide a pointwise error measure, it does gives a good indication of the overall accuracy. Similarly, the accuracy of the derivatives of the eigenvalues and eigenvectors can be evaluated using the following norm:

$$\varepsilon_2 = \frac{\left\| ([K] - \bar{\lambda}[M]) \frac{\partial\{\bar{X}\}}{\partial V} - \left(\frac{\partial\bar{\lambda}}{\partial V}[M] + \bar{\lambda}\frac{\partial[M]}{\partial V} - \frac{\partial[K]}{\partial V}\right)\{\bar{X}\} \right\|_2}{\left\| \left(\frac{\partial\bar{\lambda}}{\partial V}[M] + \bar{\lambda}\frac{\partial[M]}{\partial V} - \frac{\partial[K]}{\partial V}\right)\{\bar{X}\} \right\|_2} \tag{53}$$

The numerator is the norm of the residual from equation (3) and the denominator is the norm of the right hand side. If either of the error tolerances, ε_1 or ε_2 is not met then the corresponding approximate solution must be improved.

4.3 Improvement of the Eigensolution

The error norm ε_1 gives an indication of the accuracy of an eigenvalue and its corresponding eigenvector. If the required tolerance is not met then two possibilities are considered for improving the accuracy. The first is to improve the characterization of the reduced basis and solve for a new eigensolution (this results in increased accuracy for all the eigenmodes) or alternately, the particular eigenmodes not meeting the tolerance can be individually improved. When using static condensation, the former approach essentially involves starting over but with the benefit of additional knowledge. Improving the basis requires including the mass associated with more and/or different degrees of freedom. The approximate eigenvectors from the previous attempt are useful in this choice. In contradistinction, generalized dynamic reduction is much more amenable to improvement. The characterization of the reduced basis is augmented by performing more iterations on the existing basis vectors (or on the approximate eigenvectors) and also with additional vectors. In either case none of the information in the current basis is discarded. In addition, if only a few of the modes are found to be inaccurate, they alone are improved by cycling through the relations

$$([K] - \nu[M])\ \{\bar{X}\}^{(k+1)} = [M]\ \{\bar{X}\}^{(k)} \tag{54}$$

$$\lambda^{(k+1)} = \{\bar{X}\}^{(k+1)^T}[K]\{\bar{X}\}^{(k+1)} / \{\bar{X}\}^{(k+1)^T}[M]\{\bar{X}\}^{(k+1)} \tag{55}$$

which represent the inverse power method. Since the coefficient matrix in (54) has been decomposed previously, these procedures add little computational expense. The previous discussion brings forth some of the advantages of generalized dynamic reduction over static condensation. Due to its adaptability to the type of analysis being performed only generalized dynamic reduction is considered in the remainder of this section.

Before turning to methods for improving the accuracy of the derivatives of the eigenvectors it is useful to identify the major time consuming operations in the calculation of the eigensolution. The largest percentage results from the decomposition of the shifted stiffness matrix used in the generation of the basis vectors. Two other items that account for a large percentage of the computer time are the back substitutions performed in the generation of the basis vectors (equation (22a)) and the formation of the reduced matrices (equation (17)). Also, the back substitutions and formation of new reduced matrices required for augmenting the basis, or the back substitutions required to improve individual eigenmodes can represent significant contributions.

4.4 Improvement of the Eigenvector Derivatives

The eigenvalue and eigenvector derivatives are calculated from the reduced equations (24) to (29). Since the reduced basis is developed for representing the eigenvectors (and not their derivatives) and also since the reduced eigenvectors may not be accurate (the accuracy of the full eigenvector may have been improved), the eigenvector derivatives generally require some improvement. As discussed previously, one option would be to increase the characterization of the reduced basis. However, for the

eigenvector derivatives this is not considered viable for the following reasons:

1. The reduced eigenvalues and eigenvectors have to be recalculated.
2. In addition to reforming the reduced stiffness and mass matrices the derivatives of these matrices must also be calculated.
3. Adding more vectors to the reduced basis increases the size of the reduced equations and the cost of obtaining their solution.
4. The methods discussed previously for augmenting the reduced basis would not necessarily result in improved eigenvector derivatives.

Two methods for improving the accuracy of the eigenvector derivatives are presented subsequently.

4.4.1 Method Based on the Inverse Power Method

The well known inverse power method for the generalized eigenproblem is given by the recursion relations

$$([K] - \nu[M])\{X_i\}^{(j+1)} = (\lambda_i^{(j)} - \nu)[M]\{X_i\}^{(j)} \tag{56}$$

$$\lambda_i^{(j)} = 1 \Big/ \left(\{X_i\}^{(j)^T}[M]\{X_i\}^{(j)}\right)^{1/2} \tag{57}$$

which results in the convergence of λ_i to the eigenvalue closest in magnitude to the shift parameter ν and $\{X_i\}$ to the corresponding eigenvector. In the present study the eigenvalues and eigenvectors are already known to a required level of accuracy and iterations through equations (56) and (57) would result in very small changes. Noting this, equation (56) is differentiated with respect to an independent design variable V_k and the superscripts on the eigenvalue, eigenvector and eigenvalue derivative (but not the derivative of the eigenvector) indicating the iteration are discarded. The resulting recursion relation is

$$([K] - \nu[M])\frac{\partial\{X_i\}^{(j+1)}}{\partial V_k} = \left(\frac{\partial\lambda_i}{\partial V_k}[M] + \lambda_i\frac{\partial[M]}{\partial V_k} - \frac{\partial[K]}{\partial V_k}\right)\{X_i\} + (\lambda_i-\nu)[M]\frac{\partial\{X_i\}^{(j)}}{\partial V_k} \tag{58}$$

If the full eigenvector was improved by iteration through equation (54) it is important that the derivative of the eigenvalue be calculated from the full equation (5) instead of the reduced equation (27) since the reduced eigenvector is less accurate.

A major advantage for the procedure defined by equation (58) is that an existing decomposed coefficient matrix is used to avoid the cost of additional decompositions. This suggests an alternate development of equation (58). Returning to the full equation for calculating the

eigenvector derivatives (3a) it is noted that there is only a small difference between the matrix on the left-hand side $([K]-\lambda_i[M])$ and the existing decomposed matrix $([K]-\nu[M])$. The matrix on the left hand side can be split resulting in

$$([K] - \nu[M])\frac{\partial\{X_i\}}{\partial V_k} - (\lambda_i-\nu)[M]\frac{\partial\{X_i\}}{\partial V_k} = \left(\frac{\partial\lambda_i}{\partial V_k}[M] + \lambda_i\frac{\partial[M]}{\partial V_k} - \frac{\partial[K]}{\partial V_k}\right)\{X_i\} \qquad (59)$$

The second term on the left-hand side of (59) is then moved to the right-hand side. Using the current estimate for the eigenvector derivative, the right-hand side is evaluated and the equation solved for a new estimate of the eigenvector derivative. This relation is identical to that given by equation (58) and offers further insight into the procedure.

4.4.2 Method Using Preconditioned Conjugate Gradient Iteration

The preconditioned conjugate gradient (PCG) method for solving symmetric positive definite linear systems has been studied for many years [26,27]. In solving the system of equations

$$[A]\{X\} = \{B\} \qquad (60)$$

the PCG method attempts to accelerate the convergence of the iterative process by choosing a preconditioning matrix $[A]_o$ such that

$$[A] = [A]_o - [\bar{A}] \qquad (61)$$

The matrix $[\bar{A}]$ is the difference between the coefficient matrix $[A]$ and the preconditioning matrix $[A]_o$. At each iteration a system of equations with coefficient matrix $[A]_o$ must be solved, so $[A]_o$ should be chosen such that this system is easy to solve. In addition, the matrix $[A]_o$ should be chosen to in some way approximate $[A]$. In the present study, the splitting shown in (61) is motivated by the existence of a previously decomposed matrix.

The objective of the PCG iteration is to solve equation (3a) for the derivative of the eigenvector using the approximate result obtained from equation (24) as an initial estimate. The selection of the preconditioning matrix $([K]-\nu[M])$ as an existing decomposed matrix, results in the splitting

$$([K]-\lambda_i[M]) = ([K]-\nu[M]) - (\lambda_i-\nu)[M]$$

The PCG algorithm as presented in [28] is as follows:

1. The initial estimate $\frac{\partial\{\bar{X}_i\}^{(0)}}{\partial V_k}$ is obtained using the reduction technique.

2. For $j = 0, 1, 2, \ldots$ compute the residual

$$\{R\}^{(j)} = \{R\}^{(j-1)} - a_{j-1}([K]-\lambda_i[M])\{Z\}^{(j-1)}, \quad j \geq 1,$$

$$= \left(\frac{\partial\bar{\lambda}_i}{\partial V_k}[M] + \lambda_i\frac{\partial[M]}{\partial V_k} - \frac{\partial[K]}{\partial V_k}\right)\{\bar{X}_i\}$$

$$- ([K]-\lambda_i[M])\frac{\partial\{X_i\}^{(0)}}{\partial V_k}, \quad j = 0 \tag{62}$$

3. Solve for the preconditioned residual $\{Y\}^{(j)}$:

$$([K]-\nu[M])\{Y\}^{(j)} = \{R\}^{(j)} \tag{63}$$

4. Compute the orthogonalization coefficient, b_j, using

$$b_j = \{Y\}^{(j)^T}([K]-\nu[M])\{Y\}^{(j)} / \{Y\}^{(j-1)^T}([K]-\nu[M])\{Y\}^{(j-1)}, \quad j \geq 1,$$

$$= 0, \quad j = 0 \tag{64}$$

5. Update the conjugate search direction vector

$$\{Z\}^{(j)} = \{Y\}^{(j)} + b_j\{Z\}^{(j-1)} \tag{65}$$

6. Compute the step length along the search direction, a_j, using

$$a_j = \{Y\}^{(j)^T}([K]-\nu[M])\{Y\}^{(j)} / \{Z\}^{(j)^T}([K]-\lambda_i[M])\{Z\}^{(j)} \tag{66}$$

7. Update the solution

$$\frac{\partial\{\bar{X}_i\}^{(j+1)}}{\partial V_k} = \frac{\partial\{\bar{X}_i\}^{(j)}}{\partial V_k} + a_j\{Z\}^{(j)} \tag{67}$$

Even though the PCG method is intended for solving positive definite systems and the present equations are singular, the nonsingularity of the preconditioning matrix allows the implementation of the procedure. The effectiveness of this algorithm is discussed in the succeeding section.

V. NUMERICAL STUDIES

5.1 General

This section describes the implementation of numerical algorithms for calculating free vibration sensitivity derivatives from reduced finite element equations. Their performance compared to the exact solution is described subsequently. Henceforth, the term "exact solution" is used to denote the solution obtained using the full system of equations of the structure.

The structures considered in this study are composed of beam elements. The following three structures are considered:

1. A non-symmetric triangular double-laced lattice beam ten bays in length, supported at one end (Figure (1)).
2. An elastic line model of the Bell AH-1G Cobra helicopter (Figure (2)).
3. An orthogonal tetrahedral lattice beam ten bays in length, supported at one end. The dimensions of each bay correspond to the current design of the keel beam of NASA's space station (Figure (3)).

A simple program was written for modelling frame type structures using both displacement and mixed finite elements. The program was checked by comparing the free vibration results with those from the commercial finite element code EAL for the lattice beams and NASTRAN for the Cobra elastic line model. The primary motivation for developing this specialized code was to include the capability of assembling matrices of the derivatives of stiffness and mass coefficients of the structure and also to include mixed finite element models. Both of these tasks are not easy to implement in commercial finite element codes.

The first structure considered, the triangular lattice beam, was developed as a test bed to provide a quick means of evaluating the algorithms presented. The cross-section is non-symmetric to further simplify the problem by eliminating repeated eigenmodes. The design variables are chosen to be the cross-sectional area (axial stiffness) and moment of inertia (bending and torsional stiffness) of the longerons in the last bay (next to the support, numbered 1, 2 and 3 in Figure(1)).

The two additional cases represent more practical problems. The Cobra elastic line model is a simplified representation of the actual Cobra helicopter structure that is being used for sensitivity studies [28]. In addition to beam elements it contains linear spring and rigid body elements and uses a lumped approach in modelling the mass of the structure. The design variables are shown in Figure (2) and include the stiffness of linear spring and beam elements and certain concentrated masses. The other case considered is a ten bay section extracted from the support structure of the current proposed configuration of the NASA space station. The design variables are very similar to those chosen for the triangular lattice.

5.2 Comparisons of the Exact and Approximate Vectors

In comparing vectors obtained from the reduction method (eigenvectors and their derivatives) to those obtained from the solution of the full equations the following error norm is used [14]:

$$\varepsilon = \frac{1}{N} \sum_{i=1}^{N} [(X_i - \bar{X}_i) / |X_{max}|]^2 \qquad (68)$$

$\{X\}$ is the exact vector and $\{\bar{X}\}$ is the vector obtained from the reduction method. $|X_{max}|$ is the maximum absolute value of the exact vector and N is the number of components. This norm is similar to the r.m.s. error norm but is weighted to give less importance to the smaller components of $\{X\}$ which are usually of less practical importance.

It is important to distinguish between the norm presented here using the exact solution and the one presented in the previous section using a residual from the full equations. Experience in this study has shown that values for the exact error norm of 0.001 or less indicates an accurate approximate vector. This corresponds to an error for the largest component of a few percent or less. Values for the residual error norm of 0.1 or less show a similar accuracy. On the other hand, values for the exact error norm of 0.01 or greater indicate that the approximate vector shows very little resemblance to the exact. For the residual error norm values of 1.0 or greater indicate poor accuracy.

In addition to the error norms, portions of the exact and approximate vectors are plotted. The components and nodes for which the vectors are plotted are chosen by examining the eigenvectors for the largest displacement and rotation. These plots provide a better physical indication of the accuracy of the vectors.

5.3 Verification of the Results

To insure the reliability of the presented results they are checked by independent programs using finite difference operators to evaluate the derivatives. For the full equations, eigensolutions are calculated for a positive and negative perturbation of each design variable from the equations

$$([K]^{(V\pm\Delta V)} - \lambda_i^{(V\pm\Delta V)}[M]^{(V\pm\Delta V)})\ \{X_i\}^{(V\pm\Delta V)} = 0 \qquad (69)$$

where the superscript $(V\pm\Delta V)$ indicates the positive and negative perturbation respectively. The eigenvalue and eigenvector derivatives are then calculated from the first order central difference formulae:

$$\frac{\partial \lambda_i}{\partial V} \simeq \frac{\lambda_i^{(V+\Delta V)} - \lambda_i^{(V-\Delta V)}}{2\Delta V} \qquad (70)$$

$$\frac{\partial \{X_i\}}{\partial V} \simeq \frac{\{X_i\}^{(V+\Delta V)} - \{X_i\}^{(V-\Delta V)}}{2\Delta V} \qquad (71)$$

In the development of the reduced equations it is assumed that the basis vectors are invariant with respect to the design variables. Thus in the finite difference approximations the basis vectors are determined for the unperturbed structure and used to reduce the perturbed equations resulting in

$$[\bar{K}]^{(V\pm\Delta V)} = [\Gamma]^{(V)^T}[K]^{(V\pm\Delta V)}[\Gamma]^{(V)} \tag{72a}$$

$$[\bar{M}]^{(V\pm\Delta V)} = [\Gamma]^{(V)^T}[M]^{(V\pm\Delta V)}[\Gamma]^{(V)} \tag{72b}$$

and

$$([\bar{K}]^{(V\pm\Delta V)} - \bar{\lambda}_i^{(V\pm\Delta V)}[\bar{M}]^{(V\pm\Delta V)})\ \{\psi_i\}^{(V\pm\Delta V)} \tag{73}$$

The approximate derivatives are then calculated from the relations

$$\frac{\partial\bar{\lambda}_i}{\partial V} \simeq \frac{\bar{\lambda}_i^{(V+\Delta V)} - \bar{\lambda}_i^{(V-\Delta V)}}{2\Delta V} \tag{74}$$

$$\frac{\partial\{\bar{X}_i\}}{\partial V} \simeq [\Gamma]^{(V)}\ \frac{\{\psi_i\}^{(V+\Delta V)} - \{\psi_i\}^{(V-\Delta V)}}{2\Delta V} \tag{75}$$

In all cases very close agreement was found between the analytic and finite difference results.

5.4 Accuracy of the Derivatives Predicted by the Reduction Methods

In the present study both static condensation and generalized dynamic reduction are investigated as a means to reduce the governing equations for the displacement model of the triangular lattice beam. The results for the lowest eight vibration modes are presented in Tables (1) and (2) and the first four eigenvectors and their derivatives are plotted in Figure (4).

In the application of static condensation to the triangular lattice beam, 36 out of the total 180 degrees of freedom are retained in the analysis. These correspond to the six degrees of freedom at each of the three nodes on the first and third cross-sections of the beam, numbered sequentially from the free end. Only the lowest two eigenvalues and their corresponding eigenvectors are reasonably accurate. For higher modes the accuracy of the eigensolution falls off very rapidly. The derivatives of the eigenvalues are less accurate than the eigenvalues themselves, but are within ten percent of the exact value. Unfortunately, the derivatives of the eigenvectors show very little or no resemblance to the exact solution, even for the lowest two modes.

With generalized dynamic reduction a much higher degree of reduction is possible. Several choices for the number of basis vectors and iterations were tried and the results indicated that accurate modes could be obtained with as few as six basis vectors. Attempts at using a larger number of vectors resulted in slightly more accurate eigensolutions but had little effect on the accuracy of the eigenvector derivatives. The cost of reducing and solving the reduced equations increases rapidly with the number of basis vectors so it is generally more efficient to use the smallest number of basis vectors possible. Although fewer modes are obtained from the reduced set of equations and more shifts are required, it is still generally more efficient.

The results shown in Figure (4) and Tables (1) and (2) are obtained by using six basis vectors that are generated with four iterations on the initial random vectors. In each reduction the lowest four of the calculated modes are retained. The shift value is initially chosen to be zero and

calculated from the estimates of the higher eigenvalues on subsequent reductions. Although only the first eight modes are shown, the first twelve were calculated accurately. Even with such a high degree of reduction, the eigensolution is obtained much more accurately than with static condensation. The accuracy of the eigenvalue derivatives is also considerably better although they are still less accurate than the eigenvalues. The eigenvector derivatives in some cases resemble the exact results but for the most part, the reduced basis does not adequately characterize the eigenvector derivatives.

5.5 Implementation of the Mixed Method

In the previous section the triangular lattice is modelled with a displacement beam element. This section investigates the modelling of an identical structure with a mixed beam element. The element has 3 displacement nodes and 2 stress nodes resulting in quadratic approximation of the displacement field and linear approximation of the stresses. In contradistinction, the displacement element has two nodes and uses interpolation functions developed from classical beam theory that result in quadratic approximations for the axial displacements and cubic approximations for the bending displacements [30]. Also, the mixed element includes shear deformation and the displacement element does not. The results for the lowest four modes of the mixed model are presented in Table (3) and Figure (5). Comparing these with those obtained for the displacement model it is seen that the full equations yield almost identical results.

The full mixed model contains 900 displacement and 240 stress degrees of freedom. Through the use of generalized dynamic reduction the total number of degrees of freedom is reduced to just 6. Again comparing the results from the two formulations it is seen that the reduced mixed model does not provide quite as accurate results as the reduced displacement model of the previous section (reduced from 180 to 6 degrees of freedom) but this is probably due to the large difference in the number of degrees of freedom. However, the results are very similar in that the eigensolution and the eigenvalue derivatives are determined fairly accurately but the eigenvector derivatives are not. It is apparent from both the displacement and mixed models that some type of improvement is necessary for the eigenvector derivatives obtained from the reduction method.

The advantages of this method result from the simplified form of the governing equations. As discussed in a preceding section, this simplifies the calculation of the derivatives of the stiffness matrix when the design variables are the inverse of a cross-sectional area or moment of inertia. Also, shear deformation can be included in the formulation very easily. This study shows that the mixed model is capable of providing the same results as the displacement model.

5.6 Iterative Refinement of Eigenvector Derivatives

Two algorithms are implemented for improving the accuracy of the eigenvector derivatives that were obtained using generalized dynamic reduction on the displacement model of the triangular lattice beam. These algorithms are presented in the preceding section. The first method is based on the inverse power method and will be referred to as IPM while the

second uses a preconditioned conjugate gradient algorithm and will be referred to as PCG.

In the present implementation the IPM or PCG iterations can be terminated by three separate criteria. A maximum of two iterations is allowed, but if the residual error norm for the vector drops below 0.1 or is greater than on the previous iteration the procedure terminates. The results of using IPM and PCG iteration are shown in Tables (4) and (5) respectively for the lowest eight modes. For both IPM and PCG, the results are plotted in Figure (6). It is seen from these results that one iteration with either method in most cases provides a dramatic improvement in the accuracy of the approximate vector. In some cases a second iteration is required to meet the convergence tolerance but in a few of these cases the second iteration diverges (Table (5), PCG iteration, derivative of eigenvectors 6-8 with respect to V_2; also, not shown, IPM iteration, derivative of eigenvector 12 with respect to V_2). This may be a result of the near singularity of the matrix on the left-hand side of the governing equations. Further investigation with more iterations shows an oscillatory behavior for all the derivatives but this does not usually occur in the first two iterations. It is observed to occur after fewer iterations for cases in which the approximate eigensolution is not quite as accurate, but occurs for all modes after several iterations. Although the cases for which oscillation occurs on the second iteration do not quite meet the convergence tolerance, examination of the plots in Figure (6) show that the approximate vectors are reasonably accurate.

From the examination of Tables (4) and (5), it appears that the IPM iterations are slightly more effective at improving the accuracy of the eigenvector derivatives than PCG, since it generally leads to smaller values of the error norm. However, the plots of the vector shown in Figure (6) show the difference to be insignificant. In terms of efficiency, PCG has an advantage since the residual needed for the convergence check is a by-product, whereas in IPM iteration it must be calculated separately.

A topic of primary interest is the efficiency of the reduction method as compared to the solution of the full system of equations. The programs used in the current implementation are not optimized sufficiently to make a comparison of execution times meaningful. Also, the structures investigated are smaller than the intended application due to the central storage limitation (130560 words) of the CYBER 175 computer used in the analysis. In order to assess the efficiency, an accounting of operations is performed. The comparison is made between the solution of the full system of equations by Nelson's method (equations (5)-(7)) and the solution of the reduced equations with subsequent iterative refinement (1 iteration) by the PCG method. With two major exceptions, the operations required in both cases are almost identical. The exceptions are the decomposition of a coefficient matrix for each eigenvalue in the solution of the full equations and the reduction of the derivatives of the stiffness and mass matrices to obtain the reduced equations. Both of these have no counterpart in the other method. Considering the usual sparsity of the derivatives of the mass and stiffness matrices, the latter is usually much less time consuming. Since the decompositions usually account for a large percentage of the computer time the reduction method can result in significant savings. However, if the design variables affect large portions of the structure or there are an unusually large number of design variables, the solution of the full equations may be more attractive.

5.7 AH-1G Cobra Elastic Line Model

The Cobra elastic line model (developed by Hanson and Murthy [29]) is a very coarse representation of the actual helicopter structure as shown in Figure (2). The displacement model contains 336 degrees of freedom before the inclusion of rigid body elements and the application of boundary conditions. The rigid body elements reduce the number to 252 and the boundary conditions (chosen to eliminate the rigid body modes) further reduce the number to 246.

The lowest eight vibration modes (shown in Figure (7)) can be divided into groups according to the portion of the helicopter to which they correspond. Modes 1 and 2 represent rocking of the main rotor pylon assembly; 3, 4, 7 and 8 correspond to modes of the aft fuselage, tailboom and vertical fin; and modes 5 and 6 to the front fuselage section. Two design variables are defined within each of these sections and are marked by circled number in Figure (2). For the main rotor pylon the design variables are the stiffness of the springs supporting the pylon in the vertical direction (①) and the bending stiffness of the upper section of the rotor mast (②). For the aft fuselage modes the bending stiffness of a small section is chosen as one design variable (③) and the mass of the tail rotor as the other (④). Likewise for the front fuselage the bending stiffness of one element is chosen as a design variable (⑤) and also the mass of the gun turret (⑥).

The results obtained from the full equations (exact) and using generalized dynamic reduction with 12 basis vectors are presented in Figure (7) and Table (6). The basis vectors are obtained by performing 4 iterations on 6 random and 6 unit vectors. The unit vectors contain a single unit component in one of the locations corresponding to the masses of the main and tail rotors. This ensures that these masses are excited and improves the accuracy of the associated vibration modes. The results show that this provides good accuracy for the eigensolutions.

In examining the accuracy of the eigenvalue derivatives some very large errors are discovered, however these correspond to modes that are effectively invariant with respect to the particular design variable. Since the reduction method does find the eigenvalue derivatives to be relatively small, these large errors do not pose a problem. For efficiency logic should be included in the program to avoid computation of the associated eigenvector derivatives.

The eigenvalue derivatives of importance are predicted accurately. In addition, a few of the eigenvector derivatives are also reasonably accurate, but the majority are not. The application of PCG iteration proved very effective at obtaining accurate eigenvector derivatives.

5.8 Orthogonal Tetrahedral Lattice Beam

In addition to the previously presented triangular lattice that represents a specialized problem, it is desired to present a repetitive beam-like lattice structure with some practical significance. The keel beam of the proposed NASA space station consists of several orthogonal tetrahedral lattice beams (see Figure (3)) and for this study a ten bay length is investigated.

The beam is modelled with a displacement element and contains 240 degrees of freedom. The model is reduced using generalized dynamic reduction with eight basis vectors. For the initial reduction (shift = 0.0)

the basis vectors are obtained by performing 4 iterations on eight random vectors and the lowest two eigenmodes are retained. On subsequent reductions 6 iterations are performed on the random vectors and two modes are retained. The results for the first eight modes are presented in Figure (8) and Table (7). It is observed that for both the present case and the triangular lattice, the minimum number of basis vector required is 1/30th the total number of degrees of freedom, however the present case requires more iterations and yields a smaller number of accurate modes per reduction. The first twelve modes were calculated accurately. It is suspected that more could be calculated, however this was not attempted.

The derivatives of the eigenvalues are obtained accurately from the reduction method and PCG iteration is used to improve the eigenvector derivatives. Using the same termination criteria discussed previously, no cases are present in which the solution diverges in the first two iterations. The PCG method again demonstrates good effectiveness at improving the accuracy and in most cases only one iteration is required. However, comparing the error norms in Table (7) with the plots in Figure (8), one peculiarity is discovered. For the derivative of eigenvector 3 with respect to V_2 the exact error norm is 0.0016 after PCG iteration which indicates a reasonably accurate vector. The plot of the vector shows good agreement for the rotations but poor agreement for the displacements. This is most likely due to the difference in the size of the components (approximately two orders of magnitude) and brings out a small weakness of the procedure. In examining the remainder of the results a few more cases are discovered in which the smaller terms are not calculated accurately. However, in many practical applications these components are of little importance.

VI. CONCLUSIONS AND RECOMMENDATIONS

6.1 Summary

In the present study computational procedures are presented for calculating the sensitivity derivatives of the vibration frequencies and eigenmodes of framed structures. The procedures incorporate two key elements. The first is the use of dynamic reduction techniques to substantially reduce the number of degrees of freedom. The reduction techniques considered are static condensation (Guyan's reduction) and a generalized dynamic reduction technique. The second key element is the application of iterative techniques to improve the accuracy of the derivatives of the eigenmodes. The two procedures presented are based on the inverse power method and the preconditioned conjugate gradient technique.

Numerical studies are performed on three frame type structures using displacement and mixed finite element models. Error norms are introduced to assess the accuracy of the eigenvalue and eigenvector derivatives obtained by the reduction techniques.

6.2 Conclusions

On the basis of the numerical studies performed in this report the following conclusions seem to be justified:

1) In the structures considered, generalized dynamic reduction allowed the reduction of the equations to a small number of degrees of freedom and provided a decomposed coefficient matrix useful in improving the accuracy of the eigenvector derivatives. Static condensation was sensitive to the choice of the free degrees of freedom. Neither method was capable of reliably predicting the derivatives of the eigenvectors.

2) The mixed and displacement models used in the present study resulted in eigensolutions and their derivatives that were in very close agreement. Also, similar accuracy was obtained from the reduced models in both formulations. The advantage of the mixed formulation results from the simplified calculation of the derivatives of the stiffness matrix with respect to design variables that are the inverse of sizing quantities. Also, the simple form of the governing equations allows shear deformation to be included easily.

3) Both the exact and residual vector error norms provide a good indication of the accuracy of the approximate vectors. A good correlation was observed between the two norms, the error of the largest component and the plots of the vectors.

4) Both the PCG and IPM procedures for improving the accuracy of the approximate eigenvector derivatives proved very effective. In most cases one iteration was sufficient to obtain very accurate results. The efficiency of these procedures compared with other solution methods using the full equations depends on several factors. For cases in which the decomposition of the coefficient matrices results

in a large percentage of the full system solution time and the derivatives of the stiffness and mass matrices are sparsely populated, significant savings can be realized.

6.3 Recommendations

The following recommendations are presented in the hope that they will provide direction for future research in the topics investigated in this study:

1) The effectiveness of the proposed procedures should be investigated for structures containing repeated or very closely spaced eigenvalues. One possible way of doing this is discussed in section two but numerical studies are not performed.

2) The procedures presented in this report should be implemented in a commercial finite element code and numerical studies performed on several very large and complex structures. The size of the structures investigated in this study was limited by the central storage capacity of 130,560 words for the CYBER 175 computer.

3) Detailed studies of the numerical behavior of the IPM and PCG procedures should be performed. The methods showed a tendency to oscillate after several iterations and the causes of this should be identified.

4) The effectiveness of using static condensation to provide starting iteration vectors for the generalized dynamic reduction should be investigated.

REFERENCES

1. Adelman, Howard M.; Haftka, Raphael T.; Camarda, Charles J.; and Walsh, Joanne L.: Structural Sensitivity Analysis: Methods, Applications and Needs. NASA TM-85827, June 1984.

2. Schmidt, L. A.: Structural Synthesis - Its Genesis and Development. AIAA Journal, Vol. 19, No. 10, pp 1249-1263, 1981.

3. Adelman, Howard M.; and Haftka, Raphael T.: Sensitivity Analysis for Discrete Structural Systems - A Survey. NASA TM-86333, December 1984.

4. MacNeal, Richard H.: The Solution of Large Structural Dynamic Problems. Proceedings, Symposium on Applications of Computer Methods in Engineering, Los Angeles, CA, August 1977, Vol. 1, pp 77-86.

5. Iott, Jocelyn; Haftka, Raphael T.; and Adelman, Howard M.: Selecting Step Sizes in Sensitivity Analysis by Finite Differences. NASA TM-86382, August 1985.

6. Fox, R. L.; and Kapoor, M. P.: Rates of Change of Eigenvalues and Eigenvectors. AIAA Journal, Vol. 6, No. 12, pp 2426-2429, 1968.

7. Nelson, Richard B.: Simplified Calculation of Eigenvector Derivatives. AIAA Journal, Vol. 14, No. 9, pp 1201-1205, 1976.

8. Sutter, Thomas R.; Camarda, Charles J.; Walsh, Joanne L.; and Adelman, Howard M.: A Comparison of Several Methods for the Calculation of Vibration Mode Shape Derivatives. Proceedings, AIAA/ASME/ASCE/AHS 27th Structures, Structural Dynamics and Materials Conference, San Antonio, TX, May 1986.

9. Rudisill, Carl S.; and Chu, Yee-Yeen: Numerical Methods for Calculating the Derivatives of Eigenvalues and Eigenvectors. AIAA Journal, Vol. 13, No. 6, pp 834-837, 1975.

10. Guyan, R. J.: Reduction of Stiffness and Mass Matrices. AIAA Journal, Vol. 3, No. 2, p 380, 1965.

11. Paz, Mario: Dynamic Reduction Methods. Structural Mechanics Software Series, Vol. V, Edited by N. Perrone and W. Pilkey,University Press of Virginia, Charlottesville, VA, 1984, pp 271-286.

12. Ojalvo, I. U.; and Newman, M.: Vibration Modes of Large Structures by an Automatic Matrix-Reduction Method. AIAA Journal, Vol. 8, No. 7, pp 1234-1239, 1970.

13. Bathe, K. J.;Finite Element Procedures in Engineering Analysis, Prentice Hall, Englewood Cliffs, NJ, 1982, pp 672-695.

14. Noor, Ahmed K.; and Lowder, Harold E.: Structural Reanalysis Via a Mixed Method. International Journal of Computers and Structures, Vol. 5, pp 9-12, 1975.

15. Noor, Ahmed K.: Multiple Configuration Analysis Via Mixed Method. Technical Note, Journal of the Structural Division, ASCE, Vol. 100, No. ST9, pp 1991-1997, September 1974.

16. Noor, Ahmed K.: Recent Advances in Reduction Methods for Nonlinear Problems. International Journal of Computers and Structures, Vol. 13, pp 31-44, 1981.

17. Ojalvo, I. U.:Efficient Computation of Mode Shape Derivatives for Large Dynamic Systems. Proceedings, AIAA/ASME/ASCE/AHS 27th Structures, Structural Dynamics and Materials Conference, San Antonio, TX, May 1986.

18. Wang, B. P.: Paper presented at the Work in Progress session, 26th AIAA/ASME/ASCE/AHS Structures, Structural Dynamics and Materials Conference, Orlando, FL, April 1985.

19. Robinson, James C.: Application of a Systematic Finite Element Model Modification Technique to Dynamic Analysis of Structures. NASA TM-83292, January 1983.

20. Kim, Ki-Ook; and Anderson, William J.: Generalized Dynamic Reduction in Finite Element Dynamic Optimization. AIAA Journal, Vol. 22, No. 11, pp 1616-1617, 1984.

21. Wang, B. P.: On Computing Eigensolution Sensitivity Data using Free Vibration Solutions. Proceedings of the Symposium on Sensitivity Analysis in Engineering, Hampton, VA, September 1986.

22. Knuth, D. E., The Art of Computer Programming, Vol. 2, Addison-Wesley, Reading, MA, 1973.

23. Noor, Ahmed K.; Peters, Jeanne M.: Mixed Models and Reduced/ Selective Integration Displacement Models for Nonlinear Analysis of Curved Beams. International Journal for Numerical Methods in Engineering, Vol. 17, pp 615-631, 1981.

24. Vanderplaats, Garret N., Numerical Optimization Techniques For Engineering Design, McGraw-Hill, New York, NY, 1984, pp 260-263.

25. Washizu, K., Variational Methods in Elasticity and Plasticity, Pergamon Press, 1974.

26. Hestenes, M. R.; and Stiefel, E.: Method of Conjugate Gradients for Solving Linear Systems. J. of Res. NBS 49, 1952, pp 409-436.

27. Concus, P.; Golub, G. H.; and O'leary, D. P.: A Generalized Conjugate Gradient Method for the Numerical Solution of Elliptical Partial Differential Equations. Proceedings of the Symposium on Sparse Matrix Computations, Academic Press, 1975, pp 309-332.

28. Greenbaum, A.: Comparison of Splittings Used with the Conjugate Gradient Algorithm. Numerische Mathematik, vol. 33, pp 181-194, 1979.

29. Murthy, T. S.: Design Sensitivity Analysis of Rotorcraft Airframe Structures for Vibration Reduction. Proceedings of the Symposium on Sensitivity Analysis in Engineering, Hampton, VA, September 1986.

30. Przemieniecki, J. S., Theory of Matrix Structural Analysis, McGraw-Hill, New York, NY, 1968.

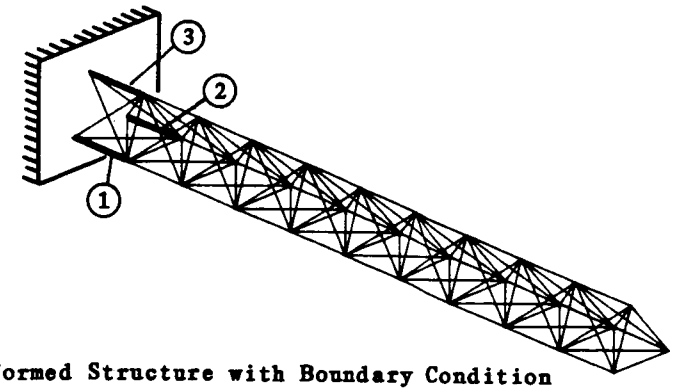

a) Undeformed Structure with Boundary Condition

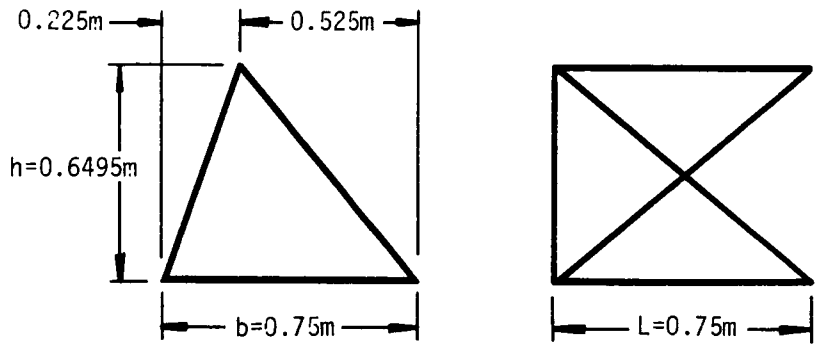

b) Repeating Module

	Cross-Sectional Area	Moment of Inertia, Axis 1	Moment of Inertia, Axis 2	Torsion Constant
Longeron	A	I_1	I_2	J
Batten	0.5A	$0.1083I_1$	$0.1083I_2$	0.1083J
Diagonal	0.5A	$0.1083I_1$	$0.1083I_2$	0.1083J

$A = 3.0 \times 10^{-5}\ m^2$ $\qquad E = 6.895 \times 10^{10}\ N/m^2$

$I_1 = I_2 = 6.0 \times 10^{-9}\ m^4$ $\qquad G = 2.652 \times 10^{10}\ N/m^2$

$J = 1.2 \times 10^{-8}\ m^4$ $\qquad \rho = 2768\ kg/m^3$

V_1 = Cross-sectional area of members ①, ② and ③

V_2 = Moment of inertia and torsion constant of member ①, ② and ③

c) Design Variables and Material Properties

Figure (1) Unsymmetric triangular double laced beamlike lattice used in the present study.

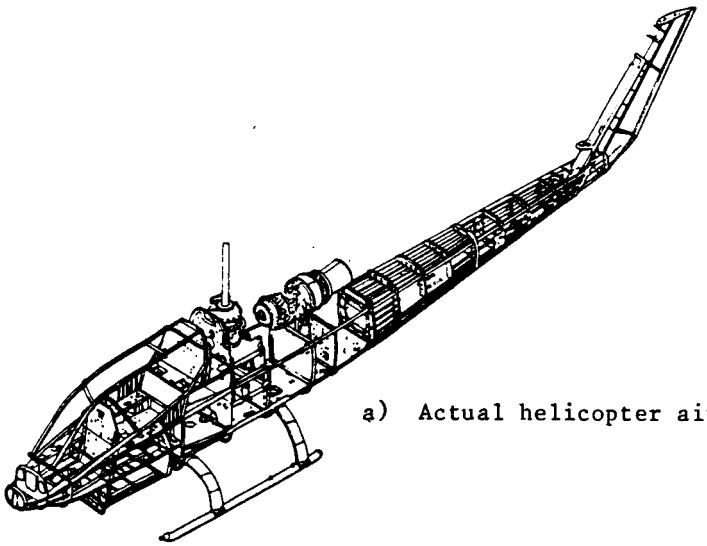

a) Actual helicopter airframe structure.

V_1 = stiffness of linear elastic elements (1) = 7.881×10^5 N/m

V_2 = moment of inertia of beam element (2) = 4.995×10^{-5} m^4

$I_1 = I_2 = V_2$

V_3 = moment of inertia of beam element (3) = 4.162×10^{-3} m^4

$I_1 = 1.167\ V_3$, $I_2 = 1.39\ V_3$

V_4 = rigid mass (4) = 13.97 kg

V_5 = moment of inertia of beam element (5) = 4.162×10^{-3} m^4

$I_1 = 1.471\ V_5$, $I_2 = 1.275\ V_5$

V_6 = rigid mass (6) = 114.9 kg

$E = 6.895 \times 10^9$ N/m^2 $G = 2.652 \times 10^9$ N/m^2

b) Design variables and material properties.

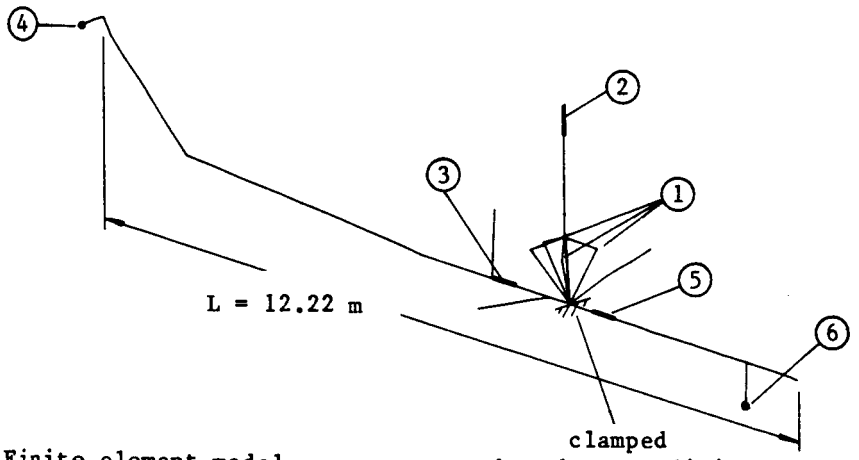

c) Finite element model.

Figure (2) Elastic line model of the Bell AH-1G Cobra used in the present study.

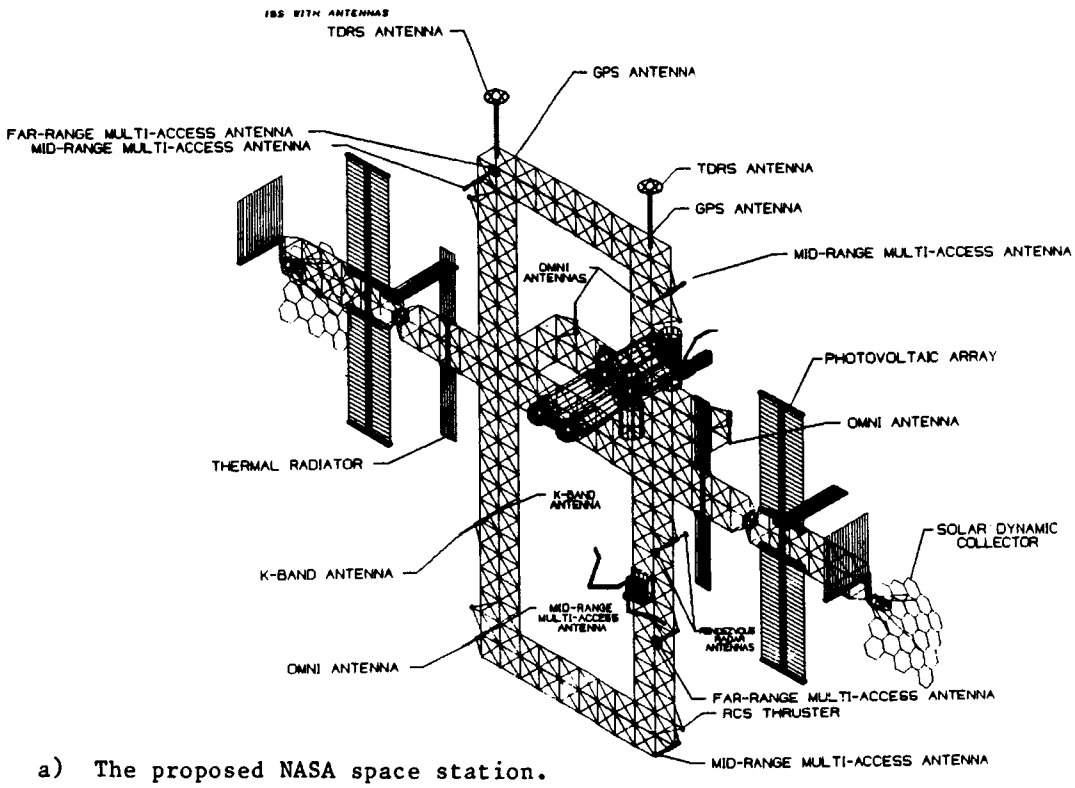

a) The proposed NASA space station.

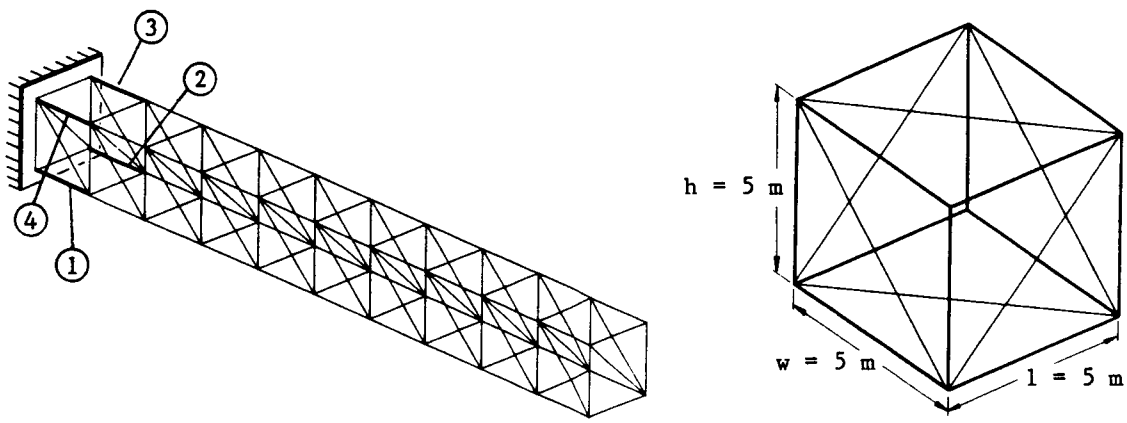

b) Undeformed structure with boundary condition.

Typical tubular member

Inner radius = 5.08×10^{-2} m

Outer radius = 5.46×10^{-2} m

Material Properties

$E = 2.76 \times 10^{11}$ N/m^2

$G = 1.06 \times 10^{11}$ N/m^2

$\rho = 1880$ kg/m^3

Design Variables

V_1 = Cross-sectional area of members ①, ②, ③, and ④.

V_2 = Moment of inertia and torsion constant of members ①, ②, ③, and ④.

c) Member and material properties, and design variables.

Figure (3) The orthogonal tetrahedral lattice beam used in the present study.

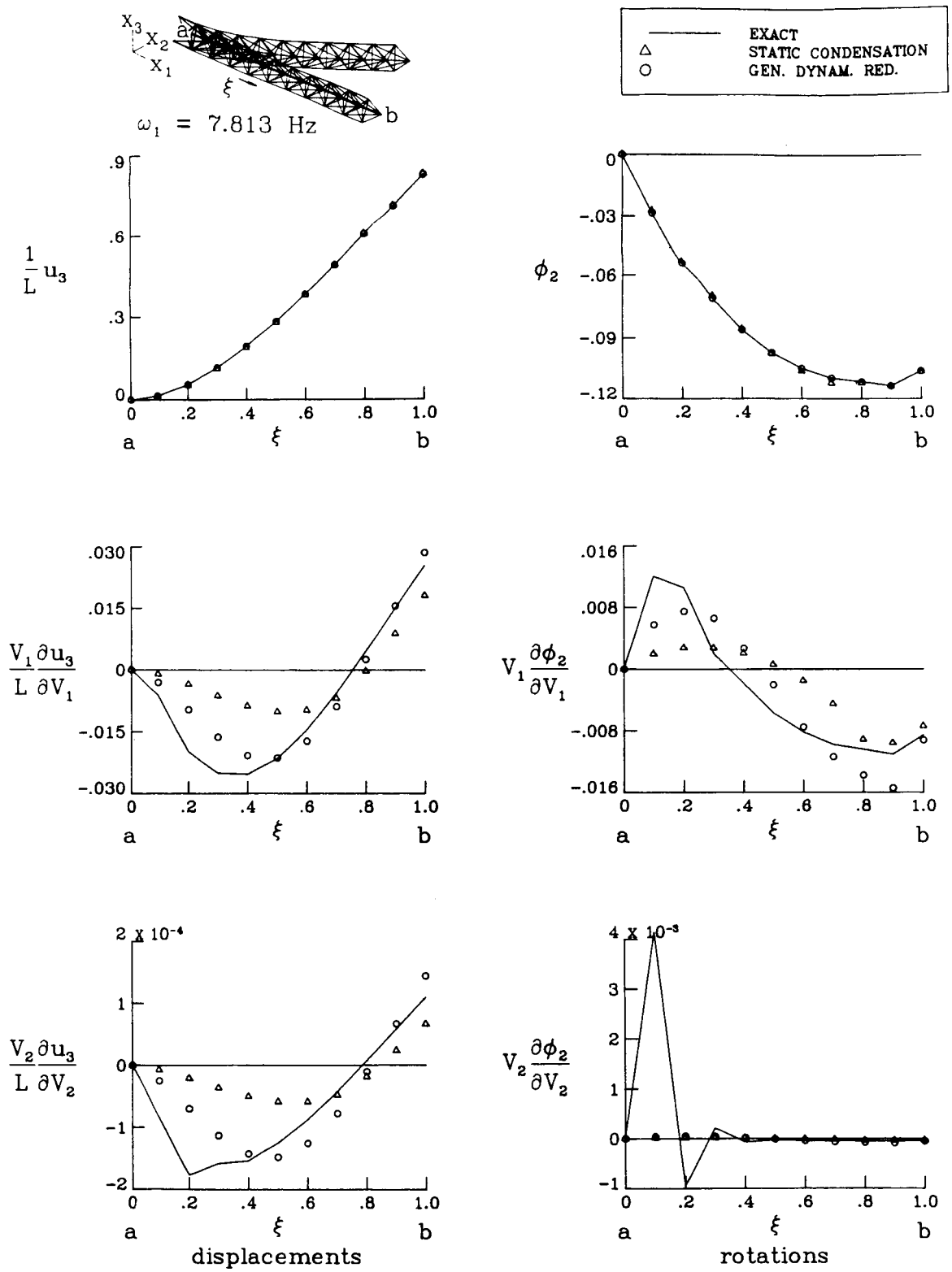

Figure 4. Accuracy of eigenvector 1 and its derivatives obtained using static condensation with 36 dof and generalized dynamic reduction with 6 dof for the ten bay triangular lattice beam (fig. 1)

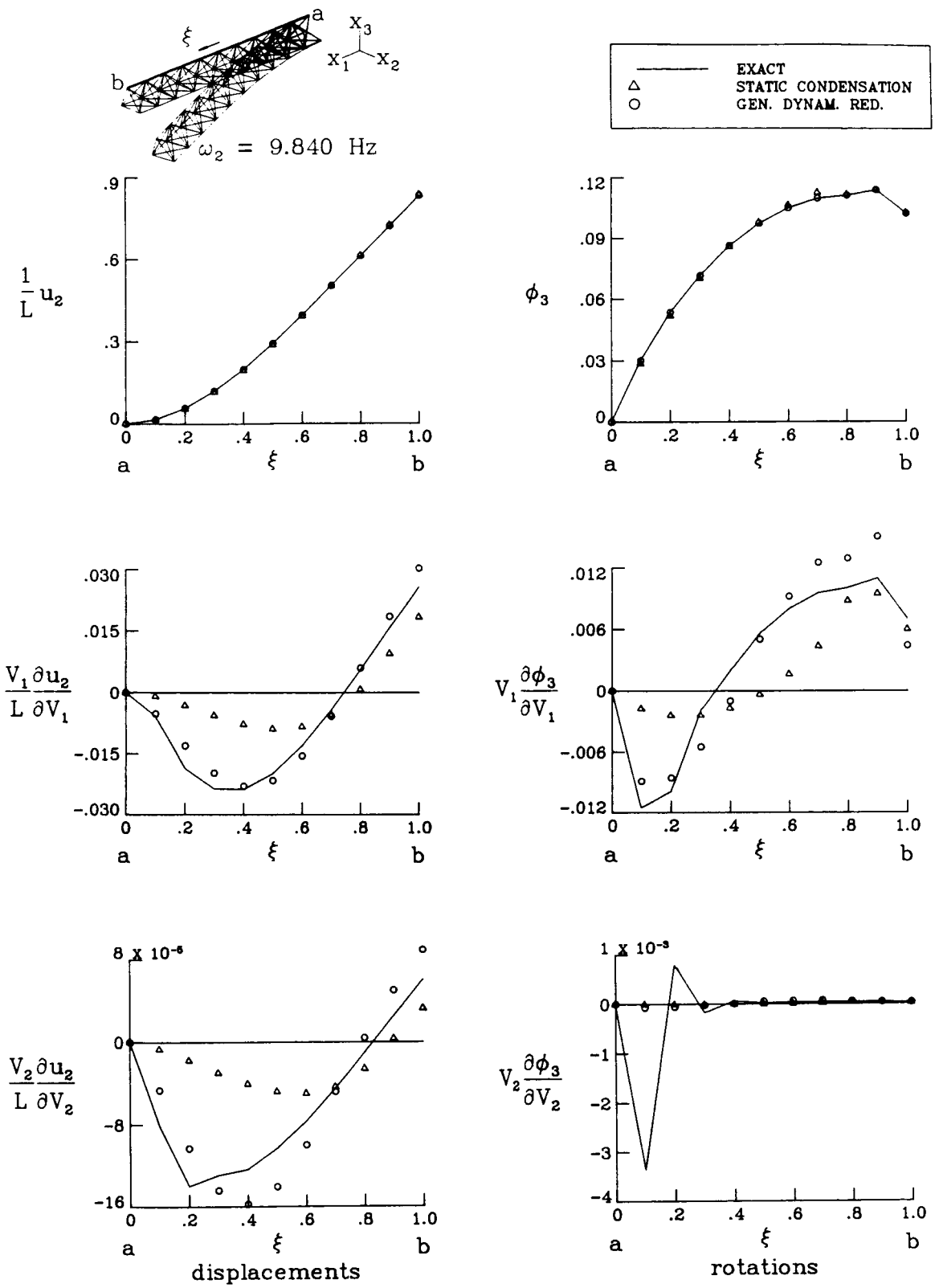

Figure 4. (Continued) Eigenvector 2

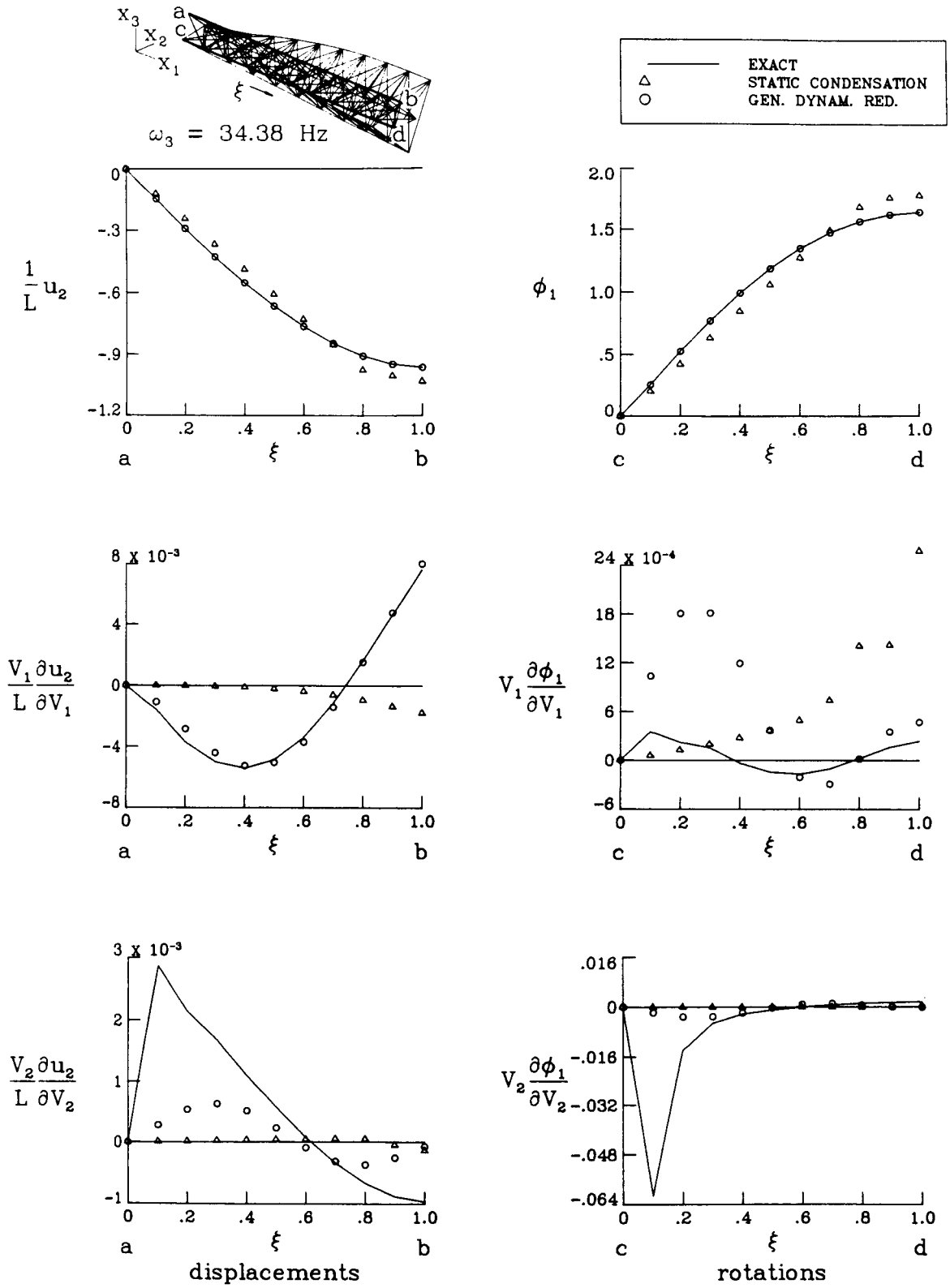

Figure 4. (Continued) Eigenvector 3

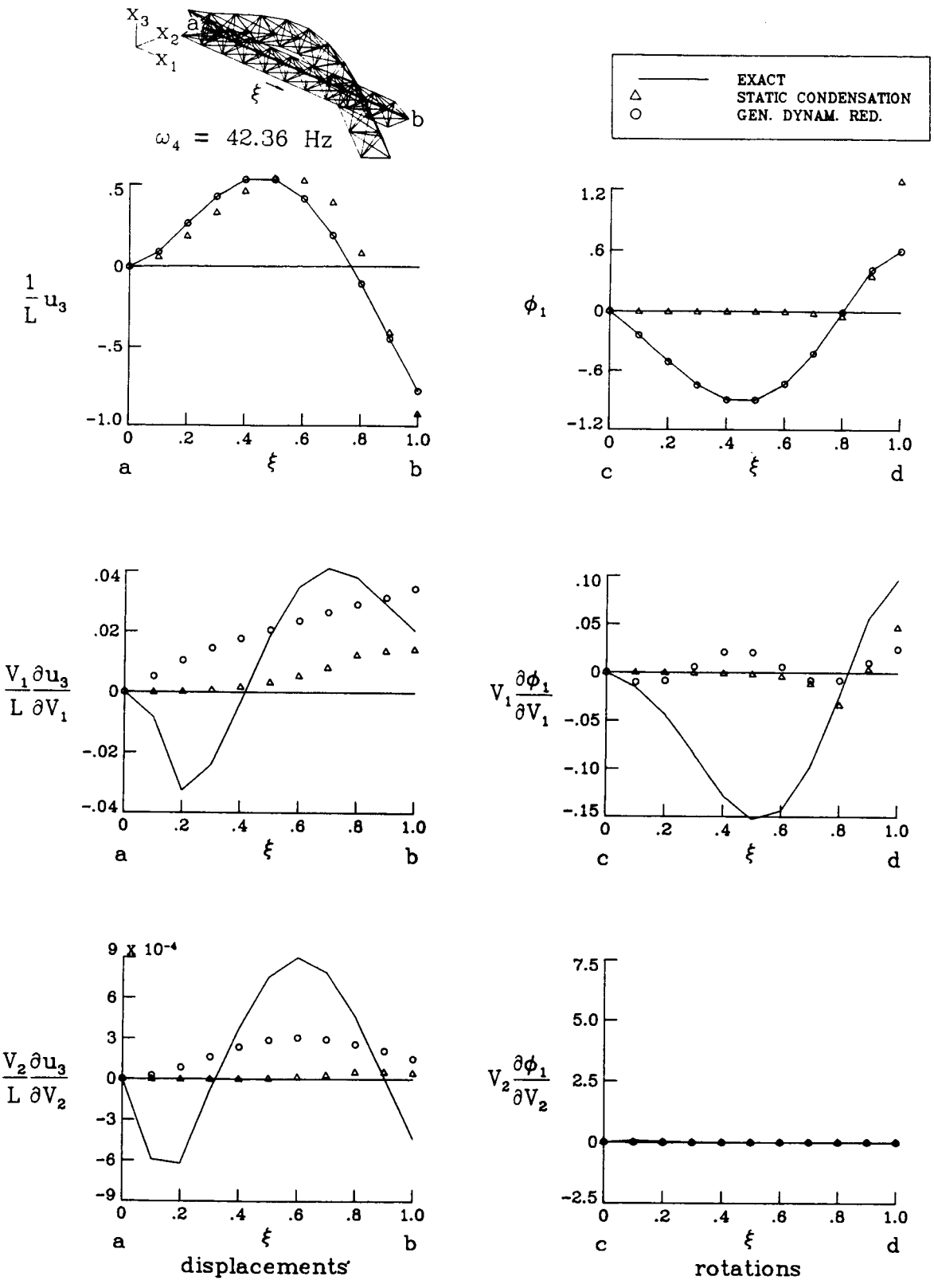

Figure 4. (**Concluded**) Eigenvector 4

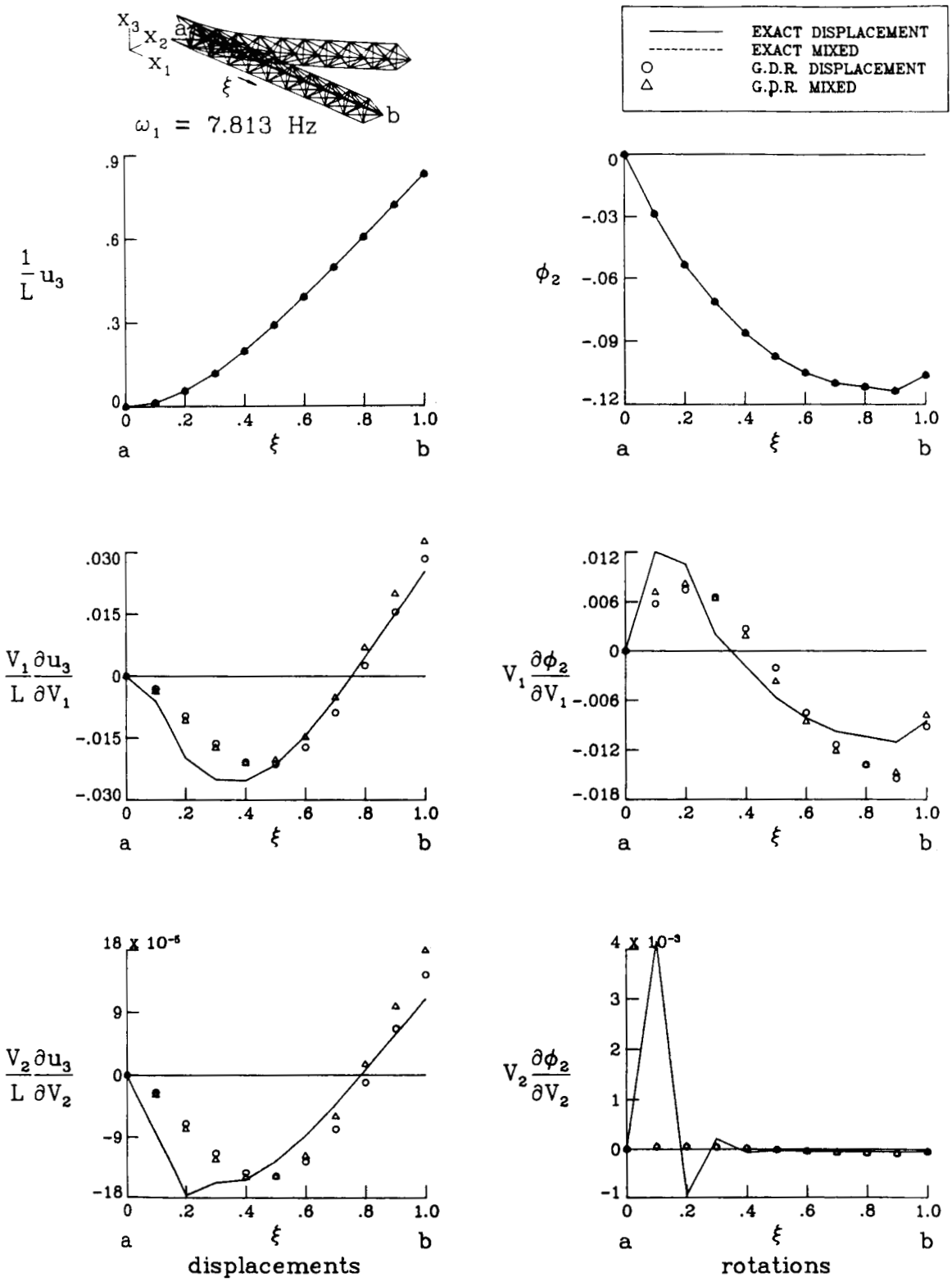

Figure 5. Accuracy of eigenvector 1 and its derivatives obtained using generalized dynamic reduction with the displacement and mixed formulation for the triangular lattice beam (fig. 1)

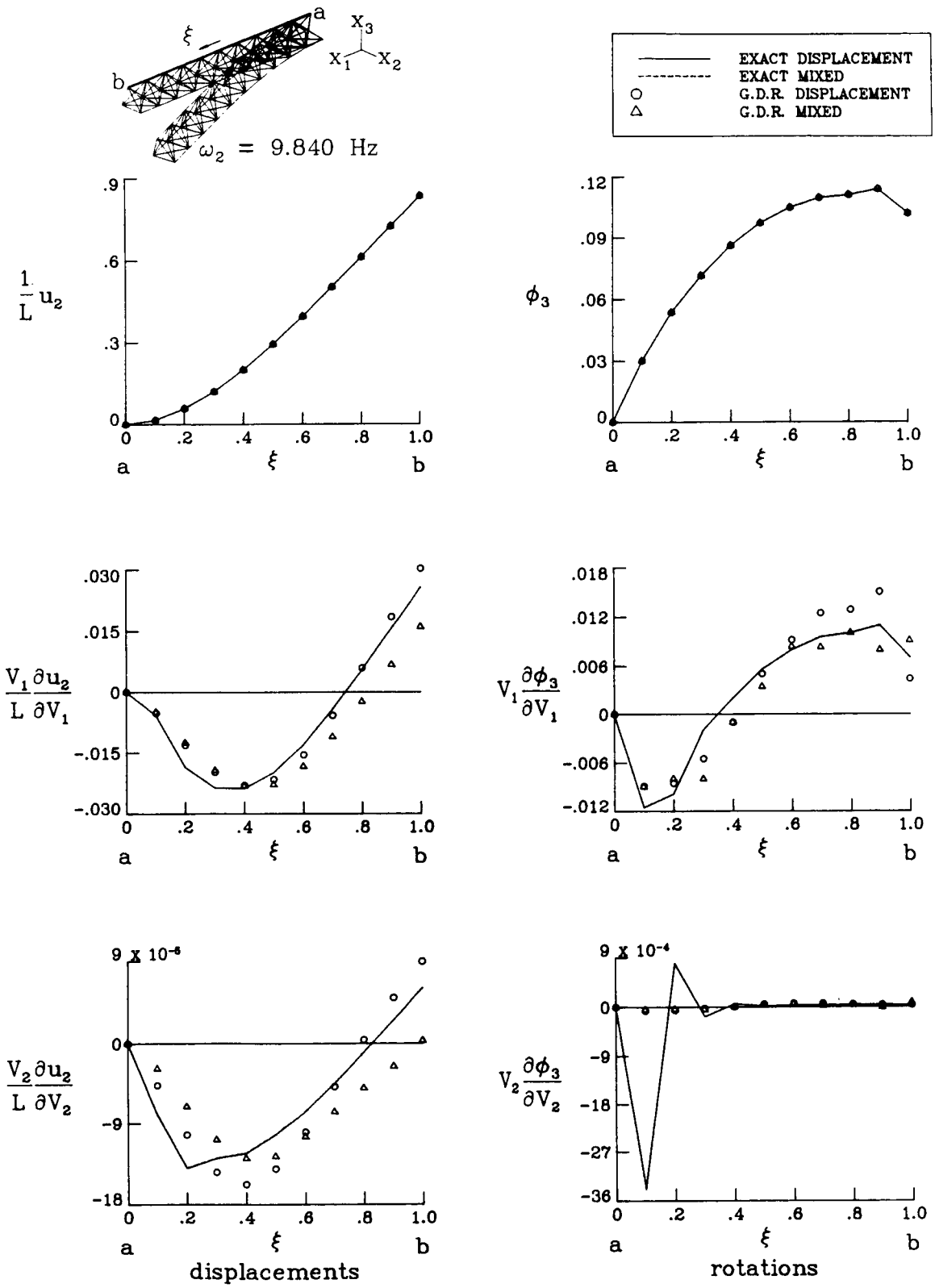

Figure 5. (Continued) Eigenvector 2

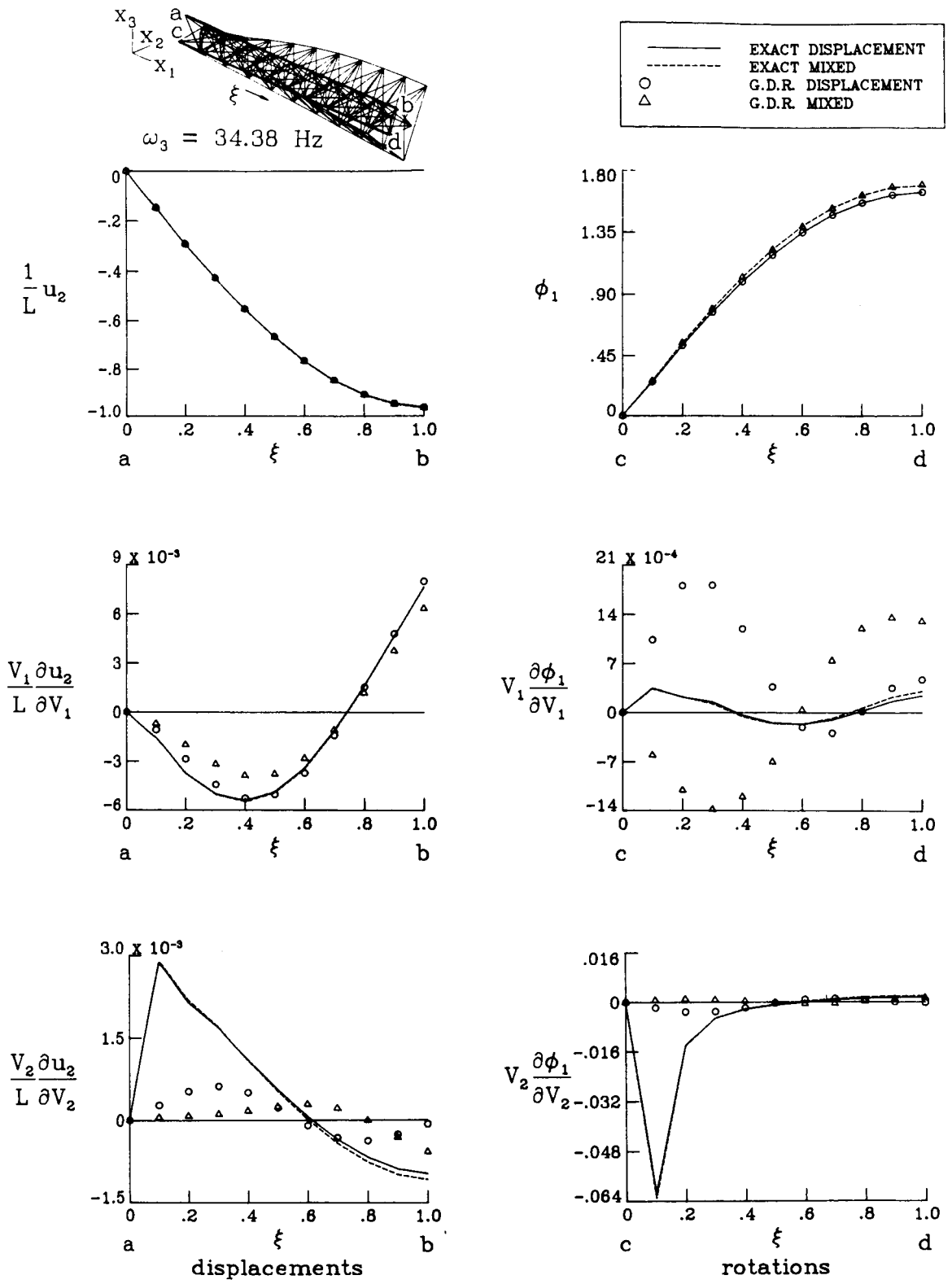

Figure 5. (Continued) Eigenvector 3

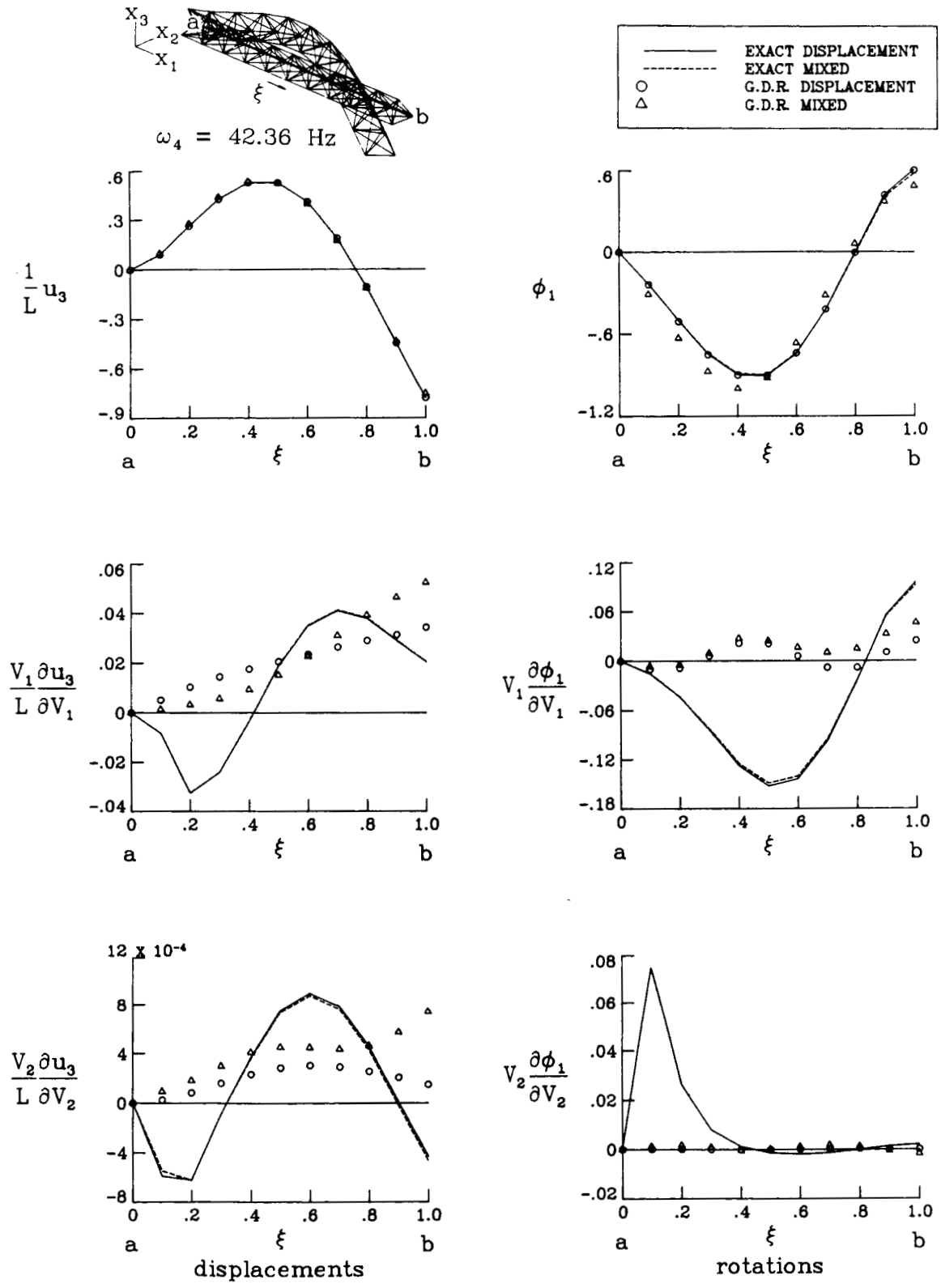

Figure 5. (**Concluded** .) Eigenvector 4

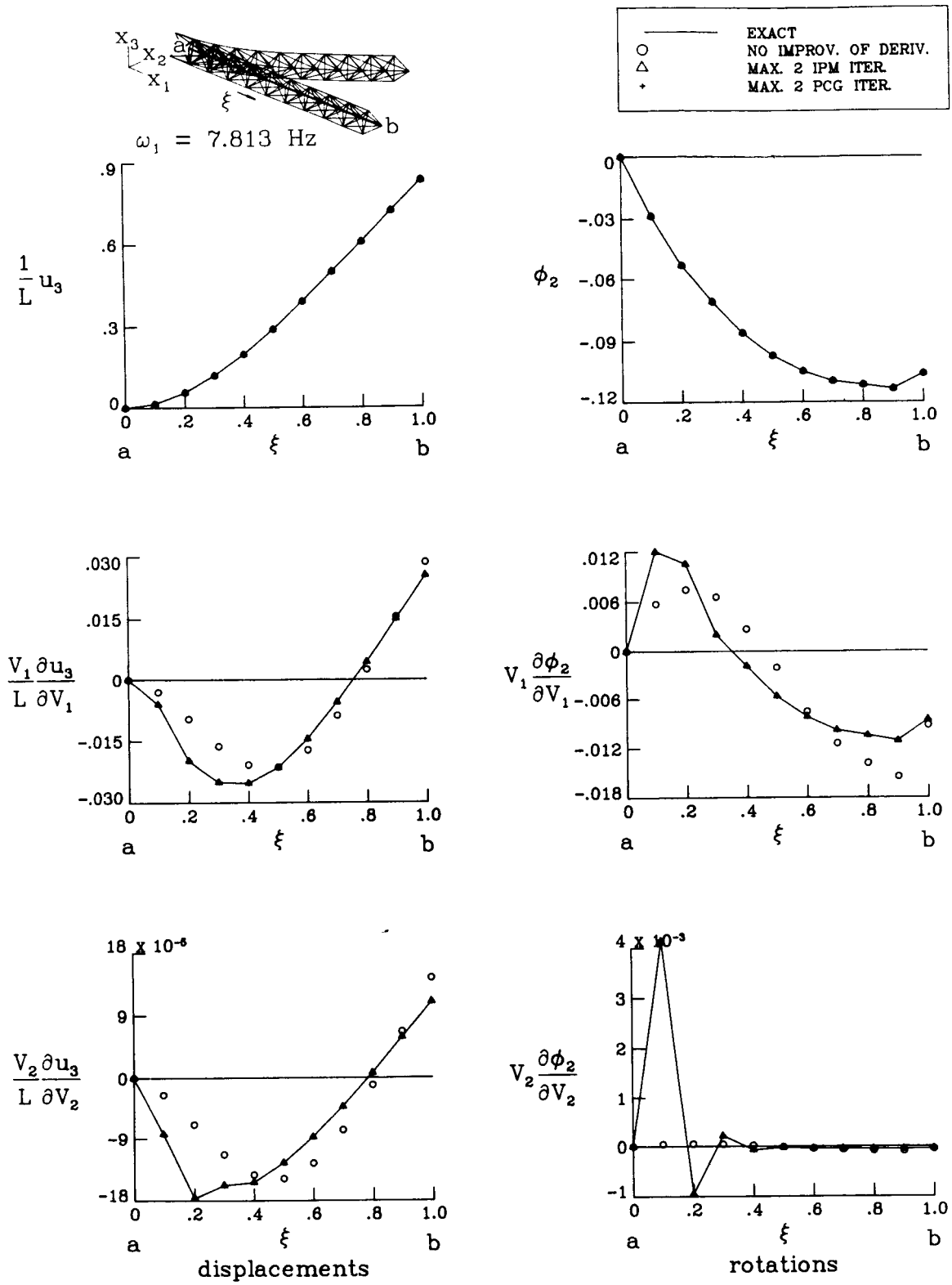

Figure 6. Accuracy of eigenvector 1 and its derivatives obtained using generalized dynamic reduction with iterative refinement for the triangular lattice beam (fig. 1)

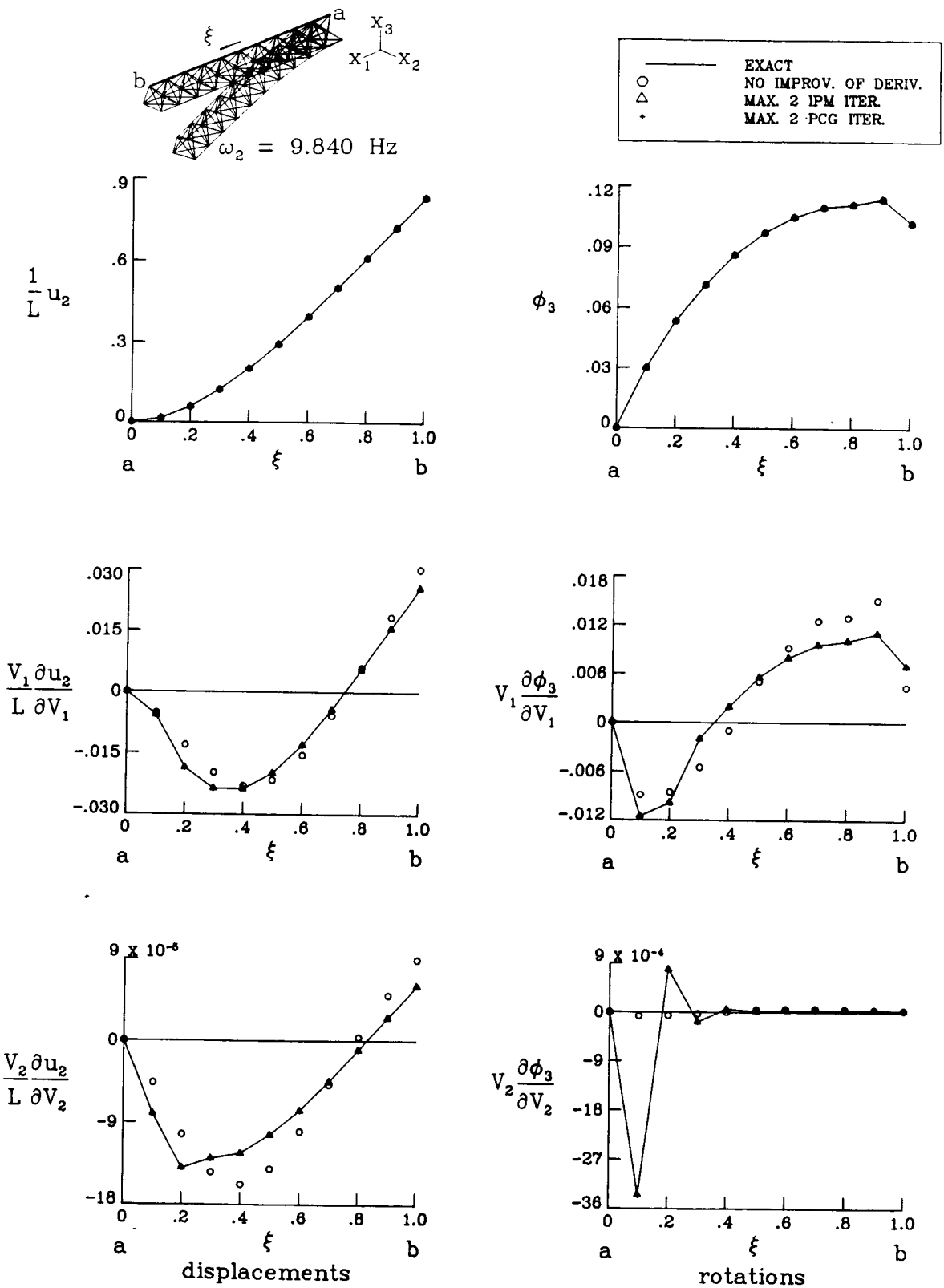

Figure 6. (Continued) Eigenvector 2

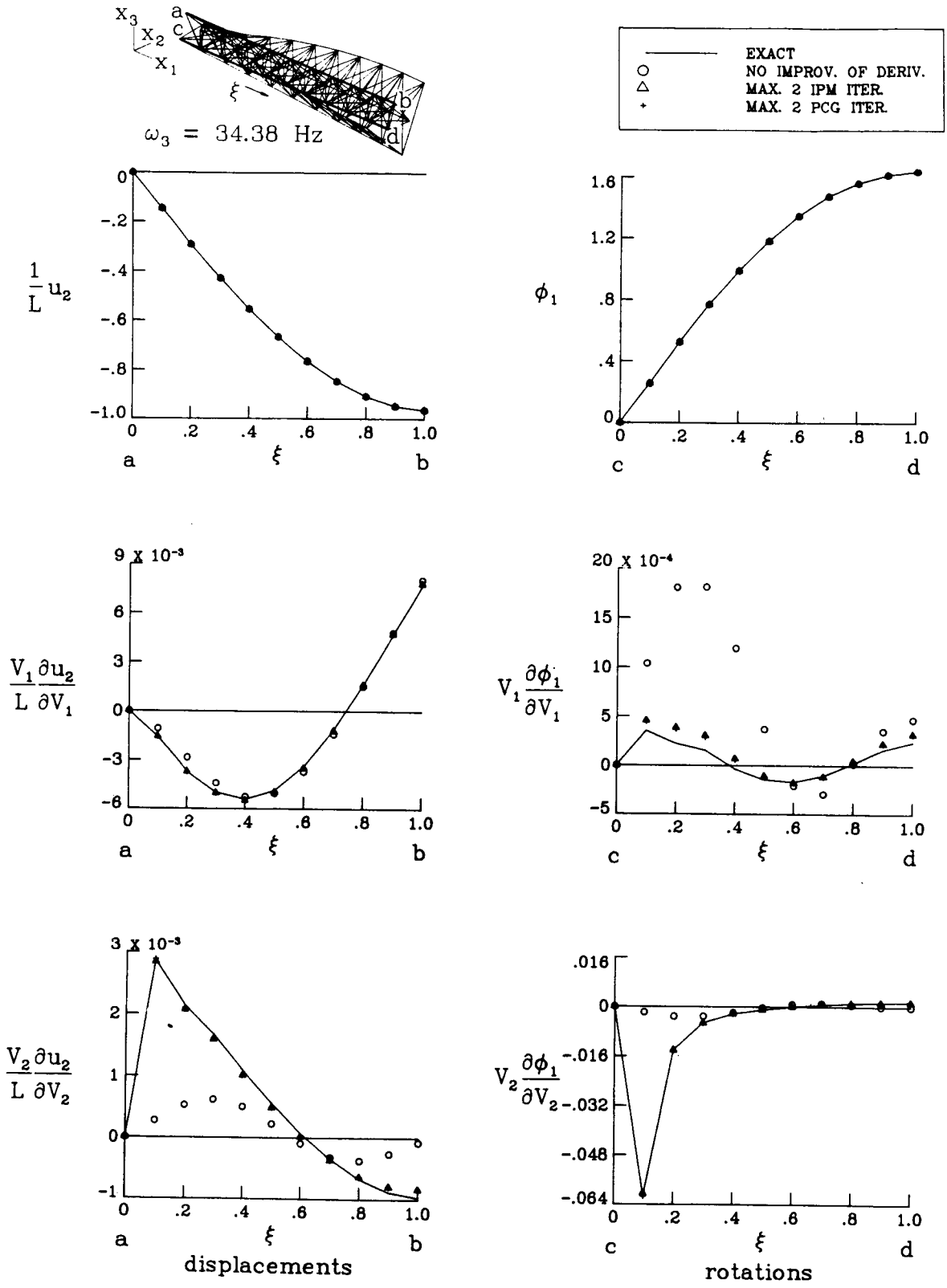

Figure 6. (Continued) Eigenvector 3

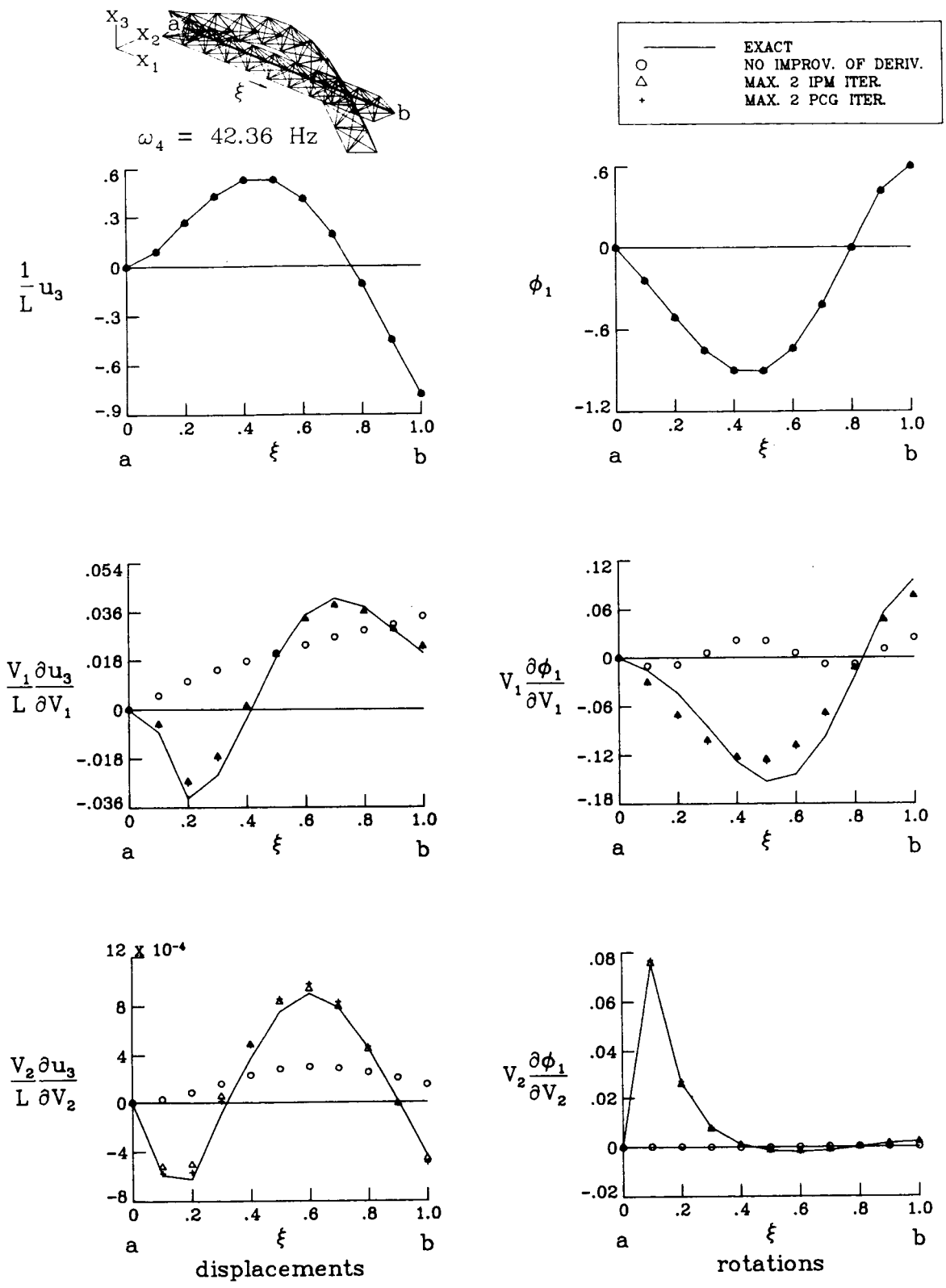

Figure 6. (Continued) Eigenvector 4

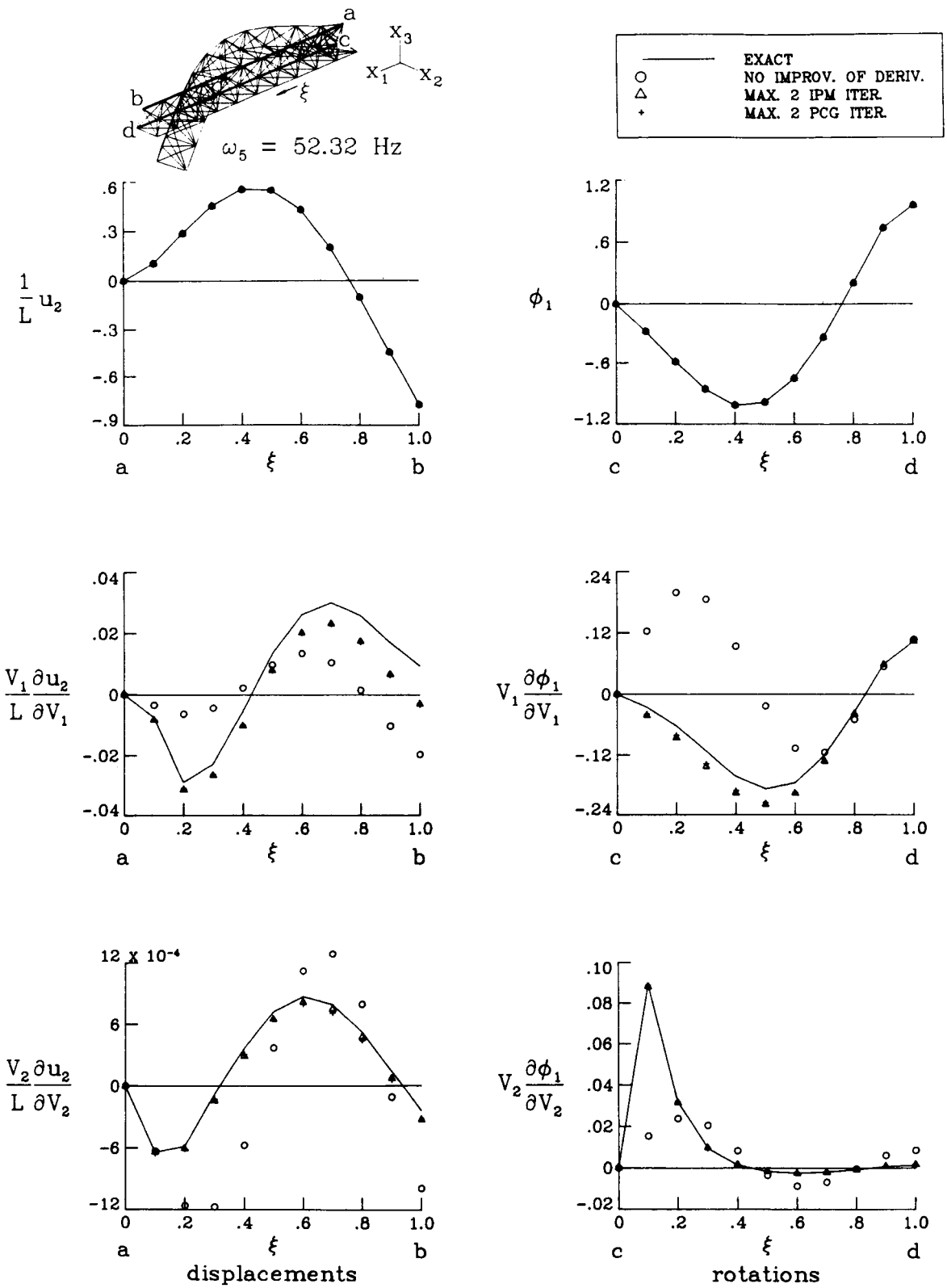

Figure 6. (Continued) Eigenvector 5

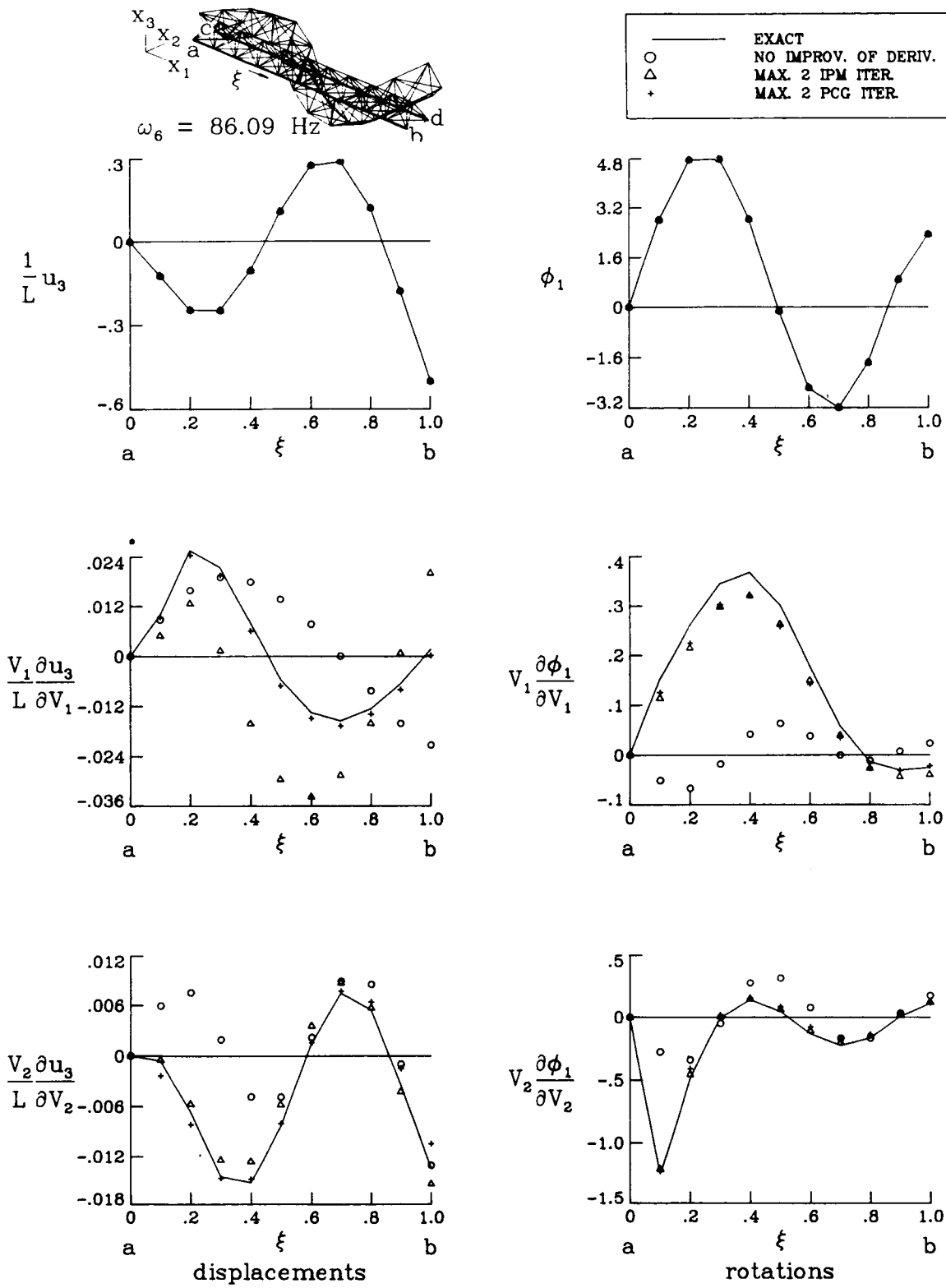

Figure 6. (Continued) Eigenvector 6

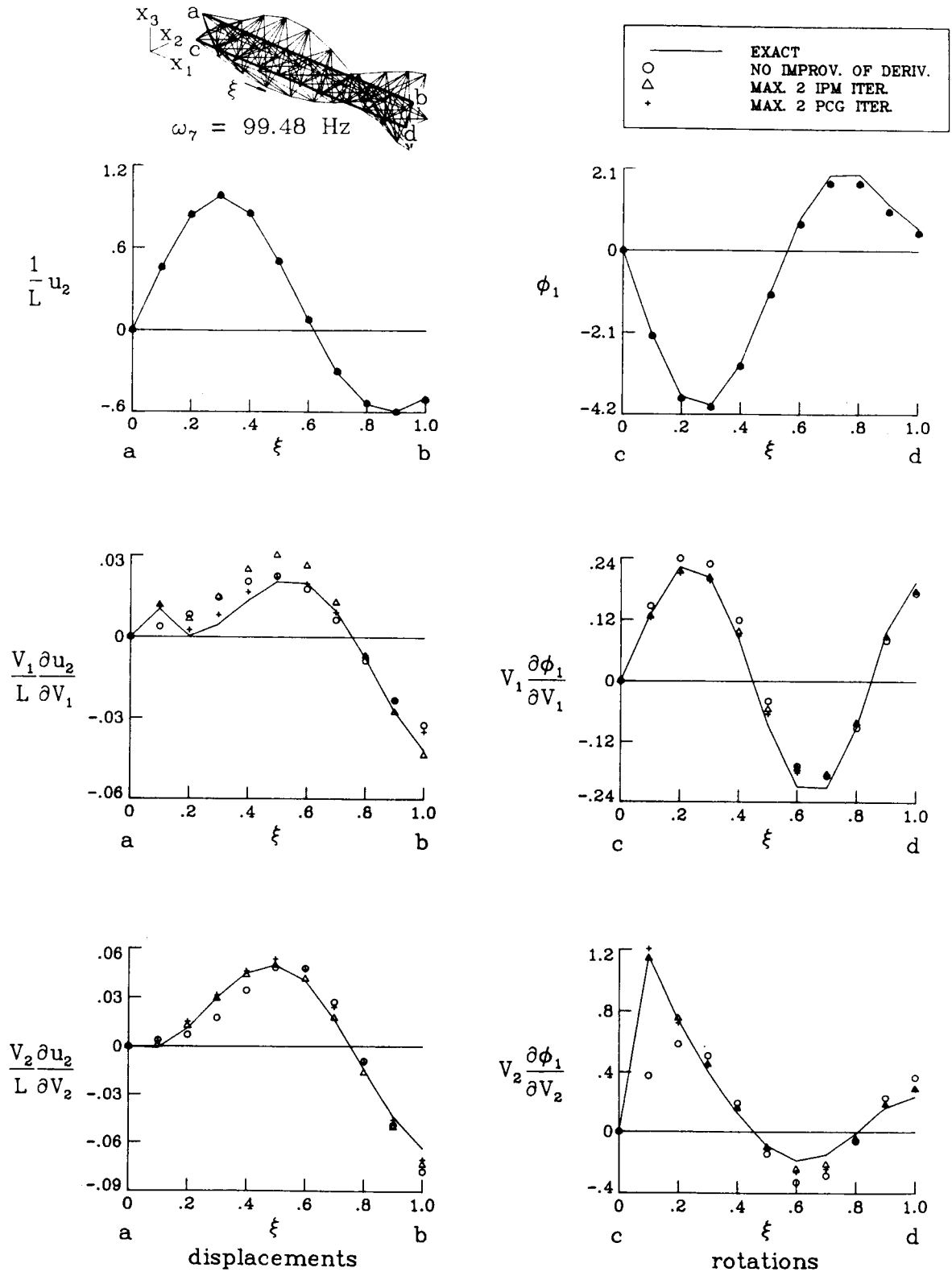

Figure 6. (**Continued**) Eigenvector 7

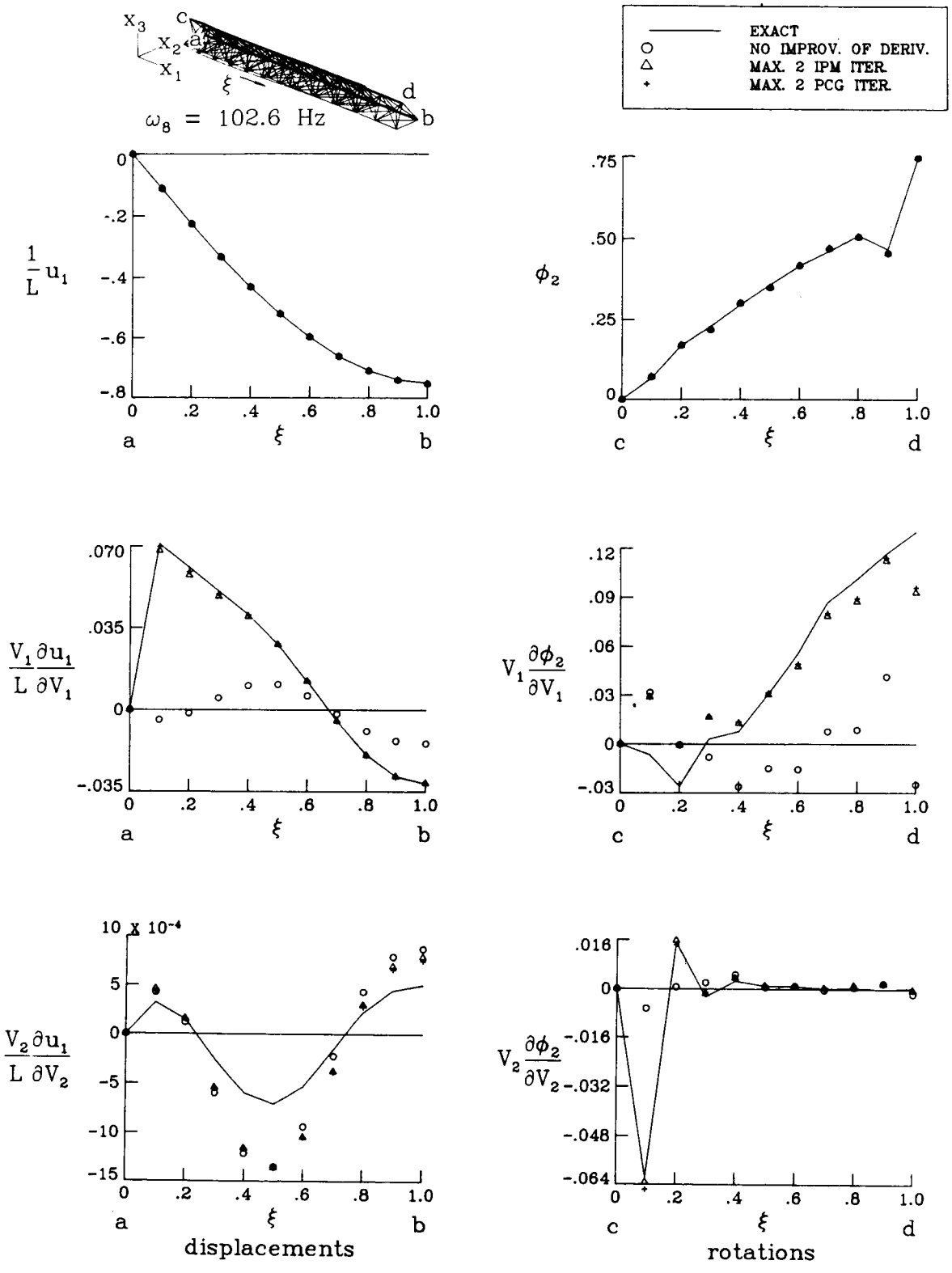

Figure 6. (**Concluded**) Eigenvector 8

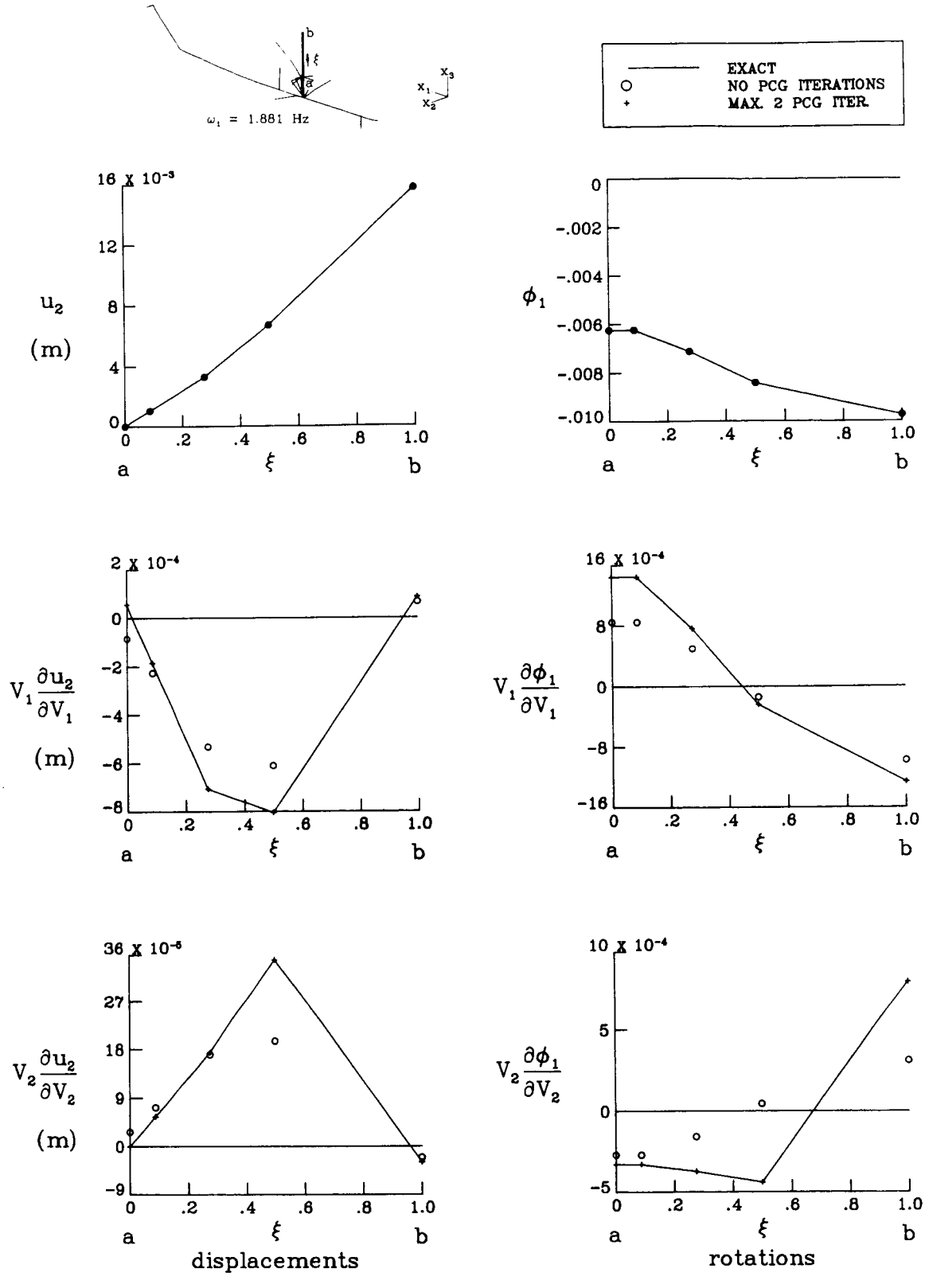

Figure 7. Accuracy of eigenvector 1 and its derivatives obtained using generalized dynamic reduction with preconditioned conjugate gradient iterations for the cobra elastic line model (fig. 2)

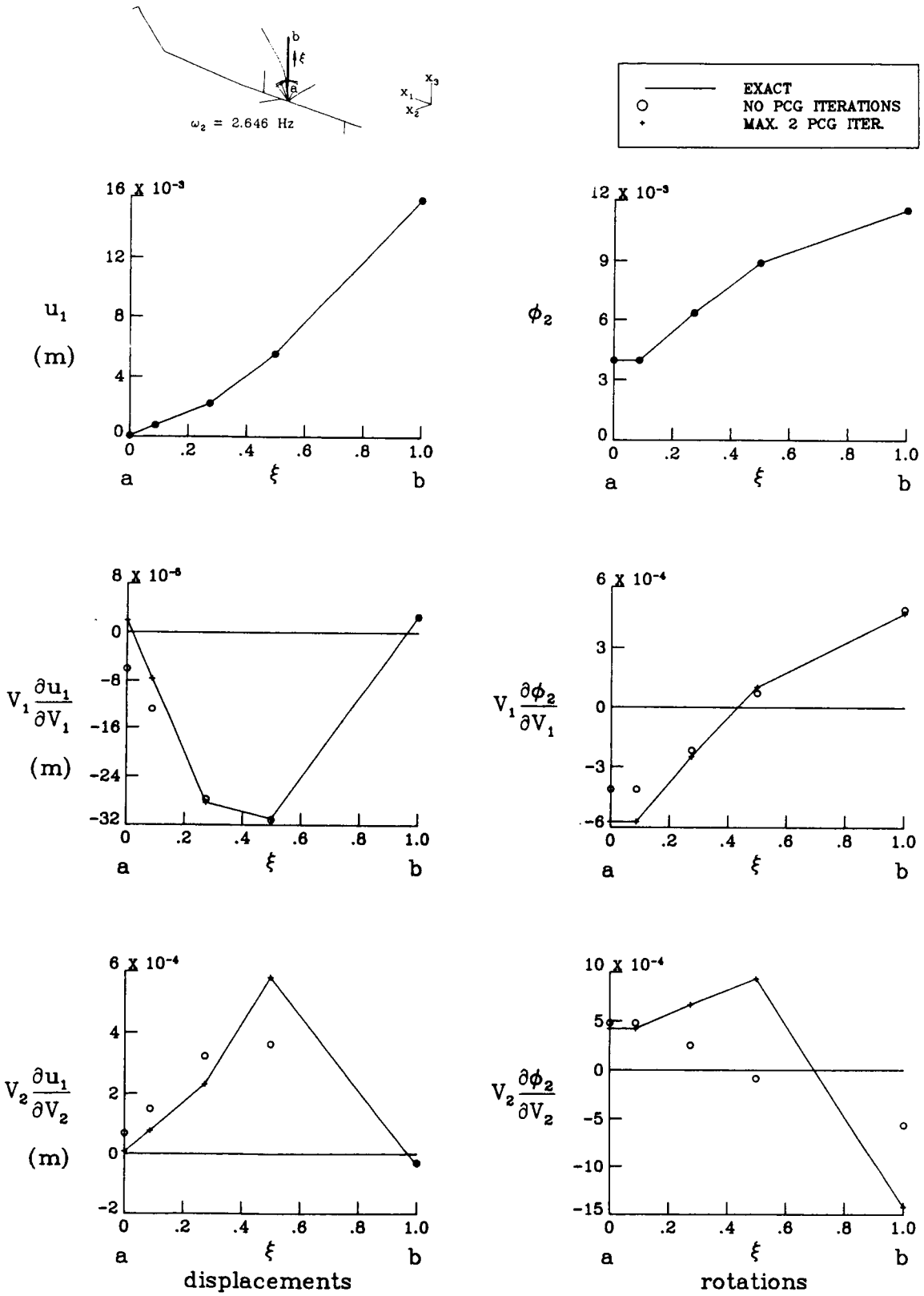

Figure 7. (Continued) Eigenvector 2

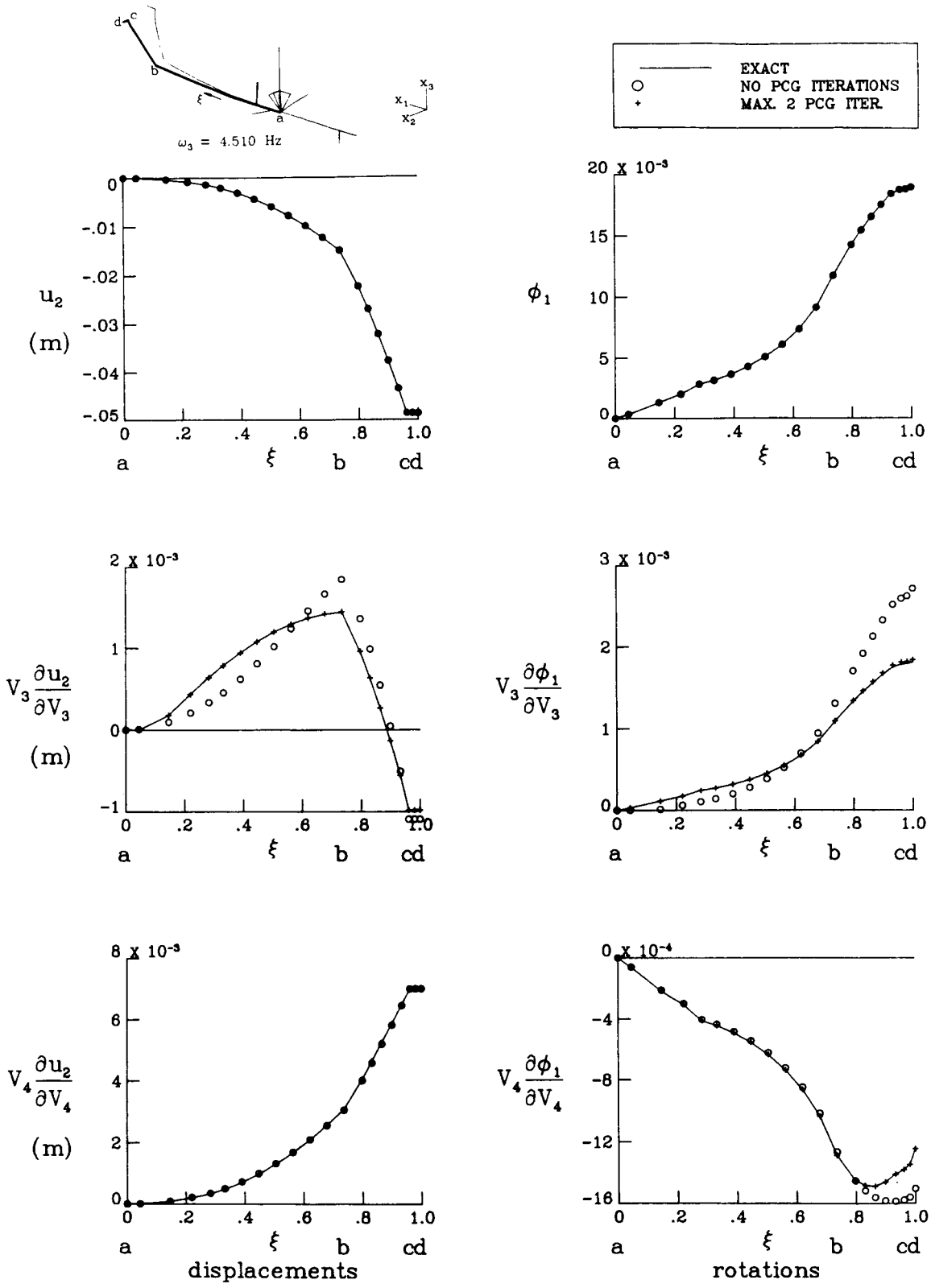

Figure 7. (Continued) Eigenvector 3

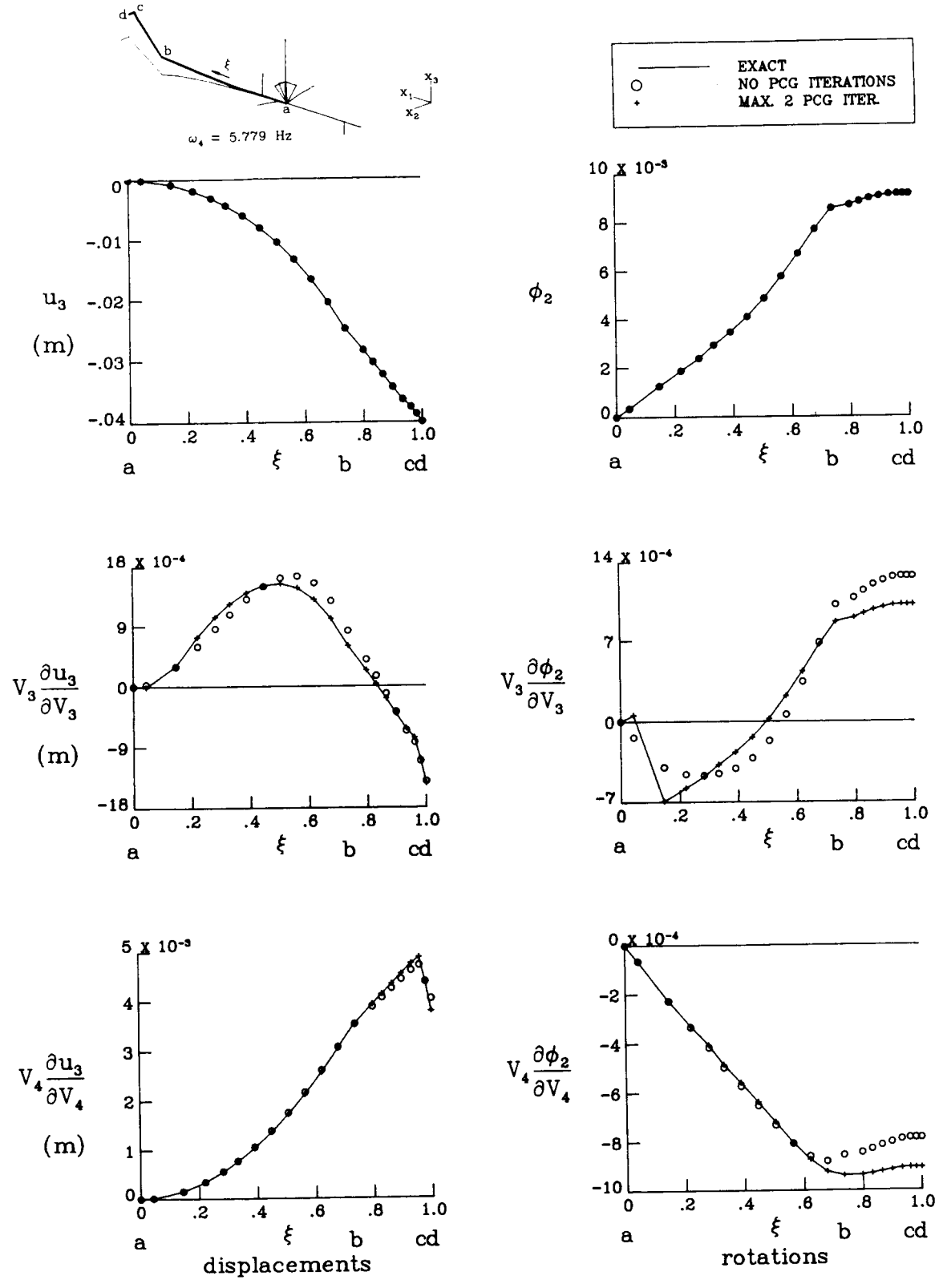

Figure 7. (Continued) Eigenvector 4

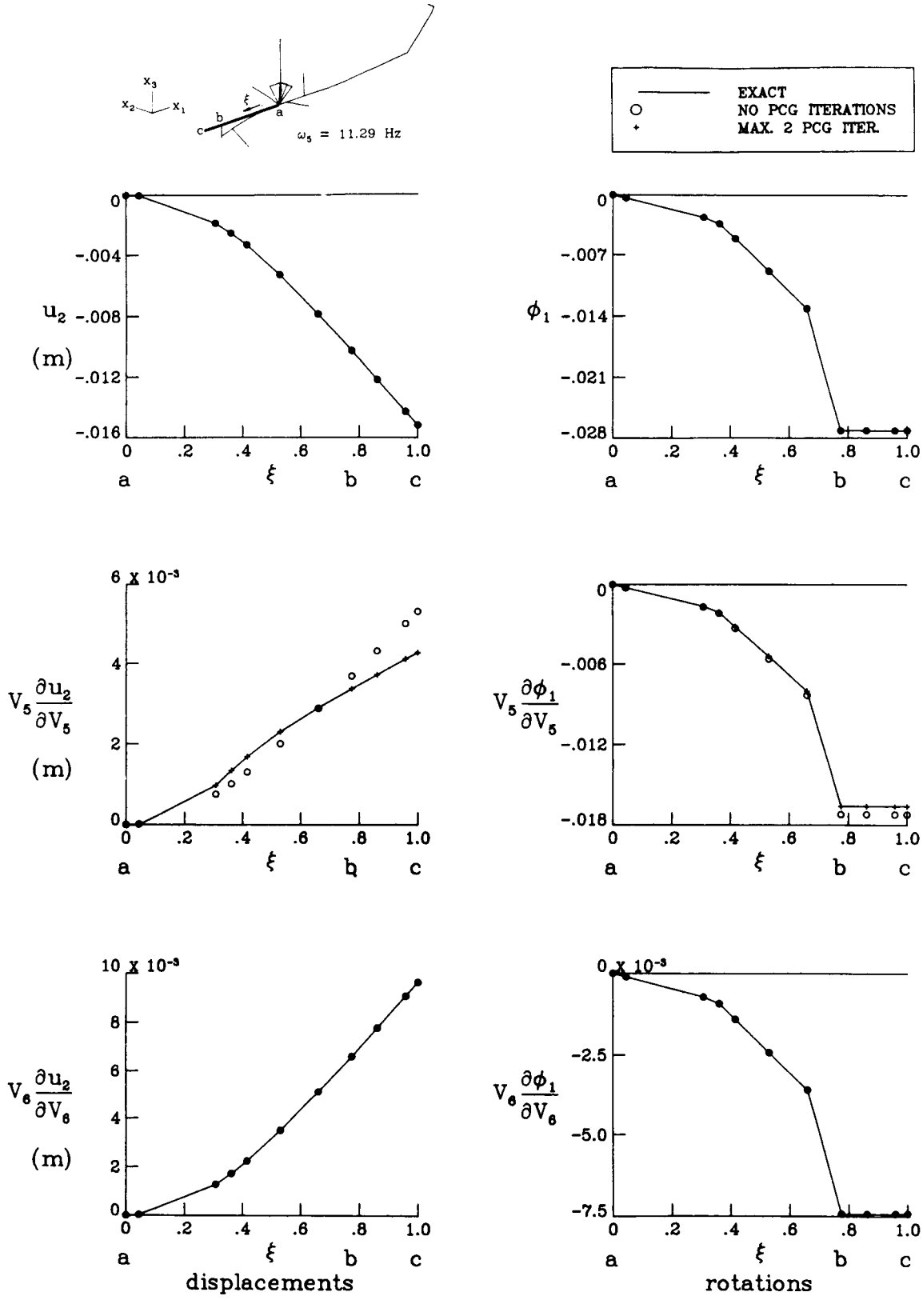

Figure 7. (Continued) Eigenvector 5

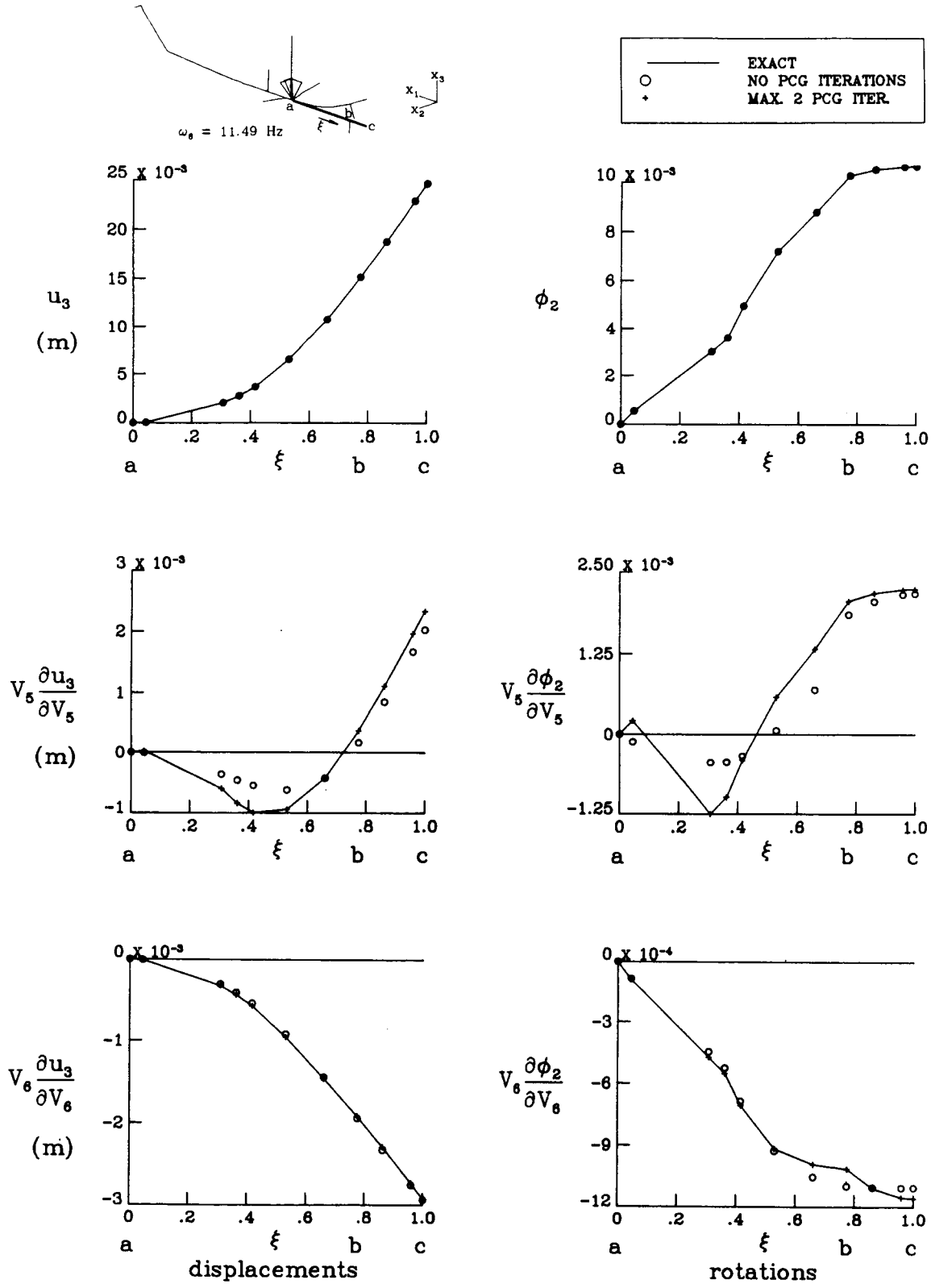

Figure 7. (Continued) Eigenvector 6

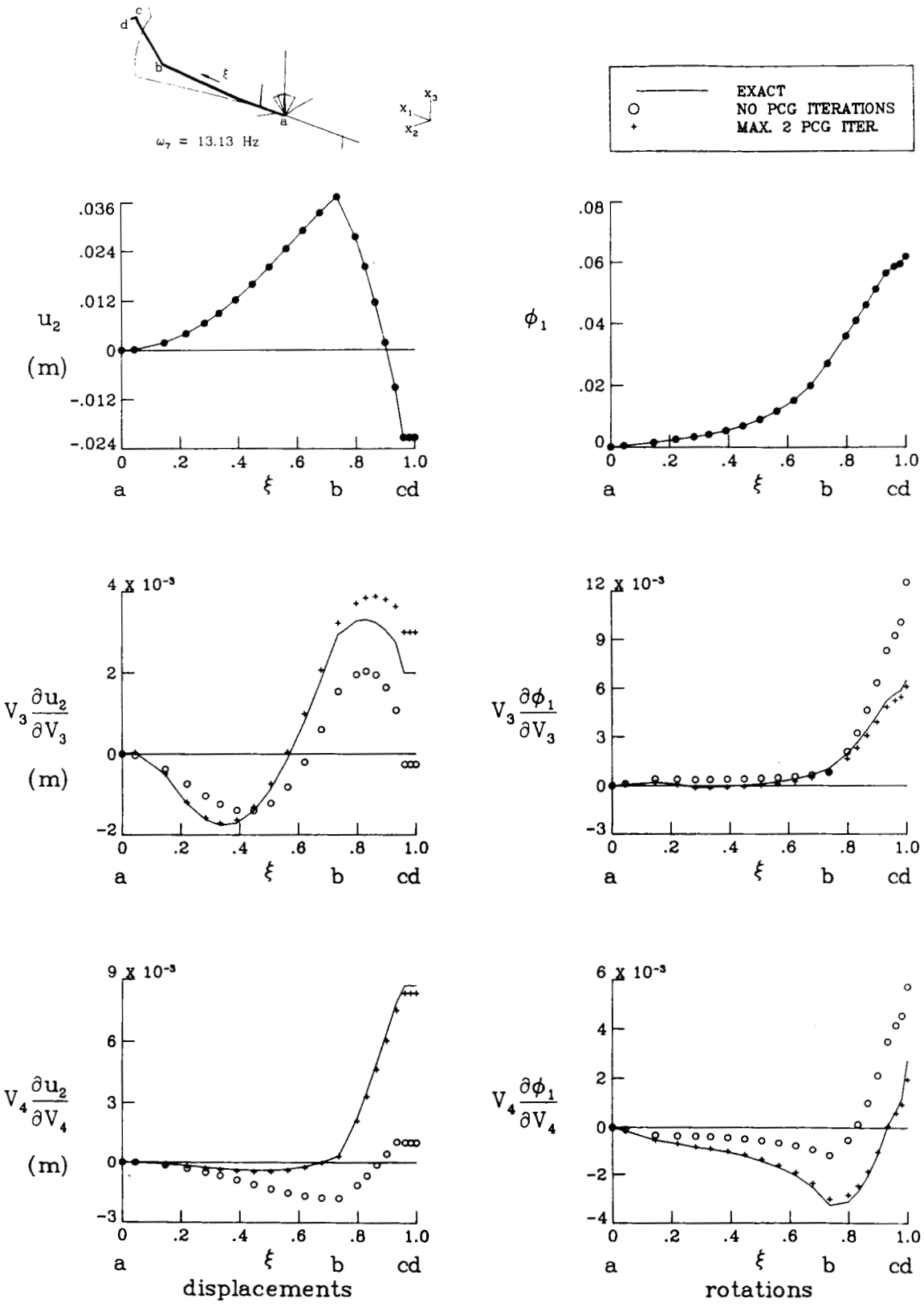

Figure 7. (Continued) Eigenvector 7

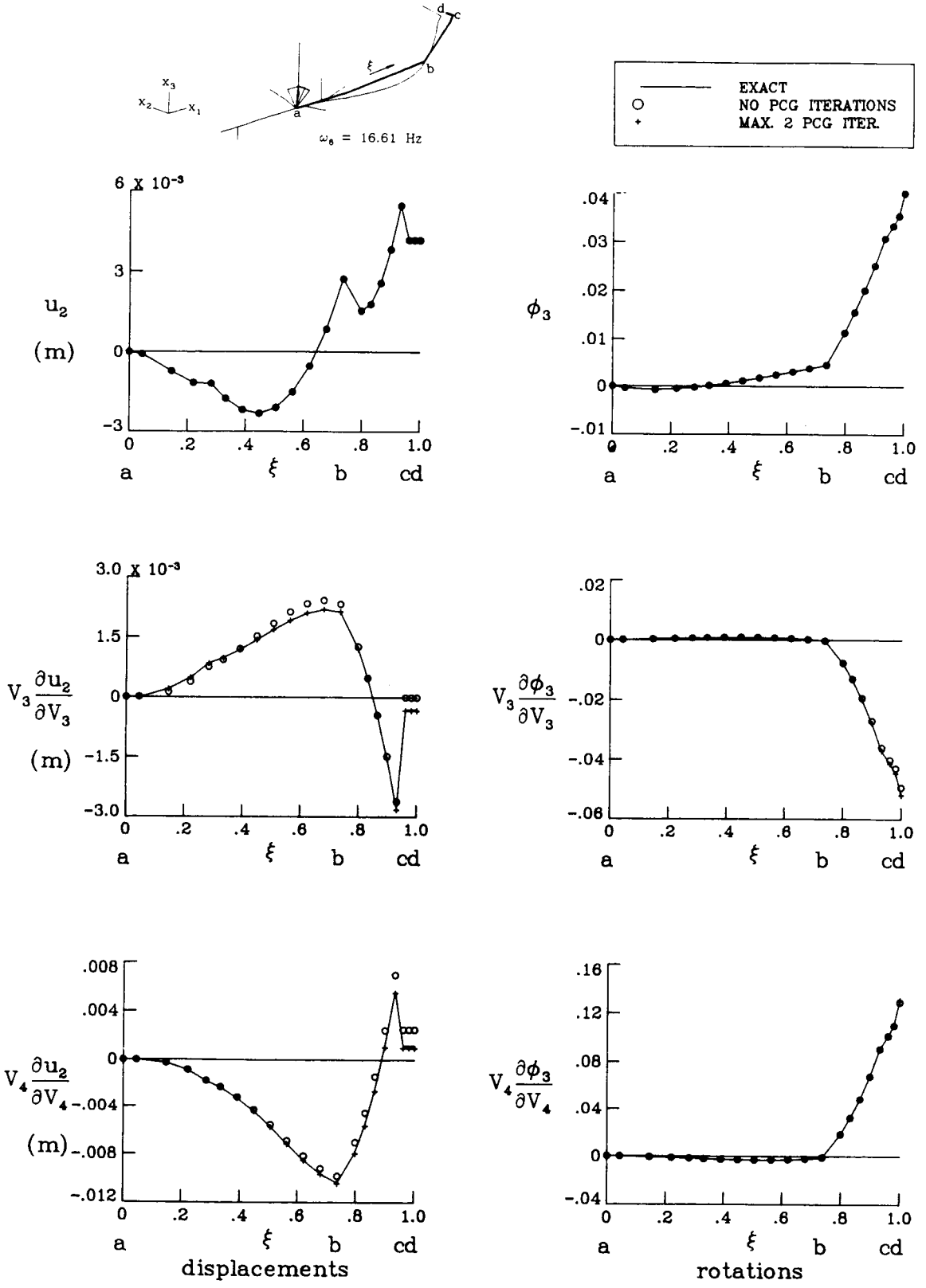

Figure 7. (**Concluded**) Eigenvector 8

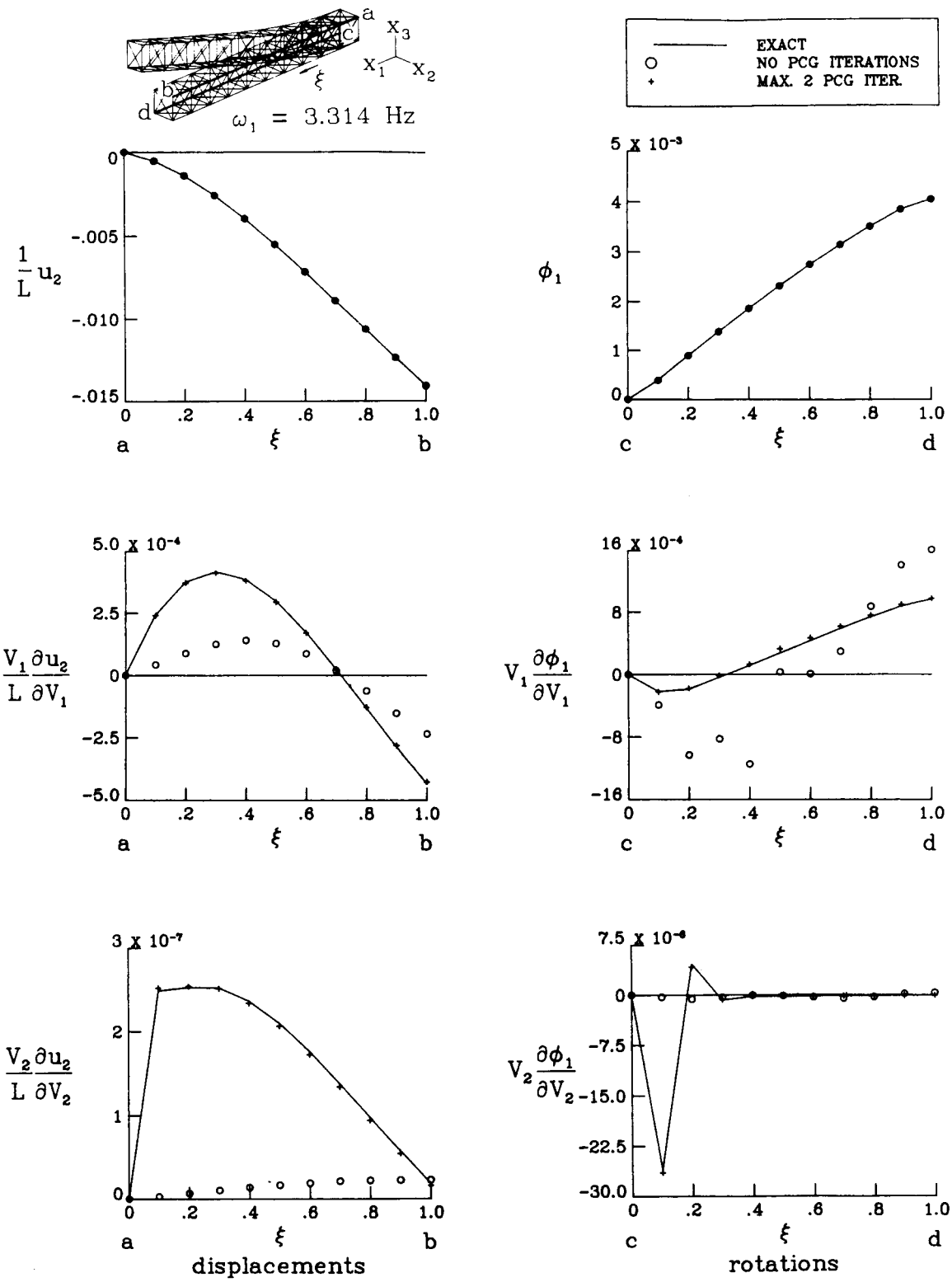

Figure 8. Accuracy of eigenvector 1 and its derivatives obtained using generalized dynamic reduction with preconditioned conjugate gradient iterations for the ten bay orthogonal tetrahedral lattice beam (fig. 3)

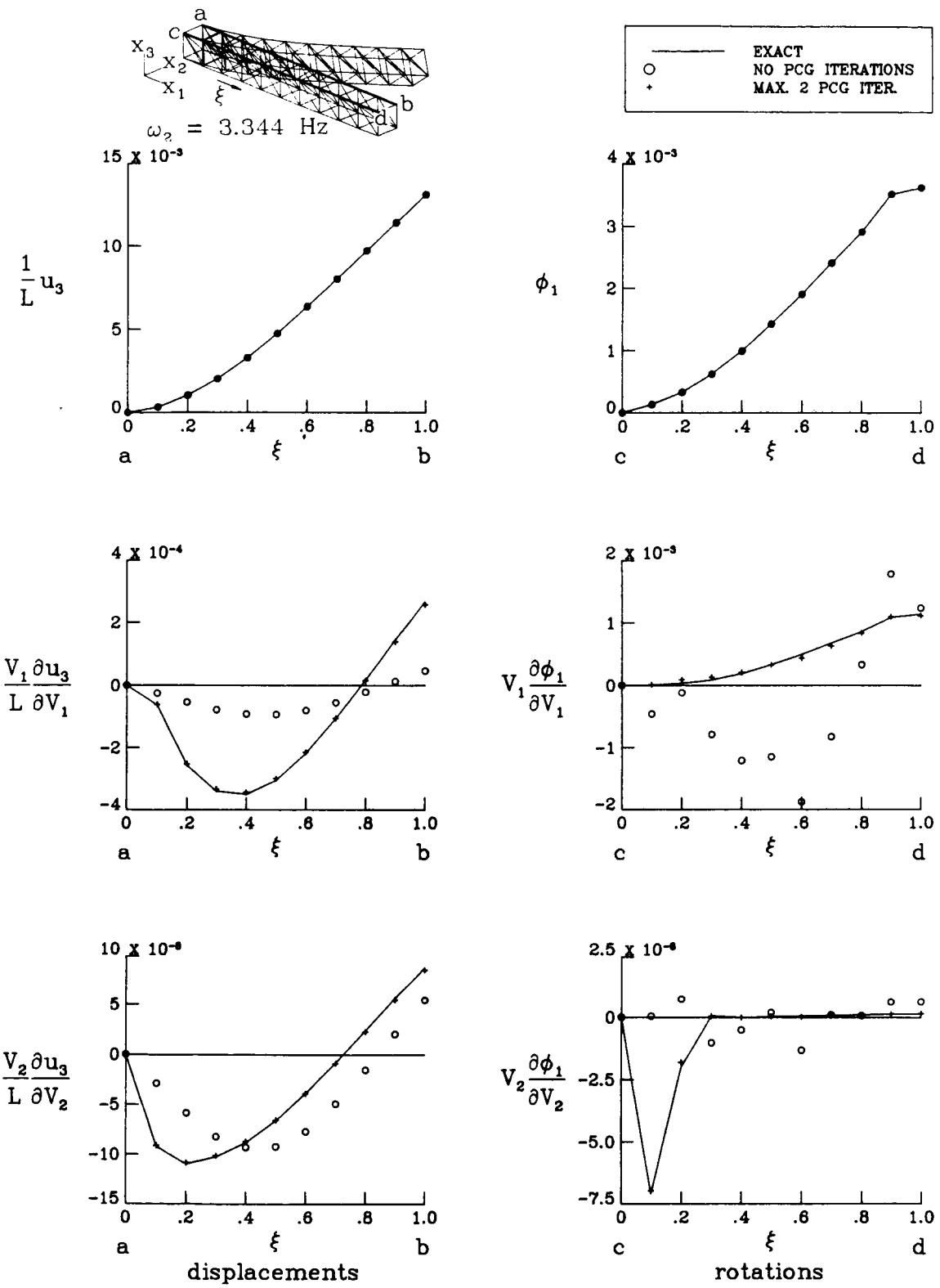

Figure 8. (Continued) Eigenvector 2

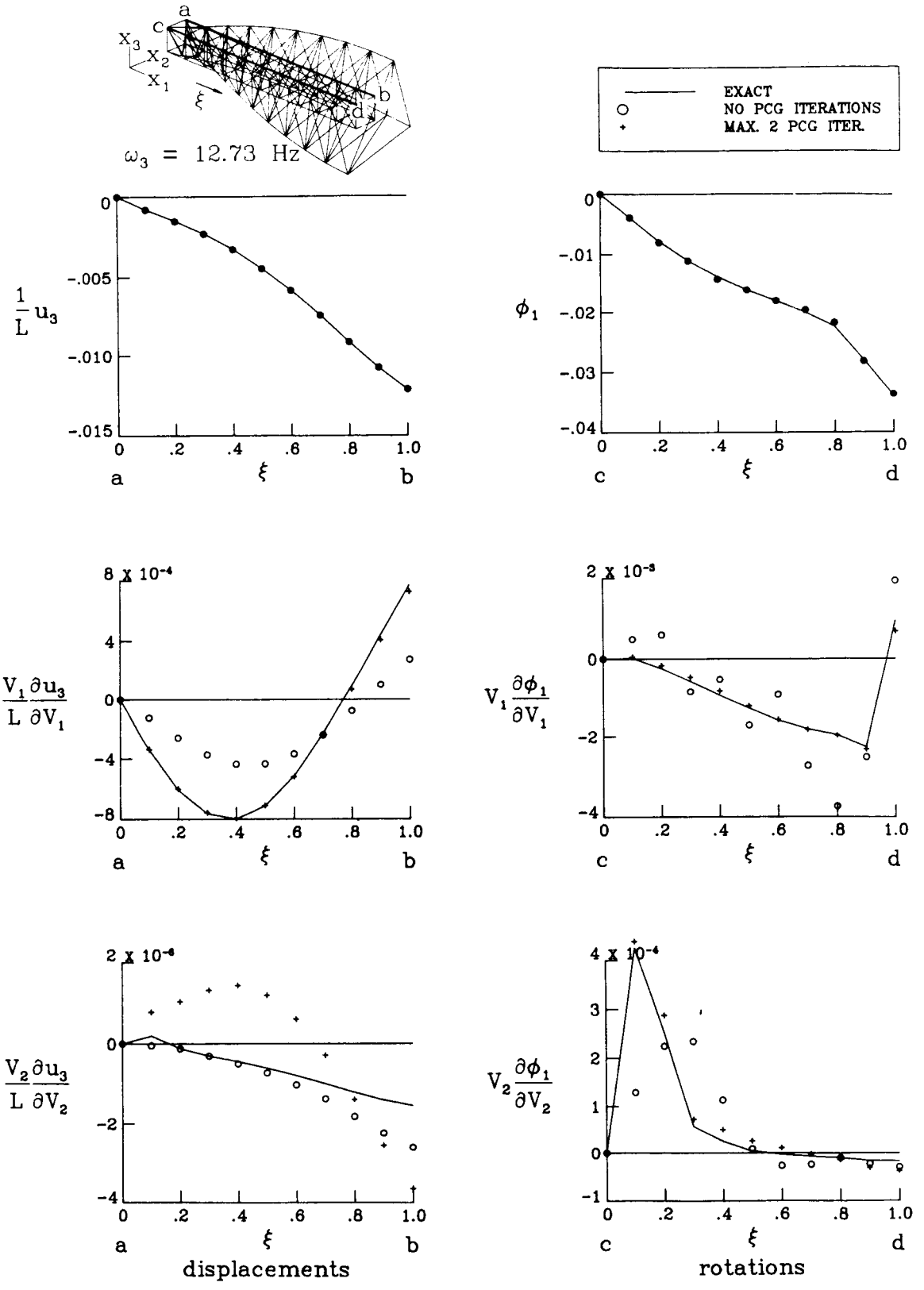

Figure 8. (Continued) Eigenvector 3

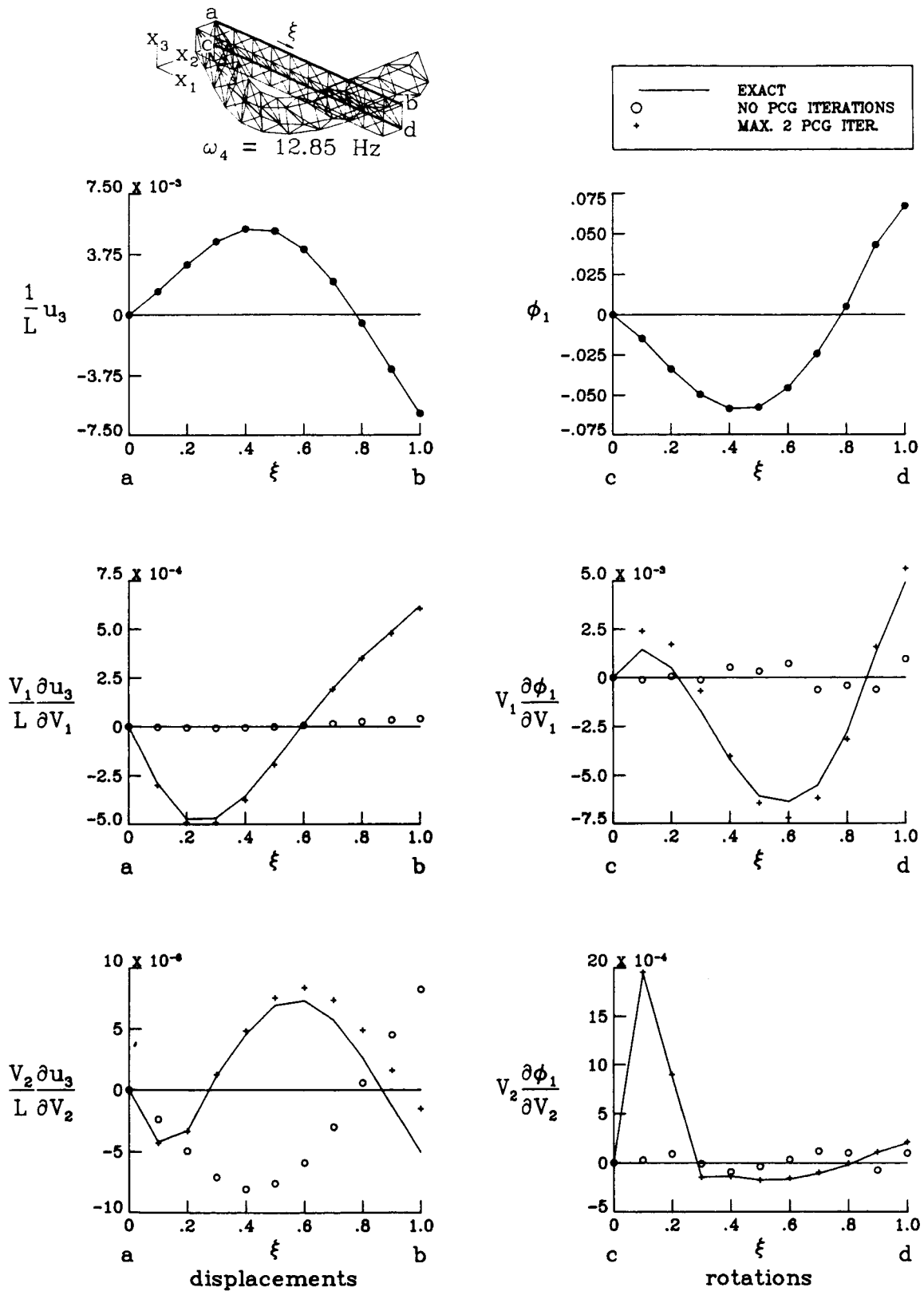

Figure 8. (Continued) Eigenvector 4

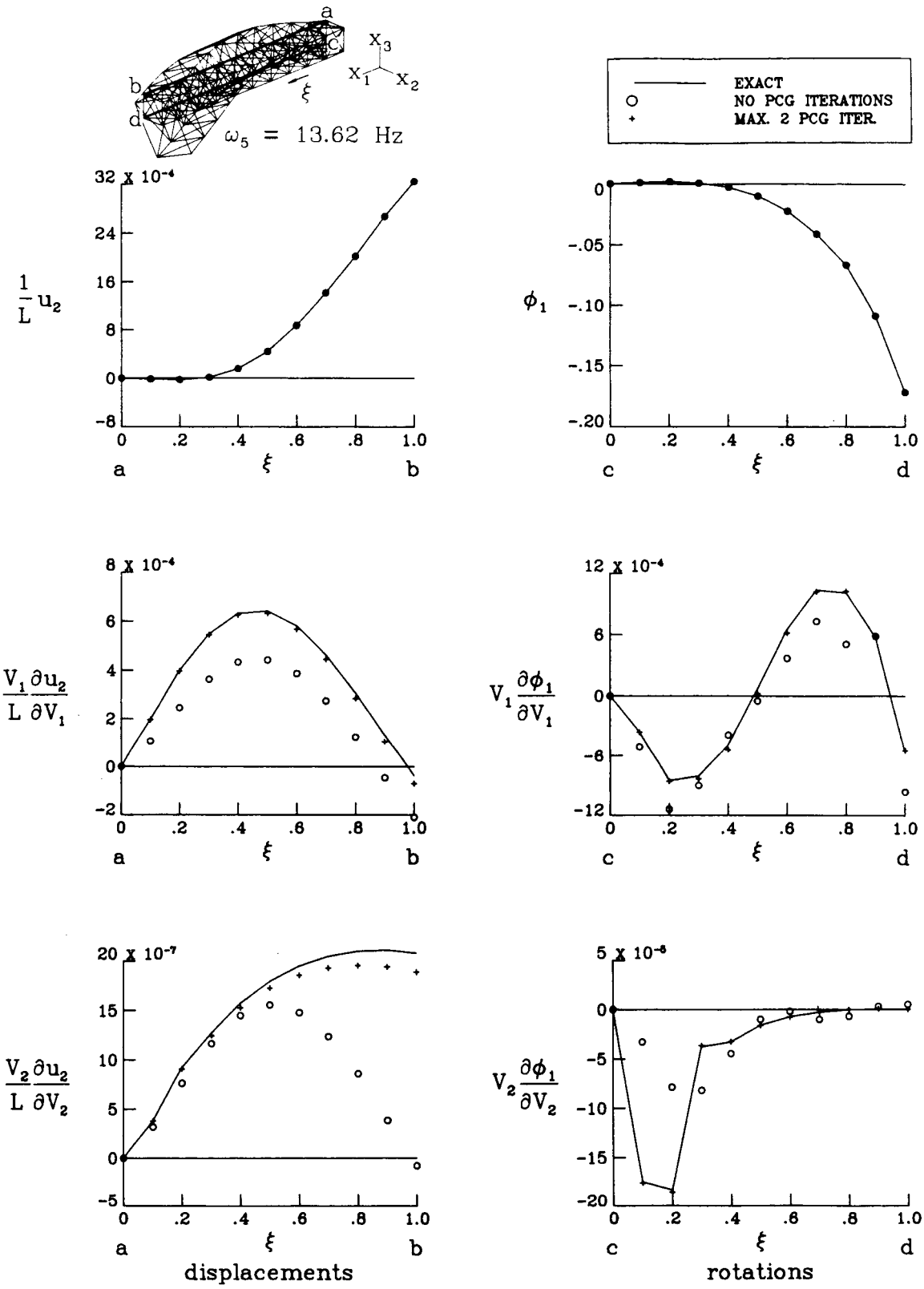

Figure 8. (Continued) Eigenvector 5

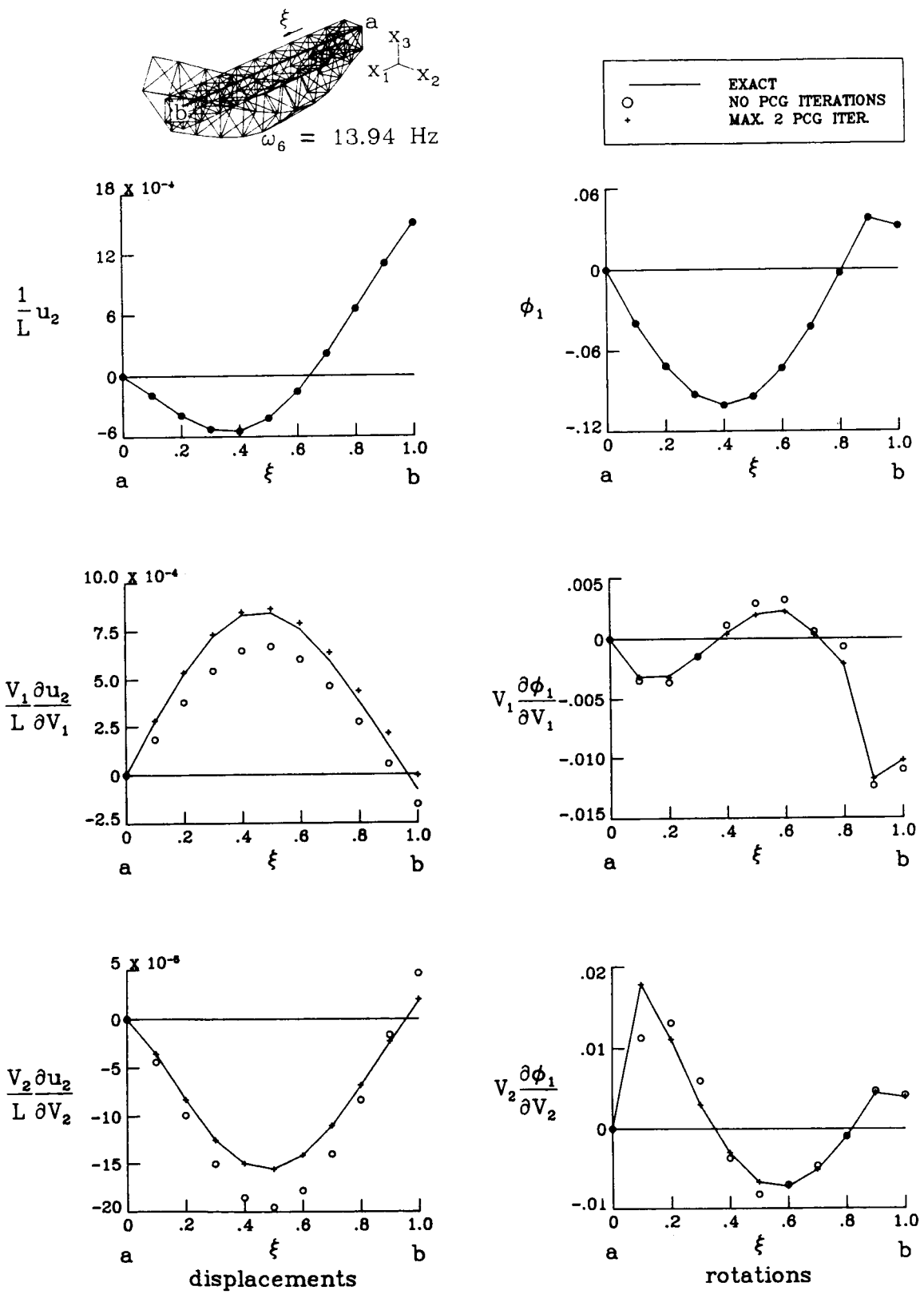

Figure 8. (Continued) Eigenvector 6

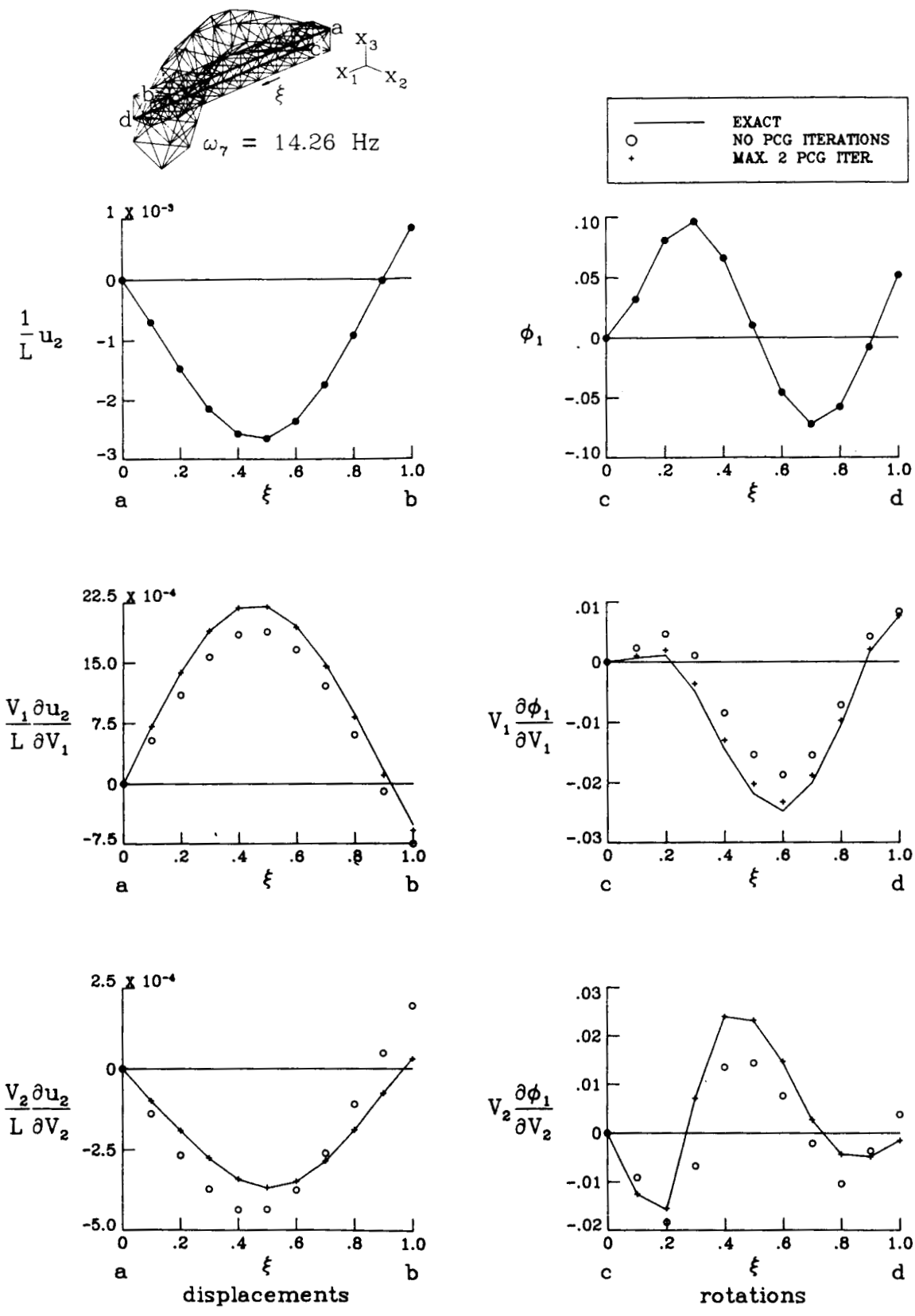

Figure 8. (Continued) Eigenvector 7

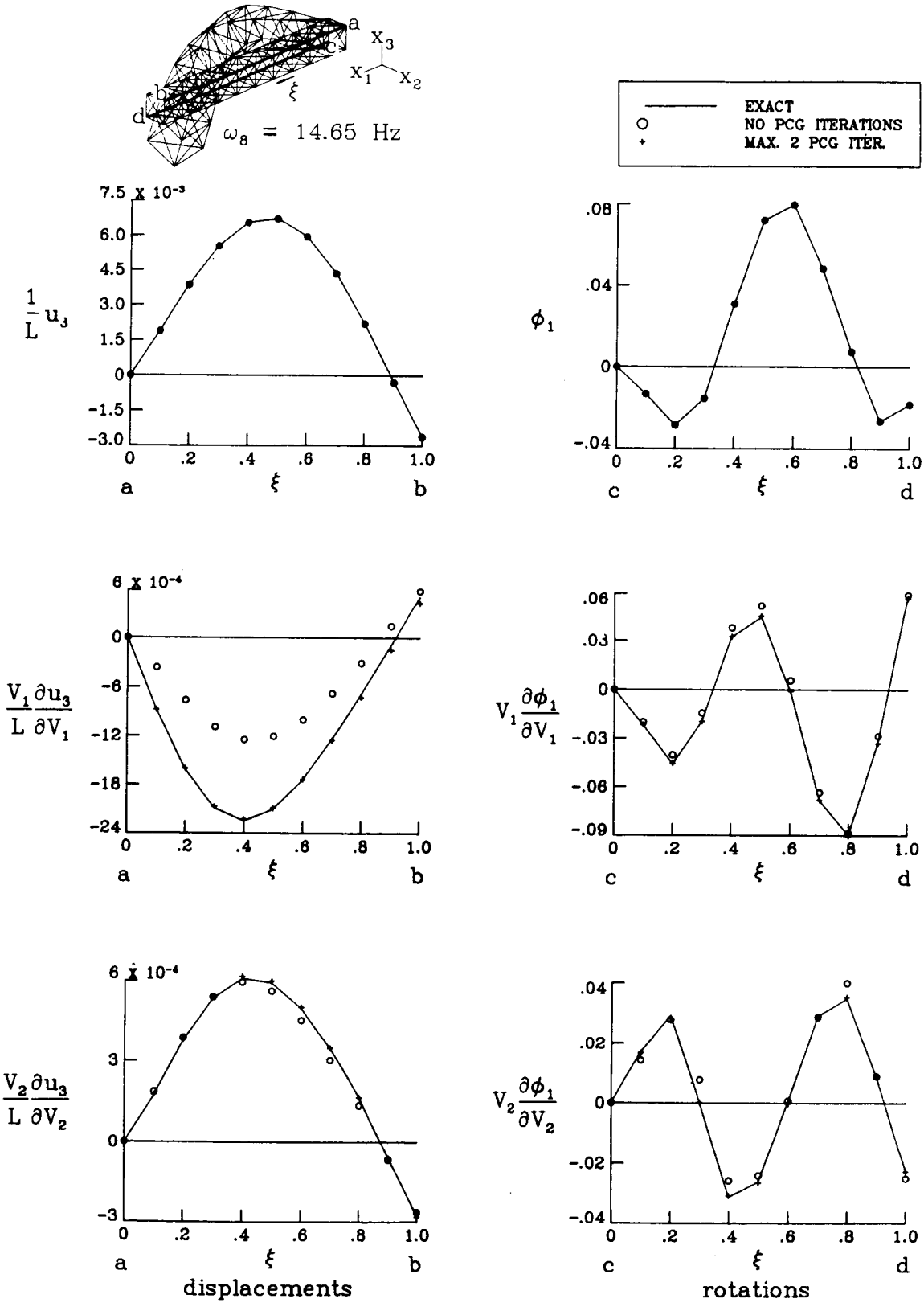

Figure 8. (**Concluded**) Eigenvector 8

Table 1. Accuracy of the eigenvalues and their derivatives.

Mode Number	Eigenvalues			Derivative of Eigenvalue with respect to V_1			Derivative of Eigenvalue with respect to V_2		
	Exact	Stat. Cond. % Error	G. D. R. % Error	Exact	Stat. Cond. % Error	G. D. R. % Error	Exact	Stat. Cond. % Error	G. D. R. % Error
1	$.241001X10^{4}$	$.347848X10^{+0}$	$-.158923X10^{-8}$	$.247151X10^{8}$	$-.491250X10^{+1}$	$-.195171X10^{-6}$	$.438882X10^{9}$	$-.827370X10^{+1}$	$-.304183X10^{-6}$
2	$.382332X10^{4}$	$.365401X10^{+0}$	$-.996056X10^{-9}$	$.384036X10^{8}$	$-.496640X10^{+1}$	$-.837162X10^{-6}$	$.463275X10^{9}$	$-.905540X10^{+1}$	$-.100450X10^{-4}$
3	$.466777X10^{5}$	$.712584X10^{+1}$	$.210180X10^{-3}$	$-.802420X10^{6}$	$-.426313X10^{+2}$	$-.664532X10^{+0}$	$.336275X10^{11}$	$-.295659X10^{+2}$	$.983986X10^{-1}$
4	$.708453X10^{5}$	$.511206X10^{+2}$	$.962984X10^{-3}$	$.328521X10^{9}$	$-.425194X10^{+2}$	$.250464X10^{+0}$	$.222657X10^{11}$	$-.702706X10^{+2}$	$.164092X10^{+1}$
5	$.108107X10^{6}$	$.521962X10^{+2}$	$.198770X10^{-3}$	$.463104X10^{9}$	$-.428125X10^{+2}$	$.510793X10^{-1}$	$.267047X10^{11}$	$-.730408X10^{+2}$	$-.345526X10^{+0}$
6	$.292597X10^{6}$	$.586066X10^{+2}$	$.431567X10^{-3}$	$.217758X10^{9}$	$.537954X10^{+3}$	$-.318201X10^{+0}$	$.986861X10^{12}$	$-.998767X10^{+2}$	$.553694X10^{+0}$
7	$.390707X10^{6}$	$.625423X10^{+2}$	$.577729X10^{-1}$	$-.114253X10^{8}$	$-.122797X10^{+3}$	$-.128613X10^{+2}$	$.573994X10^{12}$	$-.999849X10^{+2}$	$.456316X10^{+1}$
8	$.416004X10^{6}$	$.822520X10^{+2}$	$.165916X10^{-1}$	$.188734X10^{10}$	$-.999600X10^{+2}$	$-.109641X10^{+0}$	$.125338X10^{11}$	$-.984890X10^{+2}$	$.205240X10^{+2}$

Table 2. Accuracy of the eigenvectors and their derivatives. The exact error norm is given by equation (68) and compares the approximate vector to the exact. The residual error norm, given in equations (52) and (53), does not require the exact solution but uses a residual from the full equations.

Mode Number	Eigenvector			Derivative of Eigenvector with respect to V_1			Derivative of Eigenvector with respect to V_2		
	Stat. Cond.	G. D. R.		Stat. Cond.	G. D. R.		Stat. Cond.	G. D. R.	
	Exact Error Norm	Exact Error Norm	Residual Error Norm	Exact Error Norm	Exact Error Norm	Residual Error Norm	Exact Error Norm	Exact Error Norm	Residual Error Norm
1	$.402352X10^{-3}$	$.599319X10^{-10}$	$.215826X10^{-7}$	$.207283X10^{-1}$	$.310474X10^{-1}$	$.999880X10^{+0}$	$.981131X10^{-2}$	$.971090X10^{-2}$	$.100488X10^{+1}$
2	$.464169X10^{-3}$	$.866709X10^{-9}$	$.602493X10^{-7}$	$.206035X10^{-1}$	$.373177X10^{-1}$	$.999856X10^{+0}$	$.106678X10^{-1}$	$.104799X10^{-1}$	$.100933X10^{+1}$
3	$.204802X10^{-2}$	$.254341X10^{-4}$	$.346870X10^{-2}$	$.270880X10^{-1}$	$.107803X10^{-1}$	$.999801X10^{+0}$	$.984066X10^{-2}$	$.983429X10^{-2}$	$.993025X10^{+0}$
4	$.154232X10^{-1}$	$.108155X10^{-3}$	$.584248X10^{-2}$	$.155569X10^{-1}$	$.161677X10^{-1}$	$.999995X10^{+0}$	$.760068X10^{-2}$	$.759782X10^{-2}$	$.100038X10^{+1}$
5	$.157192X10^{-1}$	$.737496X10^{-4}$	$.211585X10^{-2}$	$.135881X10^{-1}$	$.203521X10^{-1}$	$.100010X10^{+1}$	$.762734X10^{-2}$	$.632193X10^{-2}$	$.110223X10^{+1}$
6	$.148434X10^{-1}$	$.487904X10^{-4}$	$.250905X10^{-2}$	$.146538X10^{-1}$	$.132615X10^{-1}$	$.100001X10^{+1}$	$.789574X10^{-2}$	$.649184X10^{-2}$	$.157067X10^{+1}$
7	$.382768X10^{-1}$	$.136385X10^{-2}$	$.991666X10^{-2}$	$.143584X10^{-1}$	$.793387X10^{-2}$	$.999801X10^{+0}$	$.927355X10^{-2}$	$.542840X10^{-2}$	$.129586X10^{+1}$
8	$.221518X10^{+0}$	$.421493X10^{-2}$	$.595339X10^{-2}$	$.149498X10^{-1}$	$.720998X10^{-2}$	$.100000X10^{+0}$	$.131801X10^{-1}$	$.127689X10^{-1}$	$.102893X10^{+1}$

Note:
Tables 1. and 2. Results for the displacement model of the ten bay triangular lattice beam (Figure 1.). The approximate results are obtained using static condensation with 36 retained dof, and also generalized dynamic reduction with 6 basis vectors.

Table 3. Accuracy of eigenvalues and eigenvectors obtained by the mixed model of the ten bay triangular lattice beam (Figure 1.). The approximate results are obtained using generalized dynamic reduction with 6 basis vectors. The exact error norm is given by equation (68) and compares the exact and approximate vectors.

Mode Number	Eigenvalue and Eigenvector			Derivative of Eigenvalue and Eigenvector w.r.t. V_1			Derivative of Eigenvalue and Eigenvector w.r.t. V_2		
	Eigenvalue		Eigenvector	Eigenvalue Derivative		Eigenvector Derivative	Eigenvalue Derivative		Eigenvector Derivative
	Exact	% Error	Exact Error Norm	Exact	% Error	Exact Error Norm	Exact	% Error	Exact Error Norm
1	$.240995X10^{4}$	$.881374X10^{-3}$	$.865581X10^{-7}$	$.247144X10^{8}$	$-.265494X10^{-3}$	$.320578X10^{-1}$	$.438772X10^{9}$	$-.128998X10^{-2}$	$.973317X10^{-2}$
2	$.382319X10^{4}$	$.639964X10^{-3}$	$.370433X10^{-6}$	$.384018X10^{8}$	$-.764543X10^{-3}$	$.472015X10^{-1}$	$.463212X10^{9}$	$-.530059X10^{-2}$	$.105772X10^{-1}$
3	$.468472X10^{5}$	$.305097X10^{-2}$	$.856726X10^{-4}$	$-.754351X10^{6}$	$-.255190X10^{+1}$	$.938631X10^{-2}$	$.346805X10^{11}$	$-.205005X10^{+0}$	$.991289X10^{-2}$
4	$.708917X10^{5}$	$.403851X10^{+0}$	$.250338X10^{-2}$	$.329159X10^{9}$	$.479938X10^{+1}$	$.166784X10^{-1}$	$.224124X10^{11}$	$.255343X10^{+2}$	$.763898X10^{-2}$

Table 4. Accuracy of eigenvectors obtained with the iteration scheme based on inverse power method.

Mode Number	Derivative of Eigenvector with repsect to V_1					Derivative of Eigenvector with respect to V_2				
	Residual Error Norm After Indicated Number of Iterations			Exact Error Norm Before and After Iterations		Residual Error Norm After Indicated Number of Iterations			Exact Error Norm Before and After Iterations	
	0	1	2	Before	After	0	1	2	Before	After
1	$.100X10^{+1}$	$.204X10^{-3}$	-	$.310X10^{-1}$	$.187X10^{-3}$	$.100X10^{+1}$	$.371X10^{-2}$	-	$.971X10^{-2}$	$.257X10^{-4}$
2	$.100X10^{+1}$	$.250X10^{-3}$	-	$.373X10^{-1}$	$.240X10^{-3}$	$.101X10^{+1}$	$.423X10^{-2}$	-	$.105X10^{-1}$	$.342X10^{-4}$
3	$.100X10^{+1}$	$.348X10^{-2}$	-	$.108X10^{-1}$	$.129X10^{-2}$	$.993X10^{+0}$	$.243X10^{-1}$	-	$.983X10^{-2}$	$.201X10^{-3}$
4	$.100X10^{+1}$	$.601X10^{-2}$	-	$.162X10^{-1}$	$.332X10^{-2}$	$.100X10^{+1}$	$.193X10^{+0}$	$.357X10^{-1}$	$.760X10^{-2}$	$.127X10^{-3}$
5	$.100X10^{+1}$	$.479X10^{-2}$	-	$.204X10^{-1}$	$.290X10^{-2}$	$.110X10^{+1}$	$.170X10^{+0}$	$.237X10^{-1}$	$.632X10^{-2}$	$.163X10^{-3}$
6	$.100X10^{+1}$	$.248X10^{-1}$	-	$.133X10^{-1}$	$.275X10^{-2}$	$.157X10^{+1}$	$.488X10^{+0}$	$.143X10^{+0}$	$.649X10^{-2}$	$.422X10^{-3}$
7	$.100X10^{+1}$	$.366X10^{-1}$	-	$.793X10^{-2}$	$.361X10^{-2}$	$.130X10^{+1}$	$.642X10^{+0}$	$.294X10^{+0}$	$.543X10^{-2}$	$.100X10^{-2}$
8	$.100X10^{+1}$	$.148X10^{-1}$	-	$.721X10^{-2}$	$.365X10^{-2}$	$.103X10^{+1}$	$.249X10^{+0}$	$.768X10^{-1}$	$.128X10^{-1}$	$.868X10^{-2}$

Table 5. Accuracy of eigenvectors obtained using preconditioned conjugate gradient iteration.

Mode Number	Derivative of Eigenvector with repsect to V_1					Derivative of Eigenvector with respect to V_2				
	Residual Error Norm After Indicated Number of Iterations			Exact Error Norm Before and After Iterations		Residual Error Norm After Indicated Number of Iterations			Exact Error Norm Before and After Iterations	
	0	1	2	Before	After	0	1	2	Before	After
1	$.100X10^{+1}$	$.675X10^{-3}$	-	$.310X10^{-1}$	$.176X10^{-3}$	$.100X10^{+1}$	$.365X10^{-2}$	-	$.971X10^{-2}$	$.184X10^{-4}$
2	$.100X10^{+1}$	$.665X10^{-3}$	-	$.373X10^{-1}$	$.221X10^{-3}$	$.101X10^{+1}$	$.420X10^{-2}$	-	$.105X10^{-1}$	$.203X10^{-4}$
3	$.100X10^{+1}$	$.108X10^{-1}$	-	$.108X10^{-1}$	$.123X10^{-2}$	$.993X10^{+0}$	$.332X10^{-1}$	-	$.983X10^{-2}$	$.113X10^{-3}$
4	$.100X10^{+1}$	$.203X10^{-1}$	-	$.162X10^{-1}$	$.319X10^{-2}$	$.100X10^{+1}$	$.182X10^{+0}$	$.246X10^{-1}$	$.760X10^{-2}$	$.180X10^{-3}$
5	$.100X10^{+1}$	$.166X10^{-1}$	-	$.204X10^{-1}$	$.258X10^{-2}$	$.110X10^{+1}$	$.142X10^{+0}$	$.132X10^{-1}$	$.632X10^{-2}$	$.101X10^{-3}$
6	$.100X10^{+1}$	$.360X10^{+0}$	$.172X10^{-1}$	$.133X10^{-1}$	$.191X10^{-2}$	$.157X10^{+1}$	$.622X10^{+0}$	$.448X10^{+1}$	$.649X10^{-2}$	$.797X10^{-3}$
7	$.100X10^{+1}$	$.352X10^{+0}$	$.462X10^{-1}$	$.793X10^{-2}$	$.318X10^{-2}$	$.130X10^{+1}$	$.880X10^{+0}$	$.500X10^{+2}$	$.543X10^{-2}$	$.125X10^{-2}$
8	$.100X10^{+1}$	$.213X10^{-1}$	-	$.721X10^{-2}$	$.362X10^{-2}$	$.103X10^{+1}$	$.345X10^{+0}$	$.887X10^{+0}$	$.128X10^{-1}$	$.857X10^{-2}$

Note:
Table 4. and 5. Results of iterative refinement for the displacement model of the ten bay triangular lattice beam (Figure 1.). The approximate results are obtained using generalized dynamic reduction with 6 basis vectors. The derivatives of the eigenvectors are refined by performing the indicated number of iterations. The exact and residual error norms are calculated as shown in equations (68) and, (52) and (53) respectively.

Table 6a. Accuracy of eigenvalues and eigenvectors.

Mode Number	Eigenvalue and Eigenvector		
	Eigenvalue		Eigenvector
	Exact	% Error	Exact Error Norm
1	$.139780X10^{3}$	$-.364716X10^{-7}$	$.263036X10^{-9}$
2	$.276482X10^{3}$	$-.242186X10^{-6}$	$.305360X10^{-10}$
3	$.803208X10^{3}$	$.142737X10^{-5}$	$.972891X10^{-7}$
4	$.131865X10^{4}$	$.148399X10^{-4}$	$.448985X10^{-6}$
5	$.503790X10^{4}$	$-.823970X10^{-8}$	$.133364X10^{-6}$
6	$.521612X10^{4}$	$-.935698X10^{-9}$	$.245186X10^{-7}$
7	$.680834X10^{4}$	$.199972X10^{-8}$	$.114681X10^{-6}$
8	$.109026X10^{5}$	$.192858X10^{-4}$	$.230128X10^{-5}$

Table 6b. Accuracy of derivatives with respect to V_1 and V_2.

Mode Number	Derivative of Eigenvalue and Eigenvector w.r.t. V_1				Derivative of Eigenvalue and Eigenvector w.r.t. V_2			
	Eigenvalue Derivative		Eigenvector Derivative		Eigenvalue Derivative		Eigenvector Derivative	
	Exact	% Error	Exact Error Norm		Exact	% Error	Exact Error Norm	
			Before PCG	After PCG			Before PCG	After PCG
1	$.239228X10^{-1}$	$-.138894X10^{-4}$	$.342773X10^{-2}$	$.177981X10^{-4}$	$.608498X10^{-1}$	$.654030X10^{-4}$	$.247875X10^{-2}$	$.173148X10^{-4}$
2	$.842153X10^{-2}$	$.226312X10^{-5}$	$.225037X10^{-2}$	$.399538X10^{-5}$	$.241423X10^{+0}$	$-.394086X10^{-6}$	$.152003X10^{-2}$	$.147141X10^{-5}$
3	$.129243X10^{-36}$	$.822776X10^{+29}$	-	-	$.370778X10^{-35}$	$.158790X10^{+30}$	-	-
4	$.493584X10^{-14}$	$.228357X10^{+8}$	-	-	$.141498X10^{-12}$	$.440856X10^{+8}$	-	-
5	$.441522X10^{-17}$	$-.957714X10^{+2}$	-	-	$.126573X10^{-15}$	$-.997873X10^{+2}$	-	-
6	$.388726X10^{-33}$	$.683526X10^{+15}$	-	-	$.543844X10^{-31}$	$.420099X10^{+17}$	-	-
7	$.130881X10^{-15}$	$.334238X10^{+3}$	-	-	$.375201X10^{-14}$	$.312476X10^{+5}$	-	-
8	$.123541X10^{-17}$	$.383604X10^{+7}$	-	-	$.314230X10^{-17}$	$.382812X10^{+11}$	-	-

Tables 6. Continued on next page

Table 6c. Accuracy of derivatives with respect to V_3 and V_4.

Mode Number	Derivative of Eigenvalue and Eigenvector w.r.t. V_3				Derivative of Eigenvalue and Eigenvector w.r.t. V_4			
	Eigenvalue Derivative		Eigenvector Derivative		Eigenvalue Derivative		Eigenvector Derivative	
			Exact Error Norm				Exact Error Norm	
	Exact	% Error	Before PCG	After PCG	Exact	% Error	Before PCG	After PCG
1	$.131631X10^{-42}$	$.292424X10^{+29}$	-	-	$-.521037X10^{-42}$	$.811033X10^{+29}$	-	-
2	$.138104X10^{-41}$	$.211996X10^{+27}$	-	-	$-.642889X10^{-39}$	$.108508X10^{+28}$	-	-
3	$.638921X10^{-2}$	$.105148X10^{-1}$	$.234402X10^{-2}$	$.431496X10^{-4}$	$-.786911X10^{+1}$	$.550639X10^{-3}$	$.635695X10^{-4}$	$.960314X10^{-6}$
4	$.256884X10^{-1}$	$.227350X10^{-1}$	$.173463X10^{-2}$	$.124308X10^{-3}$	$-.100908X10^{+2}$	$.824721X10^{-2}$	$.351065X10^{-3}$	$.111514X10^{-4}$
5	$.715246X10^{-17}$	$.329344X10^{+8}$	-	-	$-.745830X10^{-15}$	$.526654X10^{+9}$	-	-
6	$.325946X10^{-17}$	$.239365X10^{+7}$	-	-	$-.122777X10^{-13}$	$.112541X10^{+7}$	-	-
7	$.136820X10^{+0}$	$-.148975X10^{-2}$	$.545426X10^{-2}$	$.218265X10^{-2}$	$-.192418X10^{+2}$	$-.352952X10^{-2}$	$.730475X10^{-2}$	$.532075X10^{-3}$
8	$.320498X10^{-1}$	$.312914X10^{-1}$	$.306863X10^{-3}$	$.118413X10^{-4}$	$-.193920X10^{+2}$	$.247825X10^{-1}$	$.554006X10^{-3}$	$.298712X10^{-4}$

Table 6d. Accuracy of derivatives with respect to V_5 and V_6.

Mode Number	Derivative of Eigenvalue and Eigenvector w.r.t. V_5				Derivative of Eigenvalue and Eigenvector w.r.t. V_6			
	Eigenvalue Derivative		Eigenvector Derivative		Eigenvalue Derivative		Eigenvector Derivative	
			Exact Error Norm				Exact Error Norm	
	Exact	% Error	Before PCG	After PCG	Exact	% Error	Before PCG	After PCG
1	$.581406X10^{-45}$	$.360236X10^{+32}$	-	-	$-.137028X10^{-45}$	$.578543X10^{+32}$	-	-
2	$.143913X10^{-40}$	$.139385X10^{+25}$	-	-	$-.186332X10^{-40}$	$.704606X10^{+24}$	-	-
3	$.146847X10^{-39}$	$.168461X10^{+33}$	-	-	$-.560945X10^{-39}$	$.857312X10^{+32}$	-	-
4	$.304890X10^{-39}$	$.912418X10^{+33}$	-	-	$-.748631X10^{-38}$	$.113451X10^{+33}$	-	-
5	$.196220X10^{+0}$	$.807988X10^{-7}$	$.907586X10^{-3}$	$.387692X10^{-6}$	$-.123476X10^{+2}$	$-.715933X10^{-7}$	$.231513X10^{-4}$	$.231513X10^{-4}$
6	$.218462X10^{+0}$	$-.247398X10^{-5}$	$.360265X10^{-2}$	$.625635X10^{-5}$	$-.533824X10^{+1}$	$.503813X10^{-6}$	$.359601X10^{-3}$	$.418254X10^{-6}$
7	$.577945X10^{-13}$	$.146940X10^{+5}$	-	-	$-.416690X10^{-11}$	$.993028X10^{+3}$	-	-
8	$.412770X10^{-24}$	$.229253X10^{+19}$	-	-	$-.210238X10^{-22}$	$.390044X10^{+18}$	-	-

Note:
Tables 6. Results for the displacement model of the Cobra elastic line model (Figure 2.). The approximate results are obtained using generalized dynamic reduction with 12 basis vectors. The derivatives of the eigenvectors are refined using preconditioned conjugate gradient iterations. The exact error norm is given by equation (68) and compares the exact and approximate vectors.

Table 7a. Accuracy of eigenvalues and eigenvectors.

Mode Number	Eigenvalue and Eigenvector		
	Eigenvalue		Eigenvector
	Exact	% Error	Exact Error Norm
1	$.433741X10^{3}$	$.316369X10^{-6}$	$.290494X10^{-6}$
2	$.441585X10^{3}$	$.126371X10^{-6}$	$.198554X10^{-6}$
3	$.639910X10^{4}$	$.484115X10^{-2}$	$.291885X10^{-3}$
4	$.652841X10^{4}$	$.115185X10^{-3}$	$.434354X10^{-4}$
5	$.732795X10^{4}$	$-.551857X10^{-8}$	$.616662X10^{-7}$
6	$.767646X10^{4}$	$-.280291X10^{-7}$	$.642071X10^{-6}$
7	$.803260X10^{4}$	$-.369367X10^{-5}$	$.657643X10^{-5}$
8	$.847861X10^{4}$	$-.228994X10^{-3}$	$.585151X10^{-4}$

Table 7b. Accuracy of derivatives of eigenvalues and eigenvectors.

Mode Number	Derivative of Eigenvalue and Eigenvector w.r.t. V_1				Derivative of Eigenvalue and Eigenvector w.r.t. V_2			
	Eigenvalue Derivative		Eigenvector Derivative		Eigenvalue Derivative		Eigenvector Derivative	
	Exact	% Error	Exact Error Norm		Exact	% Error	Exact Error Norm	
			Before PCG	After PCG			Before PCG	After PCG
1	$.454903X10^{6}$	$.592149X10^{-3}$	$.220277X10^{-1}$	$.715613X10^{-3}$	$.246227X10^{6}$	$-.299149X10^{-3}$	$.984984X10^{-2}$	$.928875X10^{-4}$
2	$.412980X10^{6}$	$.183884X10^{-2}$	$.247654X10^{-1}$	$.898976X10^{-3}$	$.140343X10^{6}$	$.136247X10^{-1}$	$.957361X10^{-2}$	$.112305X10^{-3}$
3	$.215412X10^{6}$	$-.191396X10^{+1}$	$.135293X10^{-1}$	$.399783X10^{-2}$	$.560679X10^{7}$	$.159478X10^{+1}$	$.817695X10^{-2}$	$.160064X10^{-2}$
4	$.120456X10^{7}$	$.472150X10^{-1}$	$.190621X10^{-1}$	$.329413X10^{-2}$	$.437177X10^{8}$	$.143334X10^{+0}$	$.917554X10^{-2}$	$.159559X10^{-3}$
5	$.350430X10^{5}$	$.515644X10^{-2}$	$.930476X10^{-2}$	$.736461X10^{-3}$	$.436312X10^{6}$	$.996451X10^{-4}$	$.798418X10^{-2}$	$.165649X10^{-3}$
6	$.241314X10^{5}$	$-.312649X10^{-1}$	$.379565X10^{-2}$	$.797167X10^{-3}$	$.219680X10^{9}$	$.380166X10^{-2}$	$.492392X10^{-2}$	$.340912X10^{-3}$
7	$.115520X10^{6}$	$-.138288X10^{+0}$	$.625078X10^{-2}$	$.124098X10^{-2}$	$.620241X10^{9}$	$.384679X10^{-2}$	$.916995X10^{-2}$	$.223311X10^{-2}$
8	$.938964X10^{6}$	$.326681X10^{+0}$	$.278889X10^{-2}$	$.989256X10^{-3}$	$.325558X10^{9}$	$-.114476X10^{+0}$	$.408358X10^{-2}$	$.378197X10^{-3}$

Note:
Tables 7. Results for the displacement model of the orthogonal tetrahedral lattice beam (Figure 3.). The approximate results are obtained using generalized dynamic reduction with 8 basis vectors. The derivatives of the eigenvectors are refined using preconditioned conjugate gradient iterations. The exact error norm is given by equation (68) and compares the exact and approximate vector.

Standard Bibliographic Page

1. Report No.	2. Government Accession No.	3. Recipient's Catalog No.
NASA CR-4099		

4. Title and Subtitle	5. Report Date
Computational Procedures for Evaluating the Sensitivity Derivatives of Vibration Frequencies and Eigenmodes of Framed Structures	October 1987
	6. Performing Organization Code
7. Author(s)	8. Performing Organization Report No.
Timothy L. Fetterman and Ahmed K. Noor	
9. Performing Organization Name and Address	10. Work Unit No.
JIAFS-George Washington University NASA Langley Research Center Hampton, VA 23665-5225	505-63-11-01
	11. Contract or Grant No.
	NAG1-728
12. Sponsoring Agency Name and Address	13. Type of Report and Period Covered
National Aeronautics and Space Administration Langley Research Center Hampton, VA 23665-5225	Contractor Report
	14. Sponsoring Agency Code

15. Supplementary Notes

Langley Technical Monitor: Jaroslaw Sobieski

16. Abstract

Computational procedures are presented for evaluating the sensitivity derivatives of the vibration frequencies and eigenmodes of framed structures. Both a displacement and a mixed formulation are used. The two key elements of the computational procedure are: a) Use of dynamic reduction techniques to substantially reduce the number of degrees of freedom; and b) Application of iterative techniques to improve the accuracy of the derivatives of the eigenmodes. The two reduction techniques considered are the static condensation and a generalized dynamic reduction technique. Error norms are introduced to assess the accuracy of the eigenvalue and eigenvector derivatives obtained by the reduction techniques. The effectiveness of the methods presented is demonstrated by three numerical examples.

17. Key Words (Suggested by Authors(s))	18. Distribution Statement
Sensitivity Derivatives Free Vibration Dynamic Reduction Iterative Refinement Framed Structures	Unclassified - Unlimited Subject Category 39

19. Security Classif.(of this report)	20. Security Classif.(of this page)	21. No. of Pages	22. Price
Unclassified	Unclassified	88	A05

For sale by the National Technical Information Service, Springfield, Virginia 22161